OCCURRENCE AND SPATIAL DISTRIBUTION OF MICROBIAL BIOHERMS IN

GREAT SALT LAKE, UTAH

by

Robert LeRoy Baskin

A dissertation submitted to the faculty of
The University of Utah
in partial fulfillment of the requirements for the degree of

Doctor of Philosophy

Department of Geography

The University of Utah

December 2014

The University of Utah Graduate School

STATEMENT OF DISSERTATION APPROVAL

The dissertation of **Robert LeRoy Baskin**

has been approved by the following supervisory committee members:

George F. Hepner	, Chair	**22 October 2014** Date Approved
Richard R. Forster	, Member	**22 October 2014** Date Approved
Andrea R. Brunelle	, Member	**22 October 2014** Date Approved
Kathleen Nicoll	, Member	**22 October 2014** Date Approved
Gary E. Belovsky	, Member	**22 October 2014** Date Approved

and by **Andrea R. Brunelle** , Chair of

the Department of **Geography**

and by David B. Kieda, Dean of The Graduate School.

ABSTRACT

Microbial bioherms constitute some of the earliest forms of life on Earth. Although the primary form of life on earth during the Proterozoic (Hoffman, 1994), modern occurrences that spread over an area greater than a few square kilometers are rare. Microbial bioherms in Great Salt Lake were reported more than 75 years ago (Eardley, 1938); however, no additional studies have been done on the extent of these structures nor on how environmental factors may influence their distribution.

This dissertation documents the development of a methodology to examine the occurrence and spatial distribution of microbial bioherms in Great Salt Lake, Utah, using multiple lines of evidence including marine acoustic technologies, various spatial and aspatial analyses, Geographic Information Systems (GIS) technologies, and in situ verification of bioherm occurrence.

Microbial bioherms occupy an estimated area of more than 700 km^2 in the south part of the lake and more than 300 km^2 along the margins of the north part of Great Salt Lake. Distributions vary from statistically dispersed to clustered and are closely associated with structurally controlled, positive, microtopographical changes in the benthos. Individuals typically are circular to oblate and range in size from centimeters to over 2 meters in diameter. In some areas of the lake, bioherm heights were measured at more than 1.5 meters above adjacent substrate.

Observations, videography, and samples of microbial bioherms from the south

part of Great Salt Lake, in modern conditions of salinity averaging about 15 percent, are dark green in color, the result of an abundant surface-based phototrophic community that populates the highly rugose surface of the bioherms. Exposed shallow-water bioherms in the north part of the lake are white and not populated by either surface-based phototrophic communities or macroinvertebrate grazers. The environmental conditions in the north part of Great Salt Lake, averaging about 27 percent salinity, have exceeded the ability of bioherm-forming microbial communities to survive.

Great Salt Lake provides a glimpse into what Earth was like during the first 3 billion years of its existence and before the emergence of more complex life forms. This investigation has identified how tectonics and environmental conditions influence the initiation and growth of microbially induced carbonates in saline environments and places important constraints on the conditions for microbial life during the present and during early Earth history.

TABLE OF CONTENTS

LIST OF FIGURES

Figure

ACKNOWLEDGMENTS

First and foremost, I acknowledge the following individuals and organizations who have helped me throughout this dissertation effort. At the top of the list would be my wife Lisa and our two children Paul and Thomas for their endurance and patience. My academic advisor, Dr. George Hepner, University of Utah Department of Geography, has been a great source of inspiration and guidance throughout this process. Dr. Hepner's steadfast vigilance is very much appreciated. I truly appreciate the contributions of my committee including Dr. George Hepner (Chair); Drs. Andrea Brunelle, Rick Forster, and Kathleen Nicoll from the University of Utah, Department of Geography; and Dr. Gary Belovsky, University of Notre Dame, Department of Biology. Their wide diversity of expertise provided a synoptic view of the many factors related to microbial bioherms in Great Salt Lake. I must thank Dr. Paul Wright, Dr. Paul Milroy, and BG Group, LLC for recognizing the potential of Great Salt Lake as a virtually unknown microbial reservoir analogue and having the courage to support innovative approaches to microbialite research. Their support was invaluable in the successful completion of this research. I also am very grateful to Dr. Neal Driscoll, Professor, Geoscience Research Division, at the Scripps Institution of Oceanography, and Dr. Graham Kent, Professor, Department of Geological Sciences and Engineering at the University of Nevada, Reno, for providing equipment, software, and moral support during the collection and analysis of data from Great Salt Lake. Scientists at the State of Utah Great Salt Lake Ecosystem Program also played a critical role in the success of this research by providing logistical support during the many hours of on-lake data collection. Joe Gardner, U.S. Geological Survey, designed the base map of Great Salt Lake and vicinity. Many thanks to HyPack®, ERDAS®, and SPIP®, who provided software and temporary site licenses for use in this specific endeavor.

CHAPTER 1

INTRODUCTION TO THE STUDY

Beneath the saline waters of Great Salt Lake (Fig. 1) lies a virtually unexplored repository of environmental data that documents the tectonic, climatic, and catchment evolution of the present-day lake. As Great Salt Lake continues its evolution toward the unknown, it maintains a history of the geographic, geologic, hydrologic, chemical, and biological events that have given rise to this modern interior sea, its ecosystem, and its environs. Great Salt Lake has preserved that history using the same techniques it has used for over 12 million years. To see into the past and determine how Great Salt Lake came to be, one only needs to unravel the story written in the more than 3,000 meters of sediment that lies beneath its saline waters.

At the interface between water and sediment, the confluence of the past and present, lies the materials most influenced by the tectonic, climatic, and catchment conditions we know today. While locally held belief attests to Great Salt Lake's having an extensive muddy bottom, data from recent surveys of the lake tell a vastly different story. Hidden beneath the murky waters of Great Salt Lake resides the largest known extent of living microbial bioherms (Fig. 2) in the world, providing an analogue for a rare glimpse into the development of early Earth. Reported by Eardley (1938) as "biostromes" and little studied over the last 75 years, vast accumulations of microbial bioherms line the shallow margins of the lake and range from solitary individuals to widespread reef-like communities. A combination of life and rock, such large occurrences of these cyanobacterial communities – and the carbonate structures they build as their homes – are rare.

Great Salt Lake provides a glimpse into what the Earth was like for 3 billion of its 4.6 billion year existence and is an analogue for studying ancient earth environments. Environmental conditions in Great Salt Lake are suspected to mimic those found in the Proterozoic: an environment ripe for microbialite initiation, growth, and study. Great Salt Lake provides an area of unparalleled extent where the spatial distribution of microbial carbonates can be accurately mapped. Such an expanse allows for the development of predictive facies models and quantification of spatial distributions and factors that influence microbialite growth and survivability in a midlatitude lacustrine setting.

Microbial bioherms also are suspected to play a critical role in the ecosystem of Great Salt Lake yet detailed information about the spatial extent and function of the microbially dominated benthic zone is not available. Baseline information about the occurrence, spatial distribution, morphology, biology, and development of microbial bioherms is critical in understanding the role of this benthic community on the ecology and health of the Great Salt Lake, the long-term hydrologic history of the lake, and the effects of anthropogenic influences on the environment of the lake. Changes in climate, water use, and the introduction of waste materials from human activities adjacent to the lake threaten the stability of the lake ecosystem and the organisms depending on it for their survival. Loss of the bioherms through changes in water chemistry or by the introduction of biocidal compounds would be catastrophic.

The mere existence of this unique bioherm population in Great Salt Lake is of interest not only for its empirical presence, but because the microbial communities on the surface of the bioherms are alive and actively accreting carbonates – information that provides the unique opportunity to understand the role of varying environmental conditions on the microbial bioherm-forming communities. Many modern investigations of microbial bioherms focus on the morphology, biology, and growth history, yet little is known about controls on their occurrence and spatial distribution (S. Awramik, personal commun., August 2013). By examining modern carbonate-accreting microbial communities, one can identify possible environmental influences on their initiation and growth and infer physical, chemical, and biological controls on microbial bioherm deposits that occur in both modern and ancient lakes.

This research focuses on the occurrence and spatial distribution of microbial bioherms in Great Salt Lake, Utah, along with environmental factors that may influence their initiation and growth. Research methodology for this investigation was developed based on observations of substrate roughness in Great Salt Lake and its apparent spatial association with the occurrence of microbial bioherms. The process of methodology development involved the following:

(1) a review of historical data to examine previous research on the microbial bioherms of Great Salt Lake;

(2) formation of questions about the occurrence and spatial distribution of bioherms in the lake and definition of the objectives of a study that would address those questions;

(3) assessment of the environmental factors and processes that could influence

the initiation, formation, or preservation of the bioherms;

(4) generation of inferences on bioherm location relative to environmental processes derived from mapping and spatial analysis of bioherm distributions;

(5) selection of appropriate techniques for gathering and verifying the results from analyses of existing data;

(6) collection and analysis of data through rugosity calculations, spatial and aspatial statistics, and image processing and enhancement; and

(7) interpretation of the analyses to explain the occurrence and distribution of microbial bioherms in Great Salt Lake.

Verification of microbial bioherm occurrence and spatial distribution in Great Salt Lake involved the collection, analysis, and interpretation of data from integrated multiple remote-sensing technologies, videography/photography, and underwater benthic sampling. These data, combined with analysis techniques specifically developed for this research, GIS analytical techniques, and in situ verification, provide information about the possible controls on bioherm initiation, development, spatial distribution, and bioherm condition. This multimodal approach to the research included qualitative observations and quantitative measurement of bioherms, examination of environmental variables that could affect bioherm distributions, and an examination of the effects of salinity concentration on the viability of bioherm-forming microbial communities. Analysis of the data included spatial and aspatial statistics to define the distribution of microbial bioherms in the lake, basic measurements of microbial bioherm morphological characteristics, and identification of modern environmental factors that may influence the spatial distribution of bioherms in Great Salt Lake.

The Great Salt Lake ecosystem, including the human residents who reside in close proximity to the lake, live within the historical context of the tectonic, climatic, and catchment changes that have taken place for more than 12 million years (Morrison, 1966). While tectonic, climatic, and catchment development have defined Great Salt Lake in its broadest context, it is the last 600–800 thousand years of open lakes that preserve and define the lake environment as we now know it.

Great Salt Lake preserves an extensive history of change in the accumulated sediment beneath its waters. This research provides a glimpse of how that history can provide valuable insight about changing environmental conditions and the effects of those changes on the occurrence and spatial distribution of microbial bioherms. As an analogue for ancient environments, Great Salt Lake also provides context for environmental conditions that may have existed during the formation of ancient microbial bioherms. This dissertation presents a brief summary of the environs of Great Salt Lake, documents a methodology for studying the occurrence and distribution of microbial bioherms in the lake, addresses some basic questions about microbial bioherm distributions, examines the influence of environmental factors on bioherm distributions, and investigates if differences in environmental conditions are reflected in the patterns of occurrence for the microbial bioherms of Great Salt Lake, Utah.

1.1 Purpose and Scope

The purpose of this research is to investigate the occurrence and spatial distribution of microbial bioherms in Great Salt Lake and to better understand how environmental conditions may influence their initiation, growth, and preservation.

The scope of the research is spatially limited to microbial bioherms exposed at the sediment/water interface in the navigable areas of both the north and south parts of Great Salt Lake, Utah. Initial mapping of bioherm occurrence is based on the surrogate relation between acoustically defined substrate roughness and bioherm occurrence. Acoustic data were collected during this study in selected areas within the navigable areas of the lake for verification of bioherm occurrence. In situ observations, videography, and diving were used to examine the general physical condition of the microbial bioherms and biological activity associated with their occurrence. In situ examination and verification of acoustically based substrate classifications were primarily conducted within eight data-verification areas; however, substrate conditions were verified at random locations throughout the lake. Acoustic data included subbottom profiles of underlying sediments to a depth of approximately 50 meters.

1.2 Study Objectives

The majority of past research into microbial bioherms has focused on morphological, petrophysical, and geochemical evaluations, using that data to classify various microbial morphologies and textures into "classes." Although significant amounts of research have been conducted on microbial carbonates (representative authors include Awarmik, Grotzinger, Harris, Riding, Schopf, Walter, Wright, and others), until recently (Harris, 2012b), none of these studies have specifically examined the occurrence and spatial distribution of microbial bioherms and the range of environmental parameters that may influence their spatial distributions. To address the general what and where questions regarding microbial bioherm occurrence and spatial distribution in Great Salt Lake, the following three research objectives were defined. These objectives provide the impetus for development of a methodology for studying the occurrence and spatial distribution of microbial bioherms in Great Salt Lake.

Objective 1: Define the occurrence and spatial distribution of microbial bioherms in Great Salt Lake.

Identifying patterns in geographic space is essential for understanding the cause and effect relations of external forcing on geographic patterns. A random spatial distribution of microbial bioherms in Great Salt Lake would suggest that no deterministic link exists between physical, biological, or chemical effects and the geographic occurrence and distribution of microbial bioherms. A nonrandom spatial distribution of microbial bioherms in Great Salt Lake would suggest that at least one factor, such as depth, aspect, or salinity, influence distribution of the forms.

In the absence of prior knowledge about the occurrence and distribution of the microbial bioherms, it is commonly assumed that a systematic or random sampling design be implemented to gather the necessary data for analysis. Analysis of results from a systematic or random sampling of microbial bioherms in the lake would provide evidence of a random or nonrandom distribution and provide information about the effects of varying environmental factors on that population.

Objective 2: Determine the influence of environmental factors on the geographic distribution of microbial bioherms in Great Salt Lake, Utah.

Environmental data such as depth (and calculated variables such as aspect and slope), water level, light penetration, temperature, and salinity are available or can be derived from existing data for various locations in the lake and from varying periods of time. The effects of tectonic, climatic, and anthropogenically induced changes to Great Salt Lake can be documented and compared to characteristics and spatial trends in the bioherm distribution. Patterns of microbial bioherm distributions and tectonic, climatic, hydrologic, chemical, or biological factors can infer processes that influence microbial bioherm occurrence and spatial distribution.

Objective 3: Investigate if changes in environmental conditions affect the growth of the microbial bioherms.

Microbial bioherms are organosedimentary deposits that have a circular to subcircular morphology and are a result of benthic microbial communities trapping and binding detrital sediment and/or forming the locus of mineral precipitation (Burne & Moore, 1987). As such, they should preserve a record of changing environmental conditions as they grow. Interruptions in development of the bioherms due to changing environmental conditions should be recorded in the physical, chemical, or biological characteristics of the deposits. Major changes in the environment of Great Salt Lake have taken place during the last 100 years such as the addition of a rock-filled causeway segmenting the lake. Resultant dissolved-solids concentrations have ranged from approximately 3 percent in the south part of the lake about 27 percent in the north. The effects of these changes will affect formation and growth of the bioherm population or the organisms that form the bioherm structures, and the results of those environmental changes should be physically or chemically evident.

1.3 Relevance and Benefits

Microbial bioherms constitute some of the earliest signs of life on Earth. The first occurrence of microbial bioherms in the rock record dates back to Archaen time (3,430–3,500 million years ago) and microbialites have dominated the fossil record for over 80 percent of the Earth's history (Walter, 1994; Grotzinger and Knoll, 1999). Although the primary from of life on earth during the Proterozoic (Hoffman, 1994), modern occurrences spread over an area greater than a few square kilometers are rare (Appendix E).

Great Salt Lake can be viewed as a modern analogue to ancient lacustrine saline environments that are preserved in the rock record and currently developed, or being developed, as oil and gas reservoirs. It is one of very few settings where the spatial distribution of modern microbial carbonates can be accurately mapped both in order to develop predictive facies models and as a means of providing quantitative spatial distribution data and distribution controls for hydrocarbon reservoir mapping.

Deep-water hydrocarbon reservoirs, recently discovered off the Atlantic coasts of South American and Africa, show textures and preserved chemistries that indicate a possible microbial origin or influence. The microbial substrates in Great Salt Lake are invaluable for comparison with ancient microbial deposits because of their spatial extent, varying morphologies and internal fabrics, microbial communities, and the relatively well-defined environmental conditions in which they have formed and live. The ability to study such an extensive spatial distribution with widely varying environmental conditions also provides researchers the opportunity to extend their understanding of environmental controls on microbial bioherm distributions beyond those found in other locations.

Baseline information about the occurrence, distribution, morphology, biology, and development of microbial structures is critical in understanding the role of this benthic community on the ecology and health of the Great Salt Lake, the long-term hydrologic history of the lake, and the effects of development within its contributing drainage basins and along its shores. Microbial bioherms are suspected to play a critical role in the ecosystem of Great Salt Lake, yet detailed information about the extent and function of the microbially dominated benthos is not available. Understanding the role that benthic microbial communities play in Great Salt Lake is critical to understanding the lake ecosystem and the effects of anthropogenic influences on that ecosystem.

Microbial bioherms and similar biogenic carbonates form a stable base for adherence of benthic biological forms such as brine fly larvae and supply a base for critical primary production during periods of water-column overgrazing by brine shrimp. Changes in climate, water use, and the introduction of waste materials from human activities adjacent to the lake threaten the stability of the lake and the organisms depending on it for their survival. Loss of the bioherms through changes in water chemistry or by the introduction of biocidal compounds would be catastrophic to the ecosystem of the lake.

1.4 Unique and Valuable Contributions to the Field

Research methodologies were developed for studying the occurrence and distribution of microbial bioherms in Great Salt Lake by integrating acoustic single-beam, side scan sonar, and subbottom geophysical data along with physical, chemical, and biological data from the lake. This research produced a number of theoretical, methodological, and technical contributions that are discussed in the following sections.

1.4.1 Theoretical Contributions

This research quantified a number of currently debated theoretical issues regarding the occurrence and distribution of microbial bioherms and environmental parameters that may affect or control their distributions in lacustrine environments.

1.4.1.1 Quantified microbial bioherm distribution

This effort provides the first systematic research examining the lake-wide spatial distribution of microbial bioherms in Great Salt Lake, Utah. Although the presence of microbialites in Great Salt Lake has been known for over 70 years, this research provides the first evidence that living microbial bioherms, ranging from individual occurrences to coalesced, nearly solid reef-like structures, occupy an area of more than 700 km^2 in the south part of Great Salt Lake and over 1,000 km^2 previous to recent anthropogenic modifications to the lake.

1.4.1.2 Verified buried microbial bioherms and causes for burial

High-resolution Compressed High Intensity Radar Pulse (CHIRP) geophysical data collected during this investigation substantiates the theory that conditions favorable for microbial bioherm development previously occurred in Great Salt Lake and confirms that some microbial bioherm deposits have been recently buried by sediment. Relative downward offset of some near-surface buried bioherm deposits indicate that overlying sediments were deposited after recent tectonic activity. CHIRP geophysical data also substantiate that anthropogenic modifications in the physical characteristics of Great Salt Lake have resulted in changes to the environmental conditions in Great Salt Lake and those changes have resulted in the burial of microbial bioherms by halite and other evaporite minerals in the north part of the lake.

1.4.1.3 Identified previously unknown faults and folds

Geophysical data acquired for this investigation identified multiple previously unknown faults and folds in the sediments beneath Great Salt Lake and provide details of offsets and relative timing of fault movement. Previous research on faulting in Great Salt Lake identified larger faults along the eastern margins of the basins but utilized tools that did not have adequate vertical resolution to identify the smaller faults critical in defining the relation between bioherm occurrence and tectonically related subbottom displacement. This research has identified that the spacing, offset, timing, and orientation of these faults is important in examining the tectonic history of Great Salt Lake and in reconstructing the environmental conditions present during bioherm initiation and periods of growth. The spatial orientation and offset of subbottom structure control microbial bioherm distributions and consequently influence the statistical evaluation of microbial bioherm randomness.

1.4.1.4 Identified structural control of bioherm distributions

This research quantified that microbial bioherm occurrences in Great Salt Lake are associated with structurally controlled, positive, microtopographical changes at the sediment/water interface. The relation between abrupt fault-controlled topographic highs (1–2 meter vertical offsets), microbial bioherm occurrence on the highs of tectonically controlled footwalls, and corresponding onlapping sediments trapped in hanging wall lows is repeated in many of the surveyed areas and likely occurs throughout most of the nonsurveyed areas. Based on this observed relation, it appears that interrelated environmental conditions found at the topographic highs (light availability, sedimentation, substrate type, and/or wave-base energy) play a critical role in microbial bioherm occurrence.

1.4.1.5 Identified sensitivity to topographic changes

The sensitivity of microbial bioherm occurrence to environmental variations associated with small-scale topographic changes supports the theoretical basis of a shallow water environment for development of extensive prehistoric microbialite-rich carbonate deposits. Fine-grained onlapping sediments trapped in hanging wall lows adjacent to the microbial bioherms in Great Salt Lake exhibit wave-energy related features such as ripple marks and larger bedforms, denoting microbial bioherm occurrence above wave base.

1.4.1.6 Documented anthropogenic influence on bioherms

Comparison of bioherms and the environmental conditions immediately surrounding the bioherms in the south part of Great Salt Lake with similar occurrences in the north part of Great Salt Lake substantiates the hypothesis that the chemistry of lacustrine waters is critical in the survival of bioherm-forming microbial communities. The hypersaline environment in the north part has exceeded the salinity range in which bioherm-forming microbial communities can survive, effectively defining an upper limit of salinity for bioherm forming microbial community viability.

1.4.1.7 Identified tectonic results from Lake Bonneville regression

Faults, folds, and other tectonic features associated with bioherm occurrence extend through concordant, acoustically transparent, deposits associated with pelagic deposition from Pleistocene Lake Bonneville. Analysis of CHIRP subbottom data supports the premise that the sudden regression of Lake Bonneville resulted in faulting and folding of the sediments beneath Great Salt Lake. Directly supporting the observations of Gilbert (1890), Crittenden, (1963), and Bills and May (1987), the mapped small-scale faults and folds that interrupt the concordant sediments of Lake Bonneville are indications of isostatic rebound. Examination of faults and their vertical extension through the pelagic sediments of Great Salt Lake provides a maximum age for the small-offset faults discovered as part of this research, sediment accumulation rates in the area of the faults, and age-limits on the initiation of modern microbial bioherm deposits in the lake.

1.4.2 Methodological Contributions

Many modern investigations of microbial bioherms focus on morphology, biology, and growth history, yet little is known about controls on microbial bioherm occurrence and spatial distribution. Methodologies for examining microbial bioherm occurrence, spatial distribution, and their controls developed for this investigation are based on modifications of standard methods for marine investigations and classification of physical roughness.

1.4.2.1 Integrated acoustic technologies and GIS analysis

This research integrated multiple marine acoustic technologies with Geographic Information System (GIS) analysis tools to quantify the spatial distribution and morphology of microbial bioherm deposits in Great Salt Lake, Utah. Data from a single-beam fathometer, side scan sonar, and CHIRP subbottom profiler were integrated with Geographic Information System (GIS) technologies to provide a geographically registered, pseudo three-dimensional representation of microbial bioherm occurrence and spatial distribution in Great Salt Lake, Utah.

In situ verification insured that acoustically derived interpretations and classifications of the benthic zone and substrate were confirmed through additional lines of evidence thus limiting possible misinterpretation of acoustic data. Recording and retention of geographic registration information within each dataset insured that the data were spatially comparable and allowed for direct analysis and manipulation of the acoustic datasets within a GIS framework.

1.4.2.2 Developed automated approach to benthic rugosity analysis

This effort also resulted in the development of a unique methodology for examining variations in acoustically defined benthic roughness and successfully applied it in identifying probable areas of microbial bioherm occurrence in Great Salt Lake, Utah. Limited water-column visibility and associated difficulties in optical verification of microbial bioherm occurrence necessitated development of analytical methods for examining variations in benthic roughness from available lake-wide acoustic bathymetric data. This investigation modified techniques normally used in the machining industry to quantify the physical roughness of machined surfaces as defined by ISO-4287 (ISO, 1997).

1.4.3 Technical Contributions

This research was conducted in the hypersaline environment of Great Salt Lake, Utah, and required a number of changes to software and data processing methods. Modifications in commercial software were necessary to account for the higher sound velocities encountered in the hypersaline environment of Great Salt Lake. Two computer programs were developed to 1) calculate benthic rugosity at user-defined intervals for examining change in rugosity across a surface and 2) automate CHIRP geophysical data processing.

1.4.3.1 Provided rational for commercial software modifications

Off-nadir acoustic beam paths, governed by Snell's Law, require an accurate speed of sound to adjust acoustic imagery to its proper geographic location. The high sound velocities encountered in the hypersaline environment of Great Salt Lake exceeded the internal ability of the side scan sonar used during this study to correct for off-nadir acoustic wave paths, and consequently, postprocessing of the side scan sonar data was required. Postprocessing of the side scan sonar data involved the use of commercial hydrographic software, which also initially had limitations in adjusting for high sound velocities. The software's inability to correct for the higher velocity of sound in Great Salt Lake was identified, and methods for correcting the data were discussed with the software vendor. The vendor modified the processing software to accommodate the increased sound velocities measured in Great Salt Lake and extended the ability of their software to accommodate sound velocities that theoretically could occur in other hypersaline water bodies.

1.4.3.2 Automated benthic rugosity calculation methods

As part of the methodology for defining the occurrence and distribution of microbial bioherms in Great Salt Lake, a technique for calculating change in benthic roughness from single beam acoustic data was developed. This procedure automates the calculation of rugosity along transects in user-defined increments and assigns the average position of the selected interval to the appropriate calculated rugosity value. Calculating the change in acoustic rugosity along survey transects provides not only the change in roughness along each transect, but also locations where change occurs and the rate of change. This procedure was developed and written as a computer program for examination of multiple sample intervals and their effects on the representation of lake bottom roughness.

1.4.3.3 Automated processing of CHIRP geophysical data

An additional procedure was developed that automates processing of CHIRP geophysical data. Processing of the CHIRP data involves conversion of the native acquisition format to a nonproprietary format, modification of a specific processing script for each line segment including multiple modifications based on characteristics of the transect data, execution of the script, and production of the processed data and supporting information. Processing steps for CHIRP data were automated, utilizing a new computer program that examines file structures for standardized naming conventions and data type, extracts specific pieces of information from the CHIRP system output files, writes that information as variables into individual processing scripts, and then executes each completed script. Output files include a summary of the data collection activities and a file formatted for direct import into GIS software.

1.5 Assumptions, Limitations, Design, and Quality Controls

This series of investigations is limited to the occurrence and distribution of the microbial bioherms exposed at the sediment/water interface in Great Salt Lake, Utah, and the probable effects of selected environmental influences on their spatial distribution.

Single-beam digital acoustic data, collected over the navigable areas of Great Salt Lake (Baskin, 2005; Baskin, 2006), were used for initial determination of microbial bioherm distribution. Data analysis was conducted separately for data from the south and north parts of the lake due to the significant differences in environmental conditions between the two sections. A classified spatial distribution map was generated from the digital bathymetric data using techniques developed during this research and field verified using side scan sonar data, swept-frequency CHIRP geophysical data, videography, and in situ sampling. Utilization of environmental parameters was limited to those data available through public sources.

The timing of sampling and field investigations were affected by weather, lake condition, and equipment availability. The availability of field resources and financial constraints limited the amount of time available for data collection and analysis and consequently limited the scope of this study to the investigation of microbial bioherms and a limited number of physical and chemical environmental parameters.

Quality-control measures for collecting, processing, and analyzing verification data were established before data collection began to prevent variations in data gathered over multiple data collection episodes. Specifics on the collection, processing, and analysis of the various data are described in their appropriate sections of this manuscript.

1.6 Introduction to Great Salt Lake

1.6.1 Geographic Setting

Great Salt Lake is located northwest of Salt Lake City, Utah, and is the evaporative remnant of freshwater Pleistocene Lake Bonneville (Fig. 3). It is the fourth or fifth largest terminal lake in the world (depending on the metric used) and lies adjacent to the highly populated Wasatch Front at the eastern edge of the Basin and Range Province (Fenneman, 1931). About 2.3 million people or 75.9 percent of the population of the State of Utah live along the western flanks of the Wasatch Range (EDCUtah, 2013), where Utah's three largest cities (the Salt Lake City metropolitan area, Ogden, and Provo) are located (Fig. 1). The lake is bordered on the west by desert and on the east by the Wasatch Range.

Great Salt Lake is primarily owned and administered by the State of Utah, with large blocks of land that lie adjacent to the lake falling under the management of the Utah State Department of Natural Resources and U.S. Fish and Wildlife Service. Above the meander line, ownership is largely private. Waterfowl management areas and bird refuges line most of the eastern edge of the lake.

1.6.2 Climatic Conditions of Great Salt Lake, Utah

The climate of Great Salt Lake and vicinity, and the mountains east of the lake, from which its water supply is derived, is typical of the Western United States. Temperatures generally fluctuate widely between summer and winter and between day and night. The high mountains have long, cold winters and short, cool summers. The lower valleys are more moderate, with less variance between maximum and minimum temperatures. Average annual temperature ranges from 4.6 °C (40.3 °F) to 17.6 °C (63.7 °F) at the Salt Lake City International Airport. Average monthly maximum temperature for the Great Salt Lake drainage reaches 33.4 °C (92.1 °F) in July at the Salt Lake City International Airport, and the average monthly daily minimum reaches -18.7 °C (-1.7 °F) in January at Sage, Wyoming (U.S. Department of Commerce, 1992). Most of the inflow to Great Salt Lake originates as precipitation falling as snow during the winter months in the adjacent Wasatch Mountains and resultant snowmelt runoff during the spring. Average annual precipitation ranges from less than 25 to 41 cm (9.9–16.1 in.) on the valley floors to greater than 177 cm (69.7 in.) in the high mountain areas. Great Salt Lake has a much greater surface-area-to-volume ratio than other lakes in the region. As a result, an average of about 3,580 cubic hectometers (2.9 million acre feet) evaporates from the lake each day (Waddell and Barton, 1978).

1.6.3 Geologic History of Great Salt Lake

Great Salt Lake occupies a large Cenozoic half graben bounded on its eastern flank by a series of normal faults (Kowalewska and Cohen, 1998) and is the result of extensional forces on the area west of the Wasatch Range. The extension of the Great Basin (so named by Fremont (1845) who determined that no water drained to the ocean from the region), is characterized by low angle detachment faults with high-angle listric faults developed in areas above the low-angle faults (Morrison, 1966). These high-angle faults are predominately located along the eastern margins of the lake and conform to deep faults defined by Mikulich and Smith (1974), using data collected in 1969 (Colman, Kelts, and Dinter, 2002). The majority of the faults trend to the northwest. The exception is the Carrington Fault that separates the lake into two separate basins and trends to the northeast toward the southwestern tip of Promontory Point (Morrison, 1966; Colman, Kelts, and Dinter, 2002) (Fig. 4). These naturally formed north and south basins differ from the named Gunnison Bay and Gilbert Bay designations, designations based on the segmentation of the lake by a rock-filled railroad causeway and assigned to those areas north and south, respectively, of the railway causeway.

Displacement along the fault segments underlying the eastern margins of the lake differed for most of the late Neogene (Kowalewska and Cohen, 1998). Differential movement along the fault segments resulted in differences in sedimentation rates and varying environmental conditions between the north and south basins throughout much of the pre-Bonneville cycles (Moutoux, 1995). Subsidence rates were highest along the eastern margins of the basins, close to the faults, and subsequently had the highest sedimentation rates.

Correlation of recent seismic profiles with sediment cores indicates that the oldest post-Bonneville sediments have been displaced multiple times since their deposition including at least three episodes of movement on the East Lake fault totaling as much as 12 meters (Colman, Kelts, and Dinter, 2002). Topographic expression of faults on the lake floor, as reported by Colman, Kelts, and Dinter (2002) and Dinter and Pechmann (1999) and imaged during this research, are strong evidence that the area remains tectonically active.

1.6.4 Hydrologic Conditions of Great Salt Lake

The hydrology of Great Salt Lake is related to its catchment, climate, tectonics, and generally, to a lesser extent, to biologic and anthropogenic effects (Fig. 5). Because Great Salt Lake is a terminal lake, changes in water-surface altitude are controlled by differences between net inflow and evaporation from the surface of the lake and by structural controls limiting the complete circulation of inflow. The contributing drainage area to modern Great Salt Lake is about 55,684 square kilometers (21,500 square miles). Total annual inflow to the lake is about 3.6 cubic kilometers (~2.9 million acre-feet) with inflow and evaporation varying annually based on climatological variables (Waddell and Barton, 1978).

Three major river systems enter Great Salt Lake: the Bear, the Weber, and the Utah Lake/Jordan River systems (Fig. 6). Headwaters of the Bear, Weber, and Provo Rivers originate at the western end of the Uinta Mountains, at altitudes above 3,050 m (~10,000 ft). Much of the drainage area for Great Salt Lake lies in Utah, but it also includes areas in Idaho and Wyoming. Streams flow through the wide valleys east of the Wasatch Range, emerge through the mountain ranges to the west, and discharge into Great Salt Lake.

Throughout most of its recent history, the area surrounding and including Great Salt Lake has been a mixture of marsh, shallow lacustrine and sand flat conditions. From about 32,000 years before present (ybp) to the present, a perennial lake has existed in the basin although the presence of thick mirabilite layers in the north basin (Eardley, 1962) indicate that, at least in some parts of the basin, lake surface altitudes likely were lower than present (Spencer and others, 1984).

The physical structure of Great Salt Lake is a function of the tectonic history of the basin, wind-driven circulation patterns, and the influx and deposition of fluvial sediments. The lake is comprised of two large basins separated by a fault structure extending from Hat Island in the southwest to Promontory Point toward the northeast (Fig. 7) (Spencer and others, 1984; Bortz, Cook, and Morrison, 1985; Baskin, 2005). These two natural basins likely controlled circulation and sediment depositional patterns throughout much of the history of the lake. During periods of low lake-level elevation, the south part of the lake would segment into two separate water bodies, separating along the fault-controlled offset connecting Hat Island with Promontory Point.

In 1959, a rock-filled railroad causeway replaced a trestle bridge, constructed in

1903, that provided a rail connection between the east and west sides of the lake (Fig. 8). The rock-filled causeway effectively subdivided the north basin of the lake into north and south sections. The south part of the basin is hydrologically connected to the south part of the lake (Gilbert Bay) and the other is a separate, isolated, inflow-limited system (Gunnison Bay) (Fig. 1). The vast majority (~95 percent) of fresh water entering Great Salt Lake occurs in the south part of the lake (Waddell and Barton, 1978). Exchange of water between the south and north parts of the lake is currently limited to flow that occurs through an 82-meter wide bridge and the semipermeable causeway itself. The rock-filled causeway provided a stable long-term solution for rail traffic across the lake but effectively segmented the north part of the lake into two distinct water bodies with distinctly different chemistries and biota. The rock-filled causeway also changed wave base conditions and circulation patterns between the two basins.

In modern time, the Great Salt Lake has experienced marked fluctuations in lake level (Fig. 9). In 1963, Great Salt Lake was at its lowest water-surface altitude in recent history of about 1,277 meters (4,191 feet), covered about 2,460 square kilometers (950 square miles), and had a maximum depth of about 7.6 meters (25 feet). In 1986 and again in 1987, Great Salt Lake reached its highest water-surface altitude in recent history at about 1,284 meters (4,212 feet), covered about 6,216 square kilometers (2,400 square miles), and had a maximum depth of about 13.7 meters (45 feet).

For the area south of the causeway, area and volume calculations show a maximum area of about 2,060 square kilometers) (508,000 acres) and a maximum volume of about 11.40 cubic kilometers (~9.3 million acre-feet) at a water-surface altitude of 1,280 meters (~4,200 feet). Minimum water-surface altitude of the south part of Great Salt Lake is just below 1,270 meters (4,167 feet) in the area just south of the Union Pacific railroad causeway halfway between Promontory Point and the western edge of the lake (Baskin, 2005).

For the area north of the causeway, area and volume calculations show a maximum area of about 1,560 square kilometers (385,000 acres) and a maximum volume of about 7 cubic kilometers (~5.7 million acre-feet) at a water-surface altitude of 1,280 meters (4,200 feet). Minimum natural water-surface altitude of the north part of Great Salt Lake is the same as the minimum natural water-surface altitude of the south part (Baskin, 2006).

Water chemistry plays an important role in the survivability of the microbial communities that form bioherms. Due to differences in fresh-water inflow between the north part of Great Salt Lake and the south part, the lake now exhibits two chemically and biologically different regimes on either side of the rock-filled causeway. Before construction of the rock-filled causeway (pre-1955), the dissolved-solids concentration throughout the lake likely exhibited much less variability from north to south. Nevertheless, concentration differences would still have existed due to local variability in inflow, physical separation of the two fault-controlled basins, evaporation, currents, wind, and water density variations (Hahl and Langford, 1964). Observations by Eardley in 1934 (Rawley, 1974) indicate that the entire bottom of the lake was crusted over with halite crystals. Where sampled, the salt thickness ranged from 1 to 6 inches. Halite was not observed in the south part of the lake in 1933 or the north part of the lake in 1932. Low lake levels between 1934 and 1940 likely maintained a variable thickness salt crust over much of the lake floor; however, rising lake levels between 1945 and 1955 and the associated influx of fresh water probably dissolved the salt crust, putting the salt back into solution. Various observations by E.V. Rawley and E. Cohenhour from 1950 to 1958 confirmed the loss of the salt crust in both the north and south parts of the lake.

In the early summer of 1961, 2 years after the rock-filled causeway was completed, a layer of "hard solid salt" was observed north of Lakeside and west of Promontory Point (Rawley, 1974). Precipitation of salt in the north part of the lake likely began between 1959 and 1960, shortly after the completion of the rock-filled causeway. This early lakebed salt deposit likely is the same one that persists today. Although additional observations of salt deposition in the south part of the lake were made during the record low lake levels of 1959–1963 (Hedberg and Parry, 1971), these deposits were short-lived and subsequently dissolved as fresh-water inflows, and loss of saline brine to the north side of the causeway lowered the salinity of Gilbert Bay.

Postcauseway (1959–present) dissolved-solids concentrations in the south part of the lake have ranged from a high of about 27.5 percent (when the causeway was initially constructed) to a low of about 3.8 percent. Salinity in the north part of the lake has ranged from 15 percent to about 27 percent salinity (close to or at sodium chloride saturation) (Waddell and Barton, 1978) (Fig. 10). Present salinities average about 15 percent for the southern section of the lake and about 27 percent for the northern section. This dichotomy of salinity has a dramatic effect on the physical, biological, and chemical characteristics between the north and south parts of the lake.

The segmentation of Great Salt Lake by a solid-fill causeway provides an opportunity to examine the effects of hydrologic modification of the lake, on growth of microbial bioherms, and on changes to the ecosystem affected by the causeway and causeway on the salinity of Great Salt Lake can be found in Hahl and Langsford (1964), Madison (1970), Waddell and Bolke (1973), Waddell and Fields (1977), Wold and Waddell (1994), and Wold, Thomas, and Waddell (1997).

Water temperatures in the lake vary from below freezing in the winter to more than 80 °F in the summer (U.S. Geological Survey – unpublished data). Annual mean water temperature was greatest in July–August (25.8 °C, 78.4 °F) and lowest in January–February (1.5 °C, 34.7 °F) (Belovsky and others, 2011).

1.7 Organization of Dissertation

This dissertation is separated into six chapters and a series of appendices. The chapters progress from introductory materials that cover the purpose and scope of the research and background information on Great Salt Lake, through methodologies, methods of investigation, the examination of the environmental factors that may play a role in microbial bioherm occurrence or distribution, to analyses, results, and conclusions. Supporting information is contained in appendices.

Chapter 2 provides a brief overview of research on Great Salt Lake and Lake Bonneville and includes a summary of the geologic, paleoenvironmental, and modern histories of the lake based on published literature. An additional section is specifically included at the end of Chapter 2 in order to tie this research to the greater body of literature regarding microbial bioherm research.

Chapter 3 addresses the methodology developed for this research and methods employed to locate and analyze the occurrence and distribution of microbial bioherms in Great Salt Lake. It covers the processes and justifications for utilizing the specific equipment and methods used in the investigation. Specific techniques employed in the methodology include an initial benthic classification based on rugosity, quantification of that rugosity using a method that calculates both a rugosity value and an average position for the rugosity value, the use of geophysical techniques in verification of that classification, and the types of analyses used to determine bioherm distribution. Additional analyses address the relations between microbial bioherm distributions and small-scale topographic offsets related to tectonism and the effects of the rock-filled causeway on the microbial bioherms. Examples of imagery and information gathered as part of this study are included in multiple figures.

Chapter 4 discusses the application of spatial and aspatial tools in the analysis of data. This chapter includes techniques of analysis, including the use of rugosity to establish the spatial extent of the microbial bioherms in Great Salt Lake, analysis of subsets of the rugosity data to examine statistical variability of the data, application of spatial statistics to determine if bioherms in Great Salt Lake are randomly distributed, use of side scan sonar and CHIRP geophysical data to verify the occurrence and spatial distribution of the bioherms, and the examination of ancillary data to determine if microbial bioherm distributions are influenced by physical or chemical changes in the environment. Although analyses, and results of those analyses, are intricately intertwined, results of the analyses have been moved to Chapter 5 for clarity.

Chapter 5 contains the results of the analyses introduced in Chapter 4. This chapter presents the analytical results of spatial and aspatial statistics used in examining the randomness of the microbial bioherm population in Great Salt Lake, the influence of tectonism on the spatial distribution of bioherms, and the effects of salinity changes on bioherm characteristics. Additional information regarding observations of linear patterns of bioherms and their probable controls, along with biological activity associated with the bioherms are included in this chapter.

Chapter 6 is a review of the major implications of the dissertation and the unique contributions of the study of microbial bioherms distribution, influences on those distributions, and the use of spatial statistics in quantifying the randomness of the microbial bioherm population in Great Salt Lake. A discussion on the apparent age of the microbial bioherms is included in this chapter along with a summary discussion addressing the research questions used to guide this investigation. Chapter 6 also concludes if evidence generated using the defined methodology fulfills the objectives of the study.

Numerous supporting documents have been included in the series of six appendices at the end of this report. They include a supporting table with supplemental references, additional information on the specific equipment utilized in the investigation, and limitations to using rugosity as a surrogate for determination of microbial bioherm occurrence.

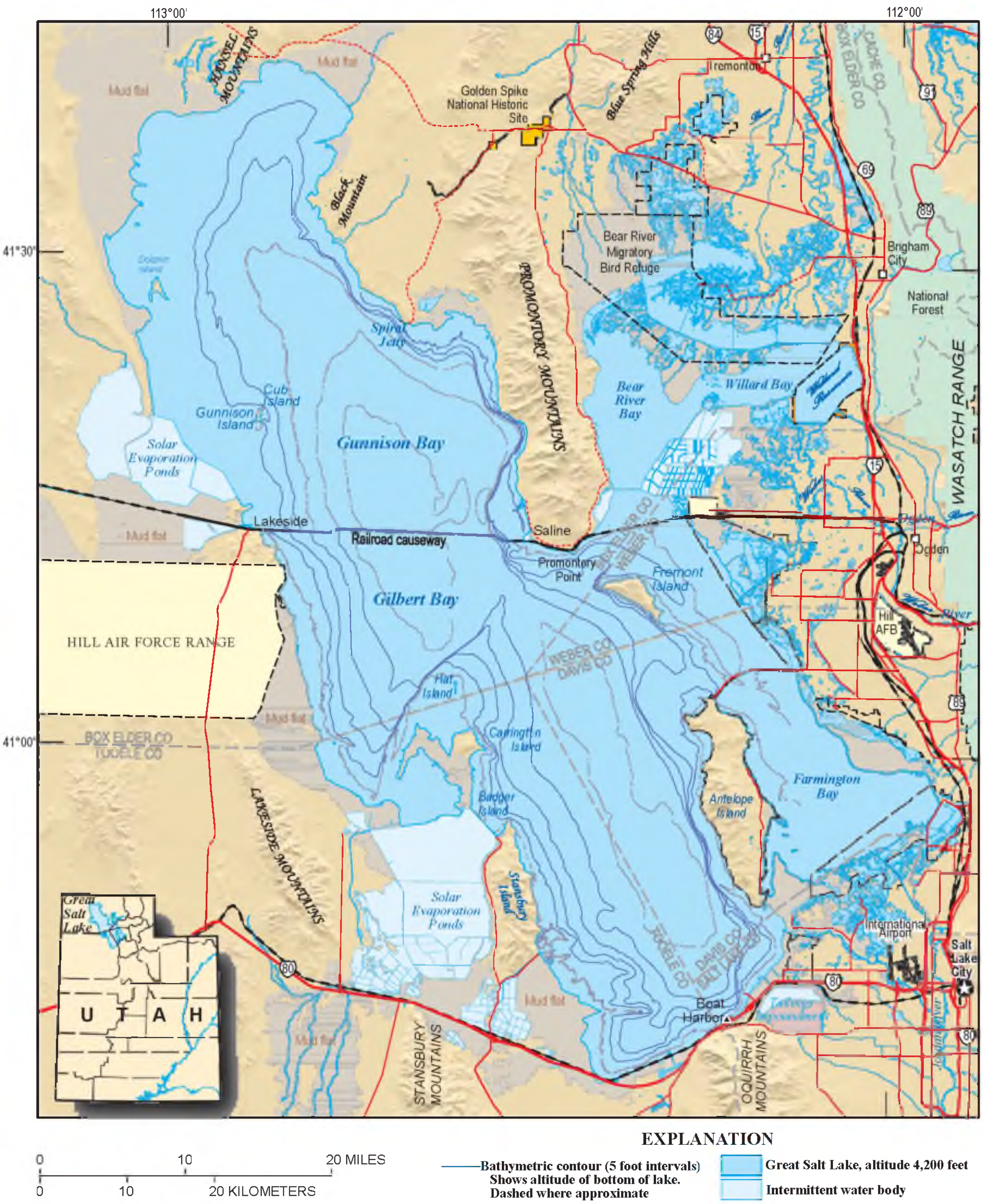

Figure 1. Great Salt Lake, Utah, and vicinity.

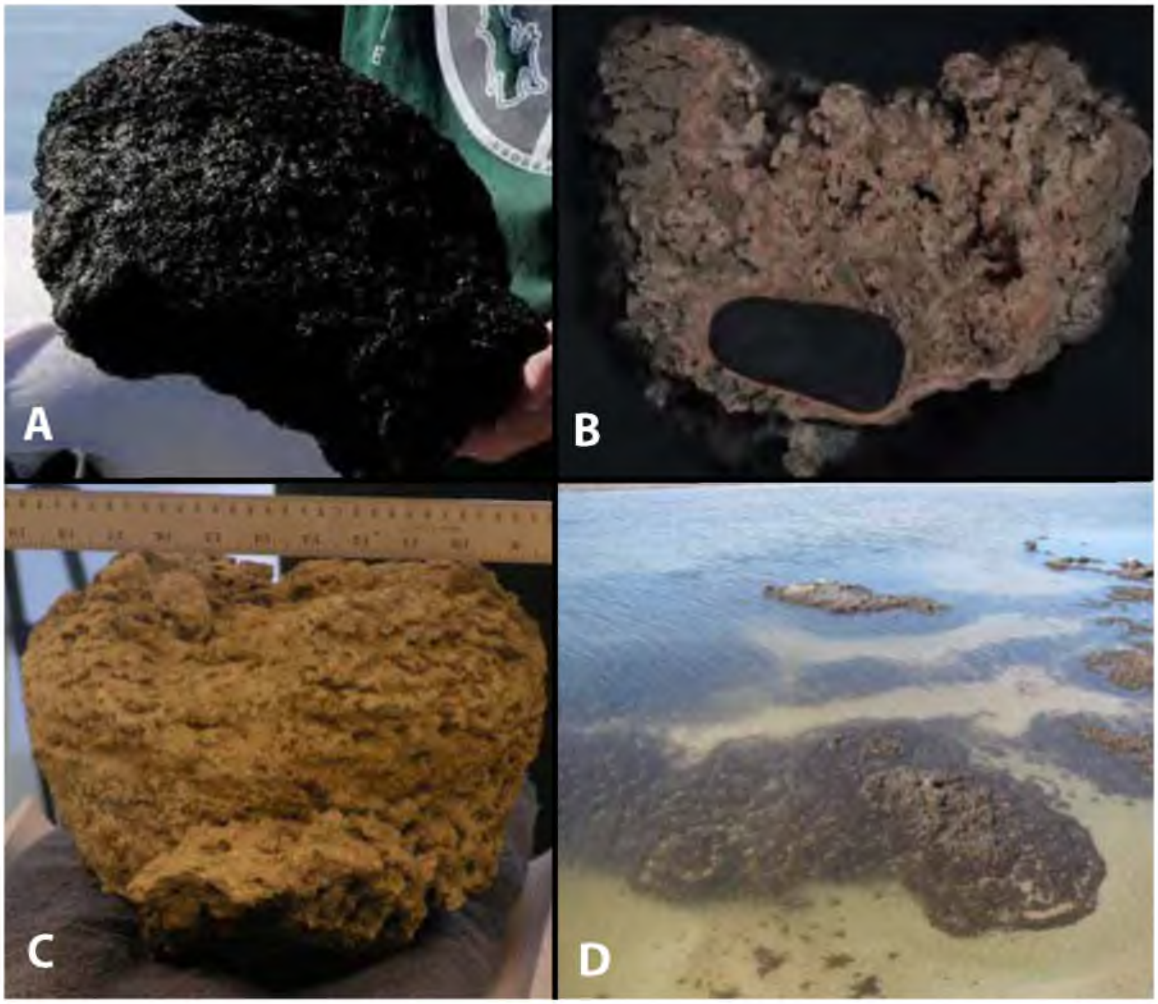

Figure 2. Microbial bioherms from Great Salt Lake, Utah: A. Sample from benthos west of Fremont Island. Dark color is from abundant phototrophic cyanobacterial community on exterior of bioherm; B. Cross-section showing interior fabric of microbial bioherm; C. Bioherm recovered from area east of Hat Island. Bioherm has been dried and cleaned for examination of fine-scale roughness; and D. Exposed bioherms along the margins of Bridger Bay.

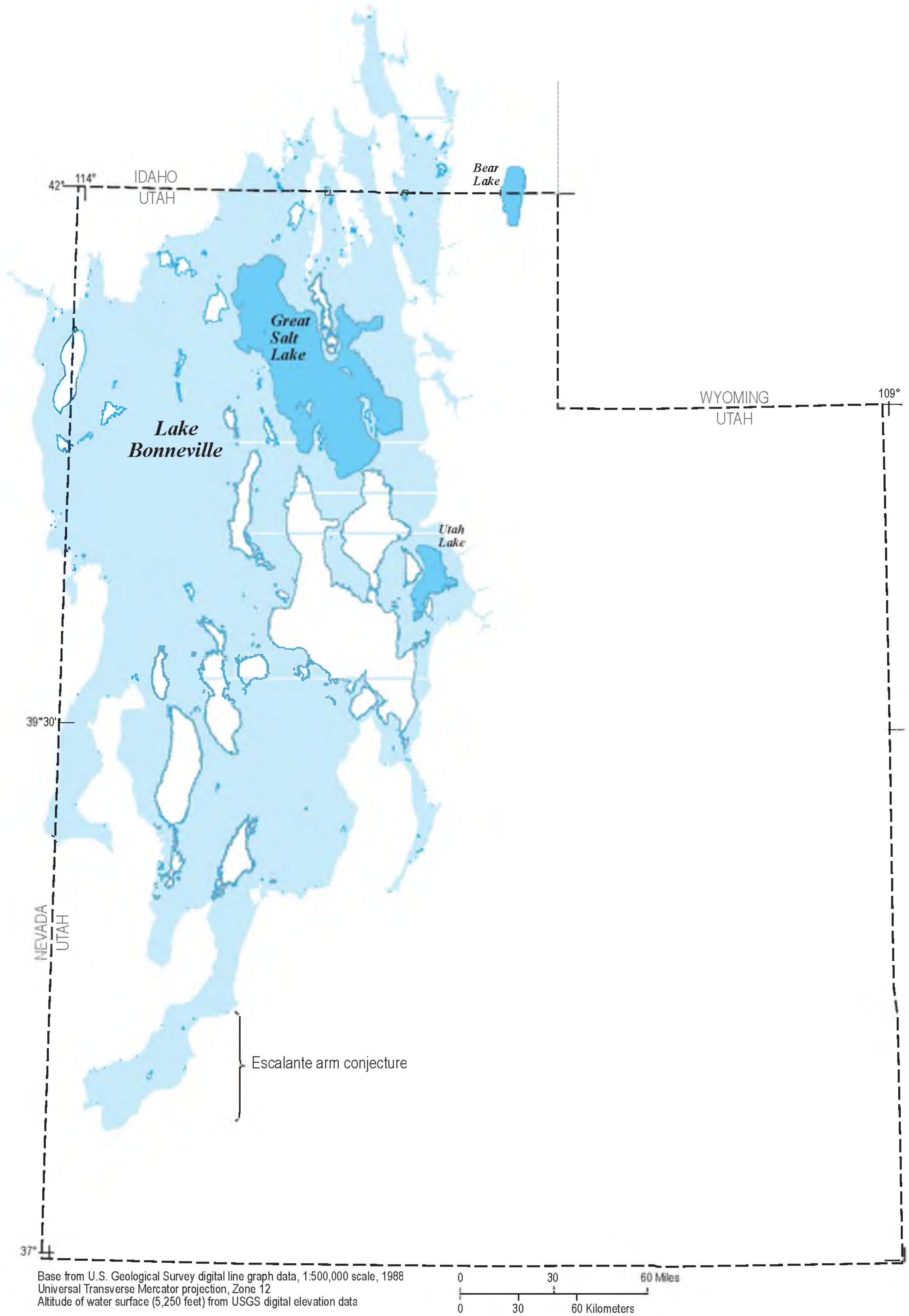

Figure 3. Approximate extent of Pleistocene Lake Bonneville, Utah, Idaho, and Nevada.

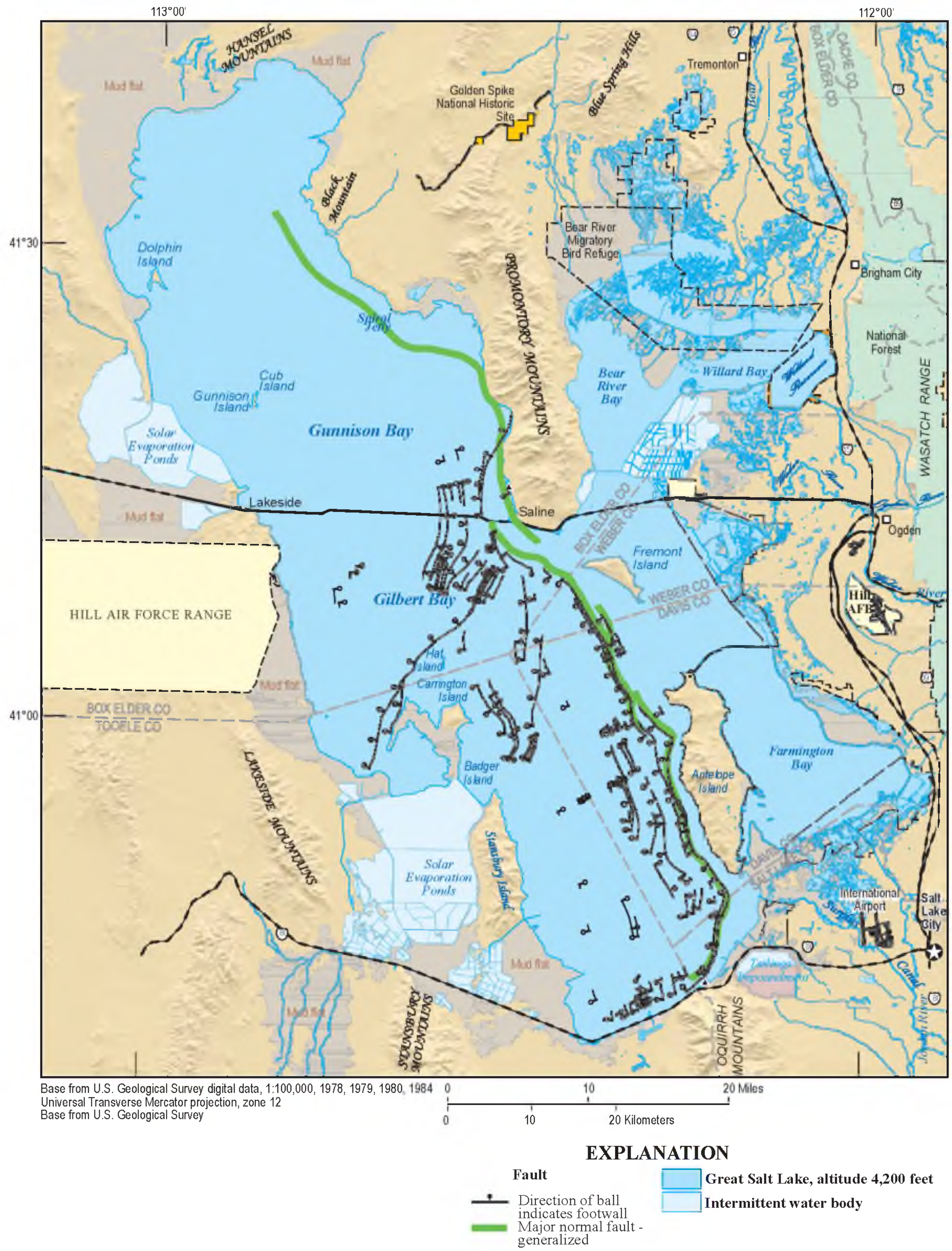

Figure 4. Mapped fault locations beneath Great Salt Lake, Utah (D. Dinter, written commun., June 2014). Locations approximated.

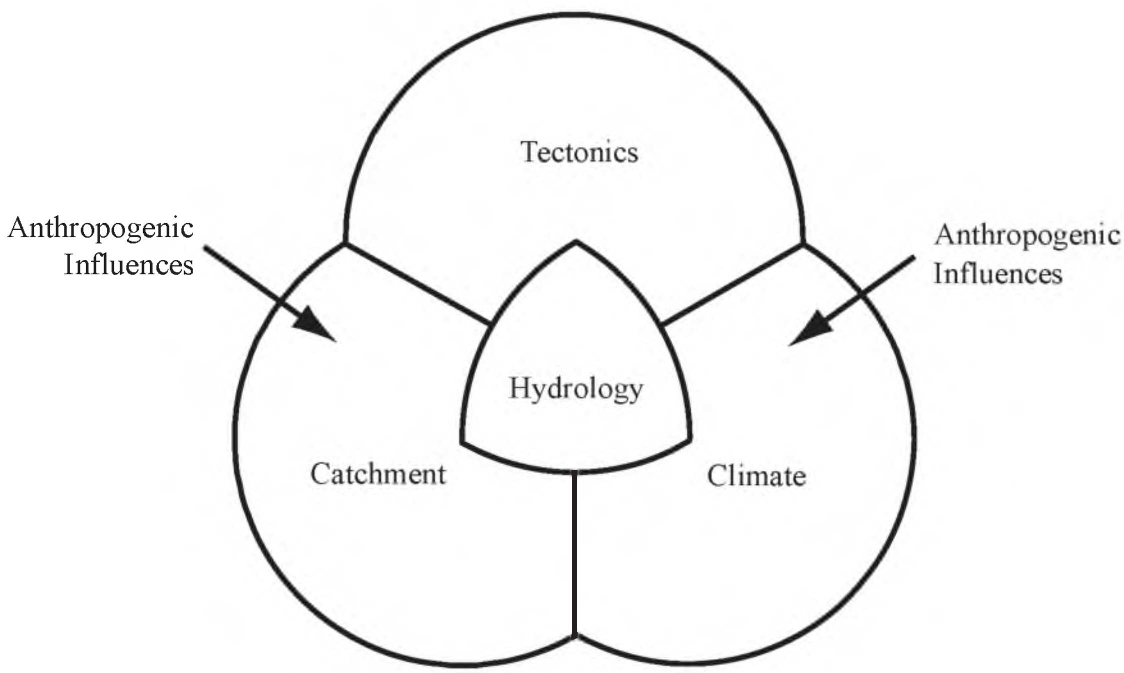

Figure 5. Major factors influencing the hydrology of Great Salt Lake, Utah.

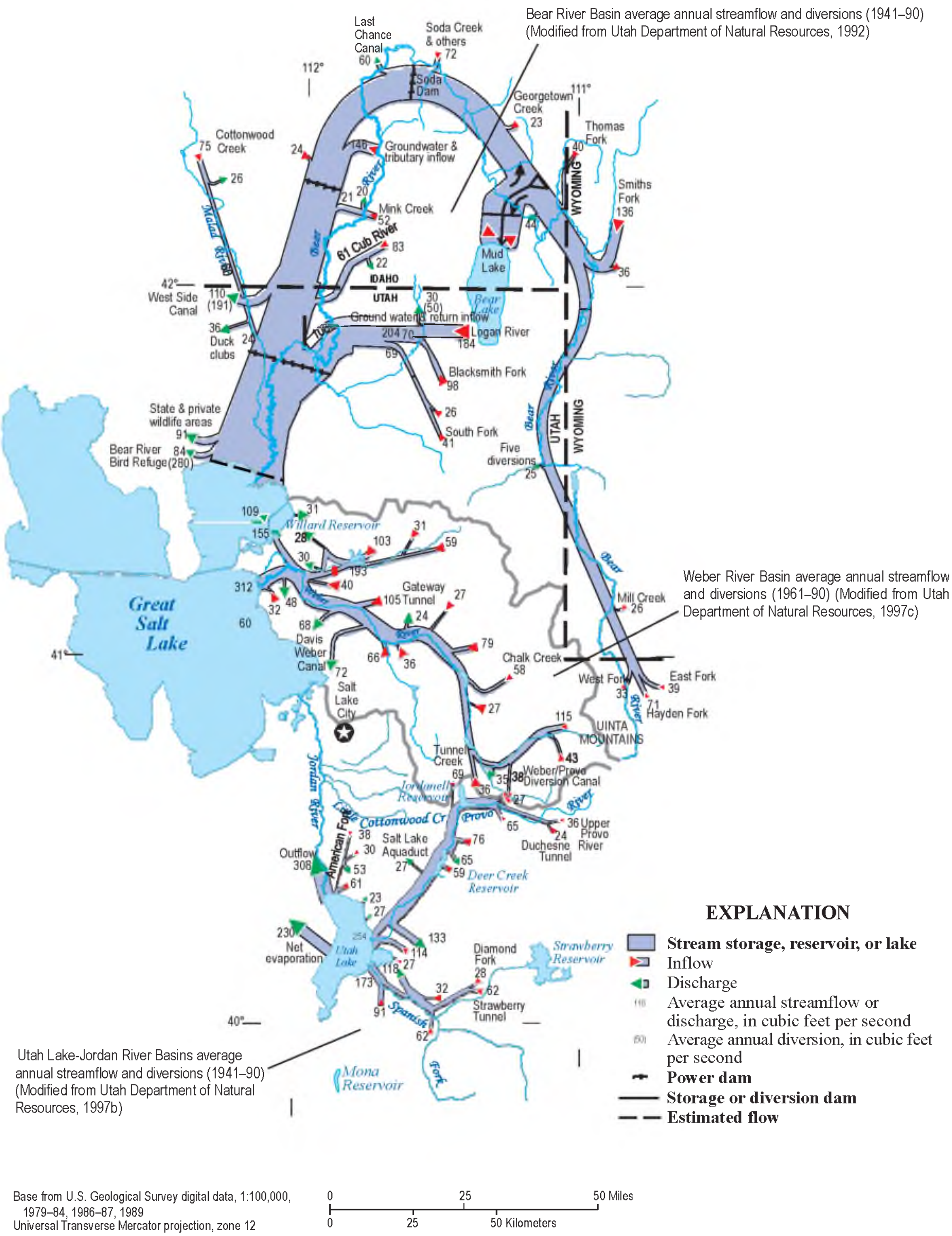

Figure 6. Major catchments and river inflows into Great Salt Lake, Utah.

Figure 7. Shaded digital elevation model of portion of Great Salt Lake bathymetry showing fault-controlled offset connecting Hat Island with Promontory Point, Great Salt Lake, Utah.

Figure 8. Natural-color satellite image of Great Salt Lake, Utah. Image shows change in lake color due to salinity-induced differences north and south of the rock-filled causeway (NASA ISSO7-E-13002, 19 August, 2003).

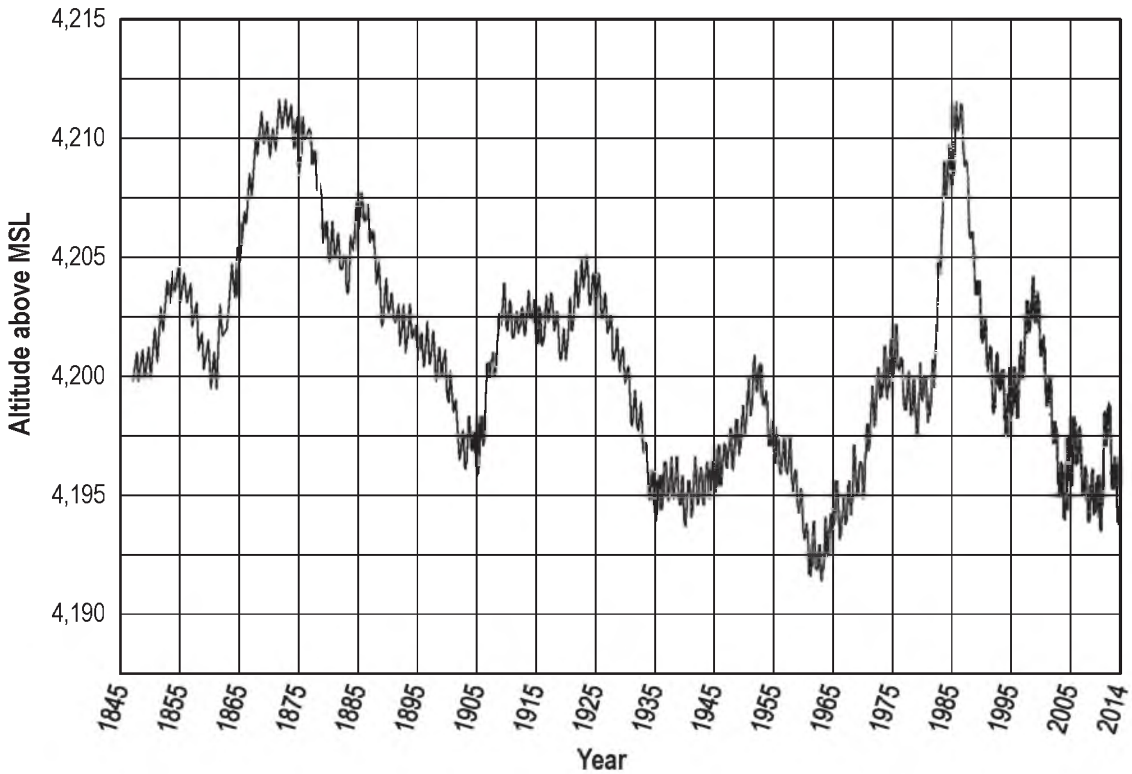

Figure 9. Historical variations in the water surface altitude of the south part of Great Salt Lake, Utah.

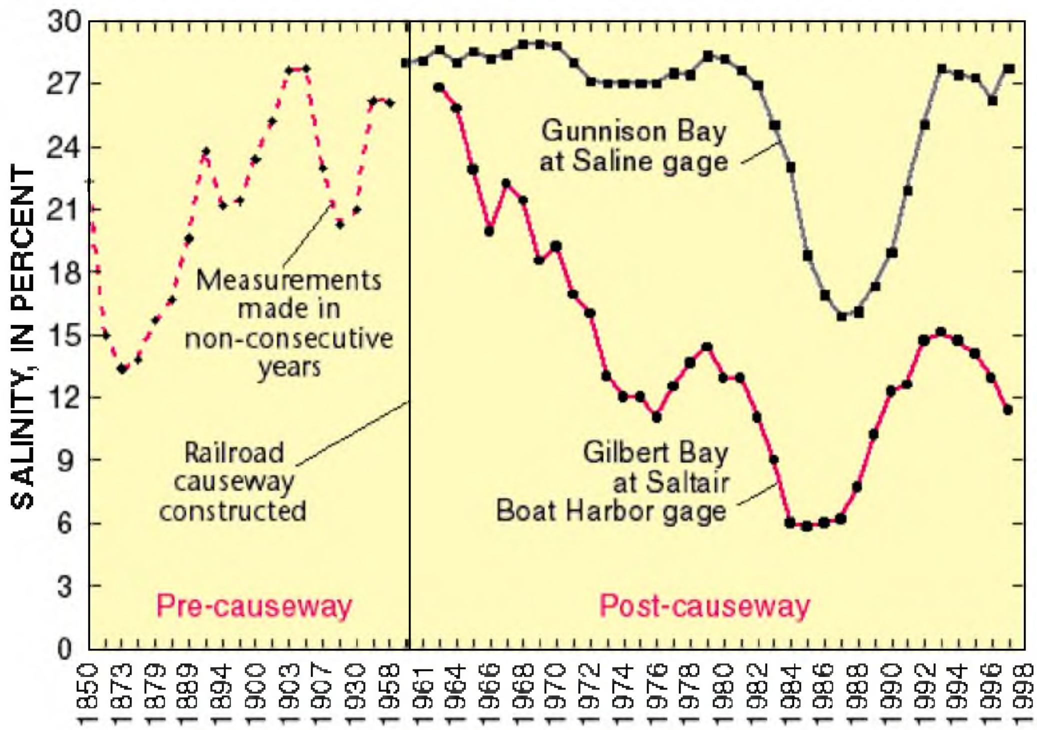

Figure 10. Pre- and postcauseway salinity concentrations in Great Salt Lake, Utah. Note differences in salinity between the north (Gunnison Bay) and south (Gilbert Bay) parts of Great Salt Lake after completion of the rock-filled causeway. Date scale is variable.

CHAPTER 2

REVIEW OF RELATED LITERATURE

2.1 Research History of Great Salt Lake/Lake Bonneville

While there are a large number of publications on Great Salt Lake and Lake Bonneville, there exist only a handful of investigations related to the benthic zone of Great Salt Lake and only a few specifically targeted at microbially formed structures within the lake. Research on the sediments of Great Salt Lake includes that of Eardley (1938, 1952, 1960, 1962a, 1973), Carozzi (1957, 1962), Halley (1976, 1977), Grim and others (1960), Pedone and Dickson (2000), Pedone and Folk (1996), Sandberg (1975), Spencer and others (1984), and Baskin and others (2005a, b and 2006a, b). Only Eardley (1938), Halley (1976), Baskin (2005, 2006), and Baskin and others (2005, 2006) have attempted to look at the entire lake and variations in the characteristics of the benthic zone. Recent efforts by Wurtsbaugh (2009, 2011) have looked at specific characteristics of microbial bioherms along the eastern edge of Great Salt Lake but have primarily focused on the capability of bioherms to sequester mercury, selenium, and other contaminants. Dinter and others (1999, 2000) and Colman and others (2002) have looked at the subbottom characteristics of Great Salt Lake in an attempt to reconstruct the paleoseismic history of the area. Reconstruction of paleoenvironmental conditions in and around the lake has been done by Oviatt (1994, 1997, 1999, 2003, 2005), Balch and others (2003, 2005), Broecker and Kaufman (1965), Benson and others (1990, 1992, 2011), Eardley (1960), Spencer and others (1984), Kowalewska and Cohen (1997), and many more. No other research on the characteristics of the benthic environment of Great Salt Lake has been located to date.

2.1.1 Literature Specific to Great Salt Lake

The earliest published work on Great Salt Lake containing specific information on the benthic environment of the lake is by Eardley (1938). His paper, published in the Journal of Geology, describes the sediments of the lake and contains a generalized benthic characteristics map along with detailed mineralogical analyses of the mud. In the most extensive study of the sediments of Great Salt Lake to date, Eardley discusses the distribution of specific substrates along the more shallow regions of Great Salt Lake and supplies a generalized map of their distribution. The majority of the paper focuses on the origin, chemistry, and life of Great Salt Lake together with the topography and hydrography of the region. Eardley's paper includes discussions about lake chemistry, chemical precipitates, physical properties of sediments, petrography, and diagenesis. Eardley focuses primarily on the distribution, petrology, and chemistry of the clays found in the lake and examines some of the oolitic sands in detail. There is little discussion of microbial bioherms or "calcareous algal bioherms," as Eardley reports. The paper concludes with a survey of the lateral variations of the sediments, the burial of the islands, and the associated structures in the process of formation. In this paper, Eardley (1938) published the first known map of sediment distributions in Great Salt Lake and included "calcareous algal bioherms, oolites, lake clays and valley alluvium, and bedrock – generally mountainous areas" in his classification. He limits their occurrence to "be 100 mi^2" with a "fair degree of accuracy."

Carozzi (1957, 1962) examined the distribution of oolites in the lake (1957) and the general morphology of biostromes near Promontory Point (1962). In his 1962 paper, Carozzi presented a detailed description of algal biostromes in the shallow area just south of Promontory Point. He concluded that the biostromes of Great Salt Lake are confined to shallow waters and shore areas, have an extent of "over 100 mi^2," and do not extend deeper than 10–12 feet. He also limited their occurrence to the western part of the lake. Carozzi (1962) utilized the same classification map as Eardley (1938), separating the sediments into four groups. The only difference between the classifications entailed Carozzi's use of the term "calcareous algal biostromes" instead of Eardley's "calcareous algal bioherms." Carozzi mapped a small section of nearshore deposits adjacent to Promontory Point and described their distribution and morphology as being a direct function of shore-line features and erosional processes due to wave action along the shore. He concluded that the algae do not have any characteristic growth pattern of their own and that the morphology of the structures is controlled by erosional channels trending at right angles to the shoreline. Though Carozzi's investigation reported on only the one locality at Promontory Point, he commented that the biostromes examined elsewhere in the lake "displayed consistent and definite morphological patterns which appeared as a direct function of shore-line features."

Grim and others (1960) examined the clay mineralogy of the sediments of Great Salt Lake, the Great Salt Desert, and the terraces of Lake Bonneville. His results showed that clays of post-Provo age, the Alpine and Provo age, and early Pleistocene have distinctive clay-mineral compositions and that only the post-Provo clays are similar to those of the modern Great Salt Lake. Although not directly applicable to this research effort, the mineralogy of clays trapped within microbial bioherms may provide information to assist in age dating the deposits.

Halley (1976, 1977) looked at textural variations of microbialites (1976) and ooid fabric and fracture patterns in the lake (1977). Halley also utilized Eardley's map showing the extent of the "aragonite algal mounds"; however, he reported an extent of only 100 km^2 (vs. Eardley's 100 mi^2 - (259 km^2) – which is perhaps a misread of Eardley's report or typographical error). Halley characterized the fabric of the algal mounds as being formed by a framework of aragonite precipitates characterized by various morphologies, internal sediments, and inorganic cements. He suggests that the varying fabrics are a function of local and periodic variations in brine concentration. Halley's (1977) publication on ooid fabric and fracture compared the ooids from Great Salt Lake with ooids from other locales around the world in an effort to determine possible processes of ooid formation. Among other conclusions, Halley's research suggested that biological processes are unimportant in ooid formation in Great Salt Lake and that the presence of broken ooids in ancient deposits may indicate nonmarine salinities if they comprise more than 1 percent of the grains in an oolite.

Spencer and others (1984) utilized a variety of approaches to study the history of the Great Salt Lake including sediment cores, acoustic stratigraphy (seismic reflection), sedimentologic analysis, mineralogy, geochemistry, paleontology, and pollen analyses. During collection of cores, and in the acoustic seismic records, Spencer identified "biohermal mounds and ridges" in the vicinity of Carrington Island and carbonate pavements between Carrington Island and Promontory Point. These "biohermal mounds and ridges" correspond with Eardley's areas of calcareous algal bioherms for the

Carrington Island area; however, the carbonate pavements mentioned by Spencer are not included in Eardley's original map. In the limited acoustic data provided by Spencer, he observed that "many bioherm mounds coincide with fault traces. The mounds also seem to be rooted in a reflector located approximately 2 m below bottom …" in areas where the "reflector indicates a buried strand line at about 1,275 m." Spencer's observations concur with the findings in this investigation.

Pedone and Folk (1996) and Pedone and Dickson (2000) performed petrographic analyses and strontium isotope ratio analysis on tufa mounds along the margins of Great Salt Lake. Pedone and Folk (1996) discuss the idea that nannobacteria may be the primary catalyst for formation of carbonate minerals, specifically aragonite. Their paper attempts to identify microscopic spherical objects in carbonate minerals in Great Salt Lake and use their occurrence to support the theory of the existence of nannobacteria and their role in carbonate precipitation. Pedone and Dickson (2000) investigated the mineralogy and petrology of a large tufa deposit located near Lakeside, Utah, along the western shore of Great Salt Lake and focused on crystal morphology, dolomitic composition, and formation of the tufa fabric. Characteristics of this deposit are morphologically different than the smaller apparently biogenically mediated forms investigated in Eardley and Carozzi. Tufa deposits studied by Pedone and others are crudely layered carbonates, cover an area of greater than 100 m^2, and are more than 2 meters thick. In contrast, the "calcareous algal bioherms" mapped by Eardley in 1933 are described as distinct, +/- 1-meter-sized structures located in subaqueous shallow areas of the lake that cover "100 mi^2." Pedone and Folk (1966) report that the bioherms are confined to shallow areas near the shore where there is strong wave activity and water circulation and at depths from 5 cm to 3.7 m.

Sandberg (1975) studied the mineralogy of oolitic sands found along the margins of the lake and contests the notion that the fabric of oolitic sands in Great Salt Lake is a function of diagenesis. He compares ooids from Great Salt Lake with the textural and mineralogical properties of altered shells to provide an indicator of original mineralogy. Using several hundred SEM examinations, he concludes that modern aragonite needles are largely algal in origin. Sandberg challenges Halley's assertion that biological processes are unimportant in ooid formation in Great Salt Lake.

Post (1977) noted that, "algae belonging to the cyanophyta grow in reeflike bioherms or biostromes in the south end" of the lake. "These consist of calcium carbonate precipitated around cells of Oscillatoria sp. and Coccochloris elebans to form domelike structures. The bioherms also occur in the north arm but may or may not be active as a result of the high salinity."

Coleman and others (2002) briefly discuss the presence of bioherm structures present above some faults and the fault-controlled ridge connecting Carrington Island and Promontory Point. Data used for the Coleman and others effort included the data discussed in Spencer and others (1984) and new data acquired in 1977 along the same transects but using different seismic data acquisition parameters.

Recent research efforts on Great Salt Lake specifically regarding microbial bioherms and the chemical environment of Great Salt Lake are being conducted by Della Porte (2011), Frank (unpublished), and Harris, Ellis, and Purkis (2012).

2.1.2 Literature Specific to Lake Bonneville

The sedimentology, chronology, and paleoenvironmental conditions of Lake Bonneville are generally well established because research in the Bonneville Basin has been a focus of research since G.K. Gilbert (1875, 1882, 1886, 1890).

Paleoenvironmental reconstructions of the Bonneville Basin began as concentrated research efforts on outcrops and geomorphic features surrounding Great Salt Lake and expanded to analyses of sediment cores and the inclusion of acoustic subbottom seismic data. Although the majority of investigations have focused on the Quaternary history of the basin, the acquisition and analysis of longer cores have extended the reconstruction of paleoenvironments for the Bonneville Basin to approximately the last 5 million years (Kowalewska and Cohen, 1998) with varying degrees of temporal resolution. Information about the sedimentology, chronology, and paleoenvironmental conditions of the Bonneville Basin can be found in publications from Gilbert (1875, 1882, 1886, 1890), Eardley and Gvosdetsky (1960), Eardley and others (1973), Spencer and others (1984), Morrison (1966), Kowalewska and Cohen (1998), Oviatt and others (1990, 1992, 1994, 1997, 1999, 2002, 2003, 2005), Sack (2009), Balch and others (2003, 2005), Colman, Kelts, and Dinter (2002), Godsey (2005, 2005a, 2011), Benson and others (1990, 1992, 2001), and many others.

2.1.3 Literature Specific to the Use of Rugosity in Marine Studies

Depth and structural complexity (roughness, rugosity) in marine environments are indirect environmental factors that play fundamental roles in macrobenthic and fish species richness and abundance (Gray, 1974) and are a common measure in coralline environments (Brown and others, 2004). Rugosity also plays an important role in substrate characterization methodologies including acoustic response analysis (ARA), E1/E2 sonar echo comparison techniques (RoxAnn method), echo shape analysis (QTC method), and other benthic classification systems (Penrose and others, 2005). Patterns of benthic roughness can infer presence or absence of bioherms and, when combined with other environmental information, the processes responsible for the occurrence and geographic distribution of the bioherm population.

Accurate measurement of one-dimensional rugosity of a marine benthic surface historically involves the use of divers using a chain-tape technique (Risk, 1972), falling-rod gauges (Leatherman, 1987), or molds (Sanson and others, 1995), although recent quantitative measures such as microtopographic laser scanning (DuPreez and Tunnicliffe, 2012) and stereo image reconstructions (Friedman and others, 2012) are now being used in high-visibility waters. The chain-tape technique calculates the ratio between a straight distance measured over the top of a surface to the distance measured along the bottom surface (using a flexible measure), accounting for all of the small-scale variations in the actual surface (Risk, 1972). These traditional methods are labor intensive, depth limited, and subject to changes in environmental conditions such as visibility, current, or wave action, which could compromise diver safety. Measurements generally are obtained using self-contained underwater breathing apparatus (SCUBA) in less than 30 m of water, which means that the majority of marine habitats cannot be described by using the chain-tape technique. Additionally, the output of measured transects using this traditional approach are calculated at a single, predefined resolution and at scales imposed by set vertical measurement distance, by transect length, and by the ability of the diver. As a result, marine rugosity surveys tend to be spatially limited to near-shore areas where environmental conditions allow the use of divers.

The development of optical imagery such as airborne bathymetric Lidar for application in determining benthic roughness continues to evolve (Irish and Lillycrop, 1999; McNair, 2010). However, many of these techniques are not suitable for use on Great Salt Lake due to refraction issues, the degree of roughness being investigated, and optical visibility through the water column.

Alternative efforts have been tested to investigate the possibility of deriving rugosity measures from bathymetric maps generated from ship-borne surveys (Becker and Sandwell, 2008; Moyer and others, 2003). However, these methods do not resolve fine-scale structure due to the general limited spatial resolution of the survey data and are not appropriate for use on Great Salt Lake.

2.1.4 Literature Specific to Microbial Carbonates

Microbial carbonates dominate the marine carbonate sedimentary record back to Archaen time (3,430–3,500 million years ago) (Awramik, 2006; Schopf, 2006), but are also major features of many saline and alkaline lake deposits (Tucker and Wright, 1990). Modern marine occurrences, such as Shark Bay, Australia (Papineau and others, 2005; Jahnert and Collins, 2011), and the Bahamas (Baumgartner and others, 2009; Bowlin and others, 2011), have provided some insights into the controls on the distribution and morphology of microbial carbonates, as have some modern lakes (Brady and others, 2010; Last and others, 2010).

Great Salt Lake is one of approximately six known areas in the world with an extensive microbial carbonate population: Bahamas (Dix and others, 1999; Bowlin and others, 2011), Belize (Rasmussen and others, 1993), Lake Tanganyika (Cohen and others, 1997a,b), Australia (Papineau and others, 2005; Jahnert and Collins, 2011), Antarctica (Parker and others, 1985), and Great Salt Lake (Eardley, 1938)). Large-scale laminated microbial buildups (commonly referred to as stromatolites) reported in the literature are included in Appendix E. Appendix E provides an overview of the reported environmental conditions identified in the literature as possibly influencing "stromatolite" formation and provides locations for known microbial carbonate deposits. Nonstromatolitic forms of biogenic carbonates remain in the table to provide additional environmental information on related forms of microbially mediated deposits.

The ability of microbial bioherms to actively grow (net accumulation of $CaCO_3$) depends on the balance of both chemical control/biological activity and the ability of the bioherm forming microbial communities to outperform competing biota. Microbial carbonates and the associated bioherm-forming communities dominated carbonate platforms during the late Archaean and Proterozoic, prior to the development of metazoans, yet are presently confined to only a few locations (Awramik, 2006). Although the direct connection between metazoan diversification and microbialite decline in the rock record is tenuous (Riding, 2006), there is evidence that metazoan diversification coincided with at least some of the recorded microbialite declines (Schubert and Bottjer, 1992; Bottjer, 1996). Despite the extensive literature on the connection between the development of higher life forms and the decline of microbialites, reef-like occurrences of microbial bioherms occur throughout the rock record, many coexisting with grazing and burrowing organisms formed in seas of varying marine salinity (Pratt, 1982; Knauth, 1998; Arp and others, 1999).

Examination of modern occurrences of bioherms show that environmental conditions in Great Salt Lake provide the appropriate conditions for growth. Grazing and competition for resources are limited by hydrodynamic (including sediment movement and deposition) and chemical controls (salinity concentrations) (Appendix E). Grazers such as herbaceous gastropods, burrowing invertebrates, and brine fly larvae are found in modern bioherm environments (Walter and others, 1973; Elser, 2005; Breitbart and others, 2009; Belovsky and others, 2011) and use benthic microbial communities for food. Nearly all of the modern environments supporting bioherm growth are void of grazers; however, those environments that support grazers exhibit no serious degradation of productivity or growth except in the case of grazing herbivores, such as cerithid gastropods (Garrett, 1970). Grazers and competition from autotrophs in the majority of locations are limited by both microbial effects (the presence of EPS or carbonate sheaths preventing or inhibiting microbial competition) and environmental controls. High sedimentation rates, strong tidal currents, and seasonal hypersalinity in the Bahaman stromatolites (Baumgartner and others, 2009) and Sharks Bay (Logan, 1961) prevent grazers from populating the bioherms in those locales. Low nutrient levels limit the snail populations in Laguna Bacalar (Gischler and others, 2011), and high salinity levels in the majority of locations limit the size and type of competition available.

The ability of bioherm microbial communities to outperform the competition is a function of their high surface area, high productivity, and ability to exist in competition-limiting environments. Even in Great Salt Lake where brine fly larvae are perhaps the most widespread and numerous of the biotic grazers, their effect on microbial bioherm production is limited by the high primary productivity (145g C/m2 – Stephens and Gillespie, 1976) of the microbial community.

2.2 Terminology

Carbonate organosedimentary structures are the oldest known evidence of life on earth and the organisms responsible for their formation are the ancestors of all complex plants and animals on earth today (Walter, 1976). The terminology used to define these structures has been in contention since their discovery as the external morphology of the forms necessarily does not reflect their internal fabric or composition. Compounding the difficulty in standardizing the terminology is the ability of mixed fabrics to be present in a single structure. Without physically sampling, breaking or cutting the sample, or using modern nondestructive examination methods such as computed axial tomography (CT or CAT scan), one cannot outwardly determine if the internal fabric is a laminated stromatolite, a clotted thrombolite, or some other microbial fabric.

Variations in terminology used to describe and classify microbial carbonate structures are based on the author's background and include such terms as bioherm, biostrome, algal mound, stromatolite, tufa, travertine, microbialite, and microbial reef. Similar morphologic forms may be classified as a variety of terms. Although the chemical mechanisms for forming "microbial" structures may be similar, the classification terminology is far from settled. Travertines and similarly formed sedimentary structures generally are associated with areas of ground-water inflow or areas where waters of differing chemical quality mix and nonbiologically mediated chemical reactions precipitate calcium carbonate. Tufa, a cool-water calcium carbonate precipitate (Glover and Robertson, 2003), occurs globally in waters enriched in dissolved calcium carbonate and is generally microbially mediated (Pedley, 1990). Bioherm, stromatolite, microbialite, and other microbial-related designations appear to have similar biological communities and calcium carbonate precipitation is biologically influenced. Actual morphological characteristics and controls over microbial bioherm growth may vary widely. Additional information on the development and history of the terminology can be found in Rezak (1957) and Riding (2011).

Many classification schemes have been developed over the years with varying degrees of adoption by other authors. Most classification schemes utilize some combination of the gross form of the occurrence, nature and orientation of the laminae (if present), and location of the occurrence as it relates to substrate and bathymetric position. Rezak (1957), Logan and others (1964), and Jahnert and Collins (2012) are three of the many researchers who have devised classification schemes for microbial formations. One of the most recent classification schemes (Janhert and Collins, 2012) attempts to quantify the usage of terminologies used to describe microbial carbonate deposits as to avoid future confusion when discussing forms with similar morphologies but different internal textures. Jahnert and Collins (2012) base their classification of microbial deposits on location within biotic zones and external organofacies, composition, and morphologies, while Logan and others (1964) used a descriptive classification based on the arrangement of the basic hemispheroid shape.

Although a variety of microbialite morphologies and fabrics occur in and beneath Great Salt Lake, the term “microbial bioherm” is used in this manuscript to describe the specific benthic-based meter-scale forms mapped during this investigation. Microbialite represents a generic term for organosedimentary deposits that are a result of benthic (prokaryotic or eukaryotic) communities trapping and binding detrital sediment and/or forming the locus of mineral precipitation (Burne & Moore, 1987). Stromatolites, thrombolites, etc., are specific forms of microbialites and can present in a variety of morphologies and type. References to microbial bioherm survivability, growth, and other inferences of life related to the bioherms refer to the carbonate-fixing microbial communities associated with bioherm formation.

CHAPTER 3

METHODOLOGY

3.1 Introduction

The development of an appropriate research methodology to study the occurrence and distribution of microbial bioherms in Great Salt Lake involved: 1) defining the research questions and primary objectives of the study, 2) examining existing data and additional data needs that address the specific processes that ultimately influence microbial bioherm occurrence and distribution, and 3) identifying appropriate methods of analysis for the types of data utilized in this research. Although previous observations on Great Salt Lake imply that the distribution of microbial bioherms is nonrandom, a quantitative examination of this issue has not been conducted heretofore.

The methodology developed for this investigation is a process based on a methodological naturalistic approach to understanding the occurrence and spatial distribution of microbial bioherms in Great Salt Lake. Assumptions as to the behavior of specific properties of water, sediment, and biological activity in Great Salt Lake are based on well-substantiated behaviors of those properties in marine environments and are assumed to be repeatable given identical conditions. The methodology defines the logistical structure and progression of activities used to link the physical factors of bioherm formation with spatial patterns of bioherms in the GSL as they are apparent using marine acoustic remote sensing techniques (Fig. 11).

3.2 Research Questions

This research effort is based on three questions about microbial bioherms in Great Salt Lake.

Question 1 - Are microbial bioherms in Great Salt Lake, Utah, randomly distributed?

Question 2 - Do environmental factors influence the distribution of microbial bioherms in Great Salt Lake, Utah?

Question 3 - Are the influences of changing environmental conditions preserved in the microbial bioherms found in Great Salt Lake, Utah?

3.3 Linking Patterns and Processes

The lack of widespread occurrences of living bioherm-forming microbial communities throughout the world indicates that suitable conditions for initiation and growth are uncommon in the modern environment. Many abiotic and biotic factors present as both synergistic and antagonistic interactions that influence the initiation, growth, and preservation of microbial bioherm communities. Patterns of occurrence depend upon the presence or absence of specific environmental factors, flux into and out of the lake, and interactions between specific physical, chemical, and biological factors.

Analysis of the geographic patterns of occurrence can provide insights into understanding the underlying environmental processes that influence microbial bioherm initiation, growth, and preservation in Great Salt Lake. However, direct observation of patterns on the lake floor generally are possible only in the shallower regions of the lake where visual inspection is possible. To examine patterns in the deeper regions of the lake, a technique must be used that does not depend on visual observations of the substrate or substrate condition.

Marine-based acoustic survey techniques allow one to identify, measure, and differentiate areas of likely bioherm occurrence at the sediment/water interface and patterns in substrate composition. Acoustically measured substrate roughness (or its calculated derivative – rugosity) can be used as an analogue to define areas of microbial bioherm occurrence and absence. When combined with geospatial reference information, occurrence of various materials at the sediment-water interface can be identified and used in the determination of spatial distribution. By linking structural changes in the lake substrate with patterns of occurrence at the sediment/water interface, one can infer underlying processes that control those patterns and distributions.

Data on recent changes in water chemistry are available for studying the linkages between water chemistry and microbial bioherm condition. Linking changes in water quality with bioherm condition(s) allows one to identify the type and degree of influence those changes have on the health and viability of bioherm-forming microbial communities. Variability in the pattern of microbial bioherm condition over short distances or in areas where physical factors remain constant, infer that a chemical or biological factor has affected the condition of the bioherms.

Due to temporal, spatial, and analytical limits on available data from Great Salt Lake, the nexus between environmental factors and bioherm distributions is limited to significant tectonically controlled structures within the lake and major variations in salinity. The linkage between some selected environmental factors (tectonics, substrate type, hydrodynamic factors, and salinity) and patterns of bioherm occurrence are discussed in the following paragraphs.

3.4 Environmental Relations Influencing Bioherm Distribution

The occurrence of microbial bioherms in Great Salt Lake can be identified in a continuum of patterns ranging from individuals to clustered populations. Examination of these patterns of occurrence can be used to infer environmental processes that inhibit or promote bioherm initiation and growth. Patterns can be the result of controlled (deterministic) or random (stochastic) processes. Where patterns are not the result of a stochastic process, external forces or events influence the distribution of objects that make up those patterns. Occurrence and distribution of microbial bioherms in Great Salt Lake likely are influenced by many of the same forces that influence the long and short-term hydrology of Great Salt Lake (Fig. 5). They are influenced by biological and chemical characteristics of the lake water along with physical conditions related to geographic, geologic, climatic, and hydrologic factors (Fig. 12). Although known factors that affect the initiation, development, and preservation of bioherms can be identified through examination of published and unpublished research, correlations between environmental factors and microbial bioherm distributions in Great Salt Lake are hampered by a dearth of long-term biological and chemical data from the lake. Most occurrences of bioherms throughout the world (Appendix E) are found in shallow, saline to hypersaline, restricted circulation environments where these controls favor the establishment, growth, and survivability of microbial communities that form biogenic carbonates.

Examination of modern occurrences of bioherms (Appendix E) shows that a combination of factors provide the appropriate conditions for growth and limit grazing and competition. Differences in sediment movement and deposition, salinity levels, and saturation of calcium carbonate provide nontectonically related opportunities to examine hydrodynamic and chemical alternatives that may affect microbial bioherm occurrence and spatial distribution.

Environmental factors related to bioherm initiation, growth, and preservation are many. While examination of a single environmental factor may show a strong correlation with bioherm occurrence, many of the factors shown in Figure 12 are interrelated by either causal means or correlated with changes in the primary controls on bioherm formation. Bioherm occurrence relies on a balance of these environmental conditions along with the presence of adequate nutrients, energy, and the introduction of the appropriate microbial community for bioherm production. As microbial bioherms are nonmobile, once established, they cannot change locations if environmental conditions vary outside of their ability to survive within those changing environmental conditions.

3.5 Components of Bioherm Initiation and Growth

Biogenic carbonate formation in Great Salt Lake requires the presence of a stable base on which a bioherm-forming microbial community can initiate and grow. Formation also requires five primary components: water, accommodation space, energy, calcium, and the existence of the carbonate-precipitating microbial community itself. Without a stable base and all five components, biogenic carbonate formation is impossible. The various physical forms and fabrics of biogenic carbonates result from variations in proportions of these five components.

3.5.1 Water Environment

First, water provides both a medium for growth and a transport mechanism for microbes. It carries with it dissolved constituents, organic and inorganic particles, nutrients, and other materials essential for the survival of bioherm-forming microbial communities. As a medium for growth, water's high albedo and its ability to circulate provide a relatively stable thermal environment for microbial growth and survival. Its ability to transmit light allows radiant energy to reach the benthos, supplying energy for photosynthesis.

3.5.2 Accommodation Space

Second, accommodation space is a critical component of both the survivability of a community and the building of large-scale biogenic carbonate formations. This space must contain the basic components for biogenic carbonate formation, appropriate environmental conditions, and nucleation sites. For expansion of the community, new initiation sites must be available within suitable environmental conditions. These can be generated by the addition of new biogenically deposited carbonates, wave and current-induced carbonate precipitation in shallow areas or removal of fine-grained sediments from the substrate, deposition of course fragments of biogenic material abraded from the microbial bioherms, transgressive water level change (including substrate tectonic modifications), and by structural failure or destructional processes along the bioherm itself.

Accommodation space can be affected by a variety of physical factors including variations in water depth, sediment accumulation (including bioherm growth), and tectonic modification of the substrate. Microbial bioherms are accretionary away from a point of origin and subsequently lessen the accommodation space within the water column as they grow. Favorable environmental conditions can increase bioherm growth rates as can the introduction of sediment for trapping and binding processes. However, increased bioherm growth also increases the rate of loss of necessary accommodation space. Increases in accommodation space can occur through erosive processes, increasing water depths (transgression), recurrent slip along faults or folds, progradation, or a combination of those factors. In Great Salt Lake, accommodation space is currently limited by short-term transgressive and regressive variations in hydrologic conditions.

3.5.3 Energy Needs

Third, requirements for growth of the microbial-forming communities in Great Salt Lake include sources of energy, "organic" carbon (e.g. sugars and fatty acids) and metal ions (e.g. iron). While discussion of the processes that cycle energy through bioherm-forming microbial communities is outside the scope of this dissertation, a discussion of the primary source of energy for the microbial communities in Great Salt Lake (solar energy) and its effects on other physical, chemical, and biological factors is necessary. Solar energy affects water temperature, drives photosynthesis, and is the primary controlling factor for life in Great Salt Lake.

Light availability (photosynthetically active radiation (PAR)) in Great Salt Lake is a function of water depth, the chemical composition of the lake waters, particles in and on the water, water-surface conditions, bathymetric position, sun angle, and solar intensity and duration. It is necessary for microbial community growth and can be both synergistic and antagonistic in providing optimal conditions for microbial bioherm formation. For example, in the presence of sufficient nutrients, increasing PAR and water temperature (to optimal photosynthetic conditions) should increase the growth rate and health of benthic photosynthetic communities. However, increasing PAR and water temperature also increases primary productivity in the water column and increases competition by phytoplankton for available nutrients and light. As the population of phytoplankton in the water column increases, there is a corresponding decrease in available nutrients and light, negatively affecting the growth of benthic photosynthetic communities. Solar radiation and its secondary effects affect the solubility of salts, rates of chemical reactions, water density, bioherm growth, movement of brine shrimp, and many other aspects of the environment of Great Salt Lake.

3.5.4 Water Chemistry

Fourth, the chemistry of Great Salt Lake waters is basically a function of climate, basin history, and the geology of the contributing drainage area. The overall concentration of dissolved solids within waters of Great Salt Lake is controlled by the long-term balance of inflow and evaporation. Distribution of salinity within the lake is affected by inflow locations, volume, and dissolved-solids concentrations, by numerous anthropogenic modifications in the lake and along its shores, lake circulation, and by deposition and solution of salts within the lake itself. Water chemistry is critical as it must provide ample dissolved calcium carbonate for bioherm formation, necessary nutrients for growth, trace elements, dissolved gasses, and at the same time provide an environment that shelters the bioherm-forming microbial communities from significant predation and competition – generally through exclusion of other biota. Changes in lake chemistry occur on a continuous basis as the balance between inputs and evaporation is in constant flux.

Fifth, the availability of calcium carbonate ($CaCO_3$) to the bioherm-forming microbial community is critical to bioherm formation. Great Salt Lake is supersaturated with $CaCO_3$ throughout the year and becomes significantly more saturated during the summer months (Corsetti and others, 2013). Increasing the temperature of water decreases carbonate solubility, thereby increasing the saturation state of $CaCO_3$ and promoting carbonate precipitation.

3.5.5 Tectonism, Patterns, and Processes

The bathymetry of Great Salt Lake and its surrounding area is primarily defined by large basin-wide tectonically formed structures. Local perturbations in the bathymetry are the result of small-scale ancillary and antithetical faults, folds, and recent sedimentary deposits. These tectonically induced, localized changes in the bathymetry are directly related to factors that may influence microbial bioherm initiation, growth, and preservation. Localized shoaling of the benthos from the formation of small-scale horsts and grabens may place the benthos within the photic zone and within wave base. This combination of light availability and wave-energy could provide the change in environmental conditions that allow bioherms to develop in such areas. Tectonically induced changes in the bathymetry can modify accommodation space or even expose bioherm communities to increased wave action or subaerial exposure. Abrupt application of tectonic forces such as earthquakes can cause the release of large volumes of sediment, water, and other disturbances to the lake. Although tectonism is a controlling factor for the bathymetry of the lake, changes in environmental factors directly resulting from tectonism can similarly and directly impact the occurrence/nonoccurrence of microbial bioherms in Great Salt Lake.

3.5.6 Hydrodynamics, Patterns, and Processes

Lake elevation and hydrodynamic conditions have both synergistic and antagonistic effects on bioherm initiation, occurrence, and preservation. Transgressive and regressive phases of Great Salt Lake result in vastly differing hydrodynamic conditions (water depth, circulation patterns, wave energy, etc.) and influence lake water chemistry, accommodation space, light availability, sediment influx and reworking, nutrient concentrations and availability, and biological communities. This variability constantly modifies the interplay between the physical, chemical, and biological factors that affect bioherm occurrence and distribution.

Changes in lake level can affect microbial growth in a variety of ways, especially in a closed basin where large seasonal or annual variations in water depth may occur. The effects of changing lake levels on bioherms are site-specific and depend in large part on the bathymetric position of the bioherm deposit. As water levels decrease, the accommodation space between bioherms and water surface lessens and the bioherms are subjected to increasing weathering and erosion from wave action. A continuing drop in water level can result in subaerial exposure, subjecting the bioherm-forming microbial communities to desiccation, predation, weathering, erosion, and extremes in temperature. Rising water levels increase the distance between the bioherms and water surface and subject bioherms to decreasing light availability, changing sediment type and volumes, different energy regimes, and changing lake chemistry.

Fetch distance also increases with rising water levels, generally allowing the transfer of more wind energy to the water and resulting in larger waves, stronger currents, and increases in wave base. Increased energy levels, in the form of waves or currents, may erode fractions of the substrate, removing fine-grained sediments and creating stable substrates for initiation/nucleation of biogenic communities. Waves and currents also affect the delivery and fate of nutrients, calcium, sediments, and other water-borne constituents critical in the microbialite-forming or destructive processes. Increases in wave and current energy beyond the holding capacity of the microbialite structures may limit or prevent preservation by creating a surface on which the microbes cannot adhere or are removed through scouring processes or by removal of the microbial structures through weathering and erosion. These processes may result in short- or long-term effects on the structures and may provide fresh nucleation surfaces for microbial bioherm expansion.

As wave base changes, sediment is eroded, resuspended, and redistributed in the lake. Changes in sediment deposition rate or sediment type may drown bioherm-forming microbial communities or create or expose a stable base on which to initiate new growth. Circulation patterns may change as water depth changes and the influence of bathymetry on circulation becomes more or less pronounced.

3.5.7 Substrate, Patterns, and Processes

Requirements for microbial bioherm formation include both suitable initiation/nucleation surfaces and the availability of accommodation space for subsequent growth of the microbial community. Occurrences of microbial bioherms initiate on nonmobile surfaces where there is sufficient physical support and substrate stability for growth to occur. The majority of modern microbial bioherms are found in areas above wave base where wave energy may provide more stable substrate conditions by reworking sediments and transporting fine-grained sediments lakeward into deeper waters. Influx of sediment during bioherm formation may inhibit or increase growth of the bioherms depending on sediment volume and size. Possible growth inhibition in high sediment deposition areas is supported by observations from ancient bioherm deposits (Johnson and Grotzinger, 2006). In contrast to substrate stability, mineralogy of the substrate does not seem to play a significant role in community nucleation or occurrence as biogenic carbonates have been found on a variety of mixed mineralogies such as limestone, dolostones, quartz, and other surfaces.

3.6 Use of Available Acoustic Data

Occurrence and spatial distribution of microbial bioherms in Great Salt Lake was quantified by examining the physical nature of acoustic returns from digital bathymetric data from earlier surveys (Baskin, 2005, 2006) and comparing those sonar returns with known microbial bioherm occurrences in Great Salt Lake. Representative rugosity characteristics derived from the acoustic data were used to identify and classify substrate type and the occurrence of microbial bioherms. Increased acoustic rugosity, results from spatial and aspatial statistics, and verification of substrate type were used to locate and map transitions between bioherm and nonbioherm substrates.

3.6.1 Population and Sample

Research on the occurrence and distribution of microbial bioherms in Great Salt Lake poses unique challenges as neither the entire extent or distribution of that population is known. Although a simple random-point sampling method would provide each location on the lake an equal chance at being included in the sample, the random point method is based on the assumption that the sample is representative of a population if it adequately describes and characterizes that population. Although technically possible, utilization of a simple random-point sampling method to characterize the population of microbial bioherms in Great Salt Lake is not feasible due to budget, geographic, and time limitations. Random sampling of the substrate itself, using methods such as sediment sampling, photography, or other direct methods, would require an unachievable large sample size to collect information defining the lateral extent and physical characteristics of the entire population.

Sampling in a marine environment where the targeted population is not visible necessarily decreases sampling bias as there is a lack of a priori knowledge of the population. Selection bias based on difficulty of access, environmental conditions, biologic or chemical hazards, and limitations due to weather are avoided in a marine environment where the targeted population is not visible. Data collection is limited only by the ability of a vessel and its crew to safely deploy and recover instrumentation, deal with the effects of wind (swells, waves, currents, etc.), and maintain adequate data quality.

To examine the spatial distribution of microbial bioherms in Great Salt Lake, digital acoustic data from previous bathymetric mapping efforts was analyzed and the rugosity of the substrate used as a surrogate for microbial bioherm occurrence. The bathymetric data were collected over the navigable waters of Great Salt Lake and provided a randomly selected, spatially distributed sample covering the full extent of the lake at a 1 kilometer north-south transect spacing (Fig. 13). The sampling method for collection of the digital bathymetric data was a probabilistic approach using a one-dimensional systematic sampling design, similar to a stratified random method. Because the data were originally collected using a random sampling design, the resultant data are appropriate for statistical examinations of distribution. Details of data collection and processing for the original acoustic survey can be found in Baskin (2005, 2006).

3.7 Methods for Single Beam Data Analysis

Natural variability of environmental parameters or distributions of factors that are mobile or mobilized by external forces such as wind or currents may temporarily alter distribution of populations in marine environments and greatly affect the usefulness of interpretations based on synoptic sampling efforts. Great Salt Lake presents a unique opportunity to examine a benthic population that is nonmobile and where control of the microbial bioherm occurrence and distribution is related to localized environmental variables rather than distributed variables where there is an open exchange of energy and materials.

3.7.1 Use of Rugosity as a Bioherm Occurrence Surrogate

For Great Salt Lake, the use of substrate roughness (or its calculated derivative – rugosity) can be used as a surrogate for microbial bioherm occurrence. Rugosity (Ra) is defined as the arithmetical mean deviation of the absolute values of the profile departure within a reference length for high-frequency components of a surface (ISO, 1997) (Fig. 14).

Rugosity is mathematically defined as…

$$R_a = \frac{1}{N}\sum_{j=1}^{N}|r_j|$$

Where… R_a = calculated rugosity (in meters)

N = number of points included in the calculation (limit of summation)

j = index of summation

$|r_j|$ = absolute value of the vertical distance from the mean line

and is statistically a very stable, repeatable parameter. Its primary use is in determining the roughness of industrial surfaces. Nevertheless, it also is used as an important ecological parameter (Friedlander and Parrish, 1998). The terms rugosity, roughness, and substrate complexity are used interchangeably in marine investigations to denote high-frequency elevation changes in substrate surfaces. The term “rugosity” is utilized for the remainder of this dissertation.

Acoustic data collected for the bathymetric survey of Great Salt Lake provided a probabilistic dataset used for statistical examinations of calculated rugosity and a surrogate for the chain-tape, microtopographic laser scanning, and other similar substrate rugosity determination methods (Risk, 1972; Brown, and others, 2004) (Fig. 15). Comparison of rugosity values from areas of known bioherms occurrence to those areas where bioherms do not occur provided the necessary information to analyze the lake-wide rugosity data and produce a classified substrate rugosity map for the entire lake.

Data analysis entailed development of new analytical methods, application of standard methods, and, in some cases, modification of those methods. Modifications to standard analysis methods generally involved redefining physical extremes to accommodate the unusual conditions encountered in Great Salt Lake or automating particular processes that define the spatial components of a particular dataset. Rugosity was calculated using the single-beam digital acoustic data and used as a surrogate for bioherm occurrence. Subsequent analyses of the rugosity data involved basic statistical analyses, classification of statistically "like" subsets of roughness data, and application of spatial analysis measures of clustering. Spatial analysis techniques provided insight about the spatial relations between bioherm occurrences, quantify characteristics of those distributions, and show changes within and between different occurrences of the bioherms or within the entire population.

Areas of relatively uniform substrate rugosity in Great Salt Lake were analyzed to define the range of rugosity in Great Salt Lake and the transitions for classifying substrate conditions as rugose or nonrugose. Polygonal areas used as classification "training" sets were selected and analyzed using aspatial statistics to determine the minimum, maximum, mean, standard deviation, skewness and interquartile range of rugosity for each area. Mean rugosity and standard deviation for each area were used to define a high, low, and medium likelihood of bioherm occurrence.

To examine the spatial distribution and randomness of microbial bioherms in Great Salt Lake, two statistical measures of clustering were utilized: Moran's *I* (Moran, 1950) and Getis-Ord Gi* (Getis and Ord, 1992). To examine the relation between the results of the Getis Ord Gi* statistic and the occurrence of bioherms in areas of increased rugosity, side scan sonar imagery showing bioherm occurrence was superimposed on the Getis Ord Gi* Z-score distribution. This comparison allowed for confirmation of increased rugosity in direct relation to bioherm occurrence.

Confirmation of bioherm occurrence in areas of increased rugosity was accomplished by visual verification and mapping of coincident rugosity values, Getis-Ord Gi* results, and side scan sonar and CHIRP datasets. Areas of probable microbial bioherm occurrence were buffered and smoothed to map changes in rugosity values and the overall distribution of microbial bioherms in Great Salt Lake.

The relation between microbial bioherm occurrence and possible environmental controls was examined by comparing verified bioherm distributions with newly acquired two-dimensional side scan sonar imagery, CHIRP subbottom profiles, and physical characteristics of the bioherms south and north of the rock-filled causeway. Subbottom profiles were geographically registered and mapped against bioherm distributions to determine if lake structural components influence bioherm occurrence.

Side scan sonar, CHIRP profiles, observations, videography, and samples of microbial bioherms from the south part of Great Salt Lake were compared with similar data from the north part of the lake to examine if the change in lake salinity has affected the condition of the bioherms. Dissolved oxygen data also were collected from the south and north parts of lake during substrate verification to supplement previous oxygen profiles on the lake that can indicate active photosynthesis at the water-sediment interface.

3.8 Methods for Verification of Bioherm Distribution

In situ verification of occurrence and spatial distribution of microbial bioherms is critical in addressing the research questions developed for this research. Due to general low visibility in the lake and the difficulties of optical verification in low-visibility waters, acoustic remote-sensing methods and direct substrate sampling were used for field-verification of bioherm occurrence and distribution. Techniques for the collection, measurement, analysis, and interpretation of data for verification of microbial bioherm occurrence were selected based on their ability to provide specific information about microbial bioherms in the hypersaline, low-transparency, waters of Great Salt Lake.

Although methods for acquiring data from low-transparency marine environments are well defined in the literature, modification of these widely accepted methods were necessary in Great Salt Lake due to the effects of the hypersaline environments. As conditions permitted, additional photography and videography were acquired to obtain site-specific information on detailed structure and biological activity associated with the bioherms.

Data-collection techniques for verification of microbial bioherm occurrence were identified based on conceptual constructs of both the lake environment and the behavior of acoustic methods of marine research. A set of mandatory criteria were established to ensure that the utilized data-collection techniques obtained unbiased, repeatable, interpretable data. Techniques used to collect, measure, analyze, and interpret data for this investigation were

1) based on an unbiased, technically defensible method of measurement;

2) widely used in marine research and well-referenced in the literature;

3) theoretically understandable with substantial performance verification testing;

4) capable of providing stable, repeatable information with regard to data quality;

5) quantifiable and interpretable data from Great Salt Lake; and

6) availability of equipment, operational limitations, and efficient data collection.

Equipment used for data verification and methods of analysis were selected based on the listed criteria. Two primary acoustic systems were selected for verification of bioherm occurrence: a two-dimensional acoustic technique for examining the occurrence and distribution of microbial bioherms on the lake floor and an acoustic subbottom profiling device to extend the two-dimensional occurrence and distribution data into the third dimension. A multibeam echosounder, although commonly utilized in modern marine surveys, was not selected for use in this investigation as frequent vertical and horizontal changes in lake salinity caused acoustic beam angle variations that could not be rectified. The inability to correctly interpret multibeam data in areas of short-distance, high vertical variation in the substrate prevented selection of a multibeam system as a useful tool for bioherm morphometric quantification.

Use of acoustic remote sensing technologies were used to verify the occurrence of microbial bioherms in areas of increased rugosity for Great Salt Lake and to identify gross morphological changes (size/shape) in the bioherms. For lake-bottom verification of bioherm occurrence in areas of increased rugosity, dual-frequency side scan sonar data were collected. For examination of subbottom characteristics, including structural control, general sediment type, and the vertical occurrence of bioherms, a CHIRP subbottom profiler was deployed (Fig. 16).

Although the side scan sonar and CHIRP systems are acoustically based remote sensing systems, their function, spatial resolution, and subsurface penetration dramatically differ. The side scan sonar system is designed to map the interface between water and underlying sediment and define features lying on that surface. Spatial resolution varies based on the pulse length and beam angle. At the frequencies used during this investigation (100 and 400 kHz), there is little to no subsurface penetration and the resultant data are represented as two-dimensional images of acoustic backscatter intensities at the sediment-water interface.

The CHIRP system is designed for acoustic penetration of the lake floor and, depending upon frequencies and power level, can range from decimeter vertical resolution to over a meter. Data are represented as two-dimensional vertical profiles through the subsurface with higher acoustic impedance reflectors appearing as darker features. Changes in acoustic impedance are related to changes in sediment characteristics and provide profiles of shallow geologic structure. Similar to the side scan sonar, repeated pulses from the CHIRP provide a series of vertical traces, which joined together, provide an acoustic profile beneath the lake bottom showing changes in acoustic impedance along the survey transects.

To ensure comparative validity of the data, acquisition system parameters for both the side scan sonar and CHIRP systems remained constant during the course of this investigation except during initial instrument tests. Details on the side scan sonar and CHIRP systems used in this investigation are included in Appendices B and C.

3.8.1 Collection of Verification Data

To verify the rugosity-based determination of microbial bioherm occurrence in Great Salt Lake, a series of systematic surveys were performed in selected areas of the lake that exhibited increased single beam acoustic rugosity. Geophysical data from the side scan sonar and CHIRP systems were gathered in blocks of overlapping transects in eight areas, along randomly located transects, and in areas of widespread bioherm occurrence where time and budget constraints otherwise prevented collection of overlapping transects (Fig. 17). Five of the verification sites were located in the south part of the lake and the remaining three in the north. Data were gathered as overlapping transects to provide a larger two-dimensional distribution of benthic bioherm occurrence. Additional randomly collected transects were obtained also for use in validating the rugose/nonrugose classification and to verify the extent of larger bioherm distributions.

The eight principal areas selected for verification of microbial bioherm occurrence were based on the change in the acoustic characteristics of the benthic zone, proximity to mapped faults, orientation of changes of rugosity of adjacent transects, lake salinity, aspect, and depth. All eight areas included transitions between mapped rugose and nonrugose areas in an attempt to capture changes in substrate conditions. Additional verification data were randomly collected to check the validity of the classification rugose/nonrugose classification.

To optimize available time and opportunity, data collection procedures were designed to provide information that could be used to concurrently examine all three research questions, as found in Section 3.2. For example, side scan sonar data were used to verify bioherm occurrence, map patterns of bioherm occurrence, and examine the morphology and general characteristics of the bioherms.

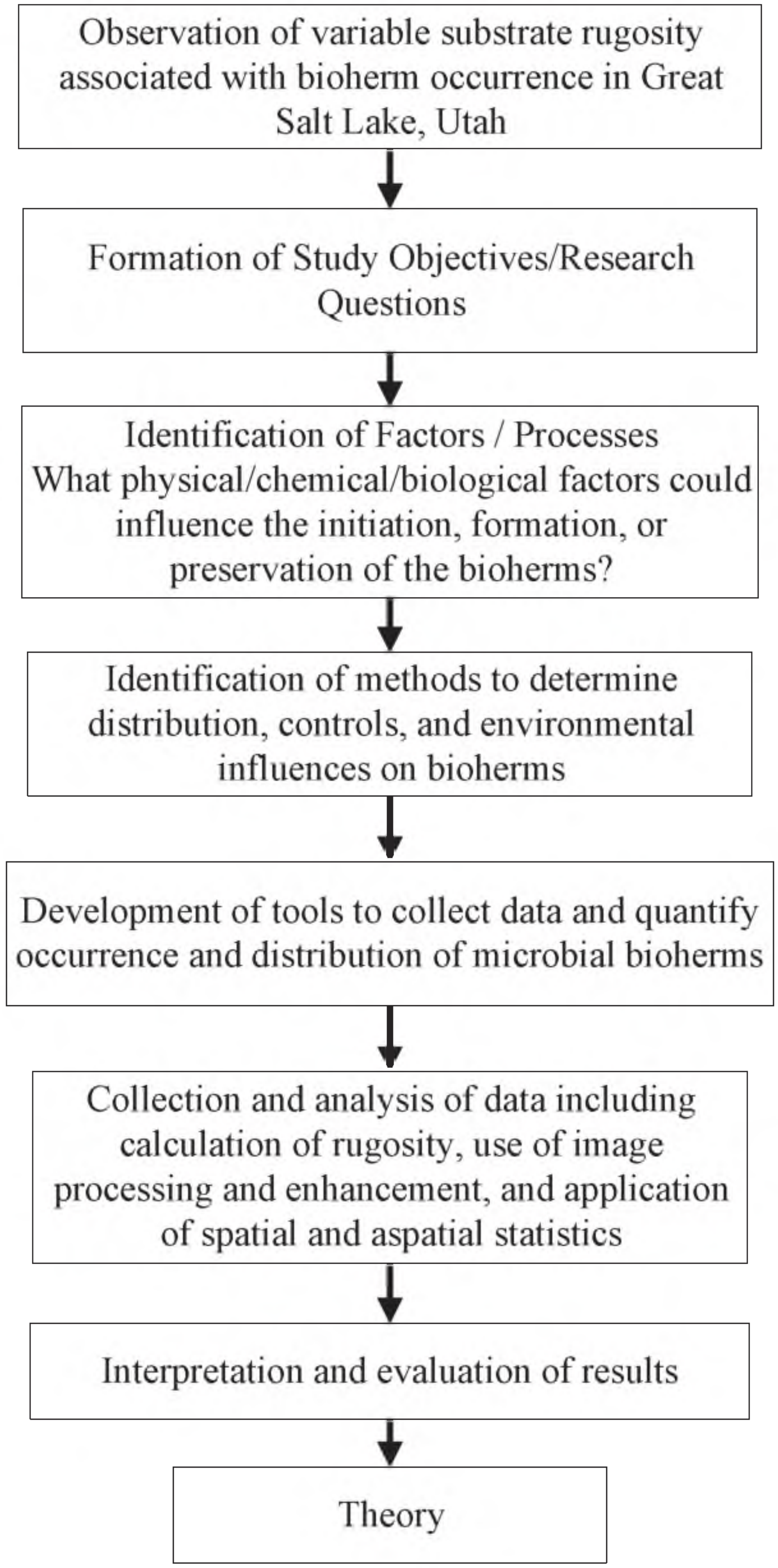

Figure 11. Diagram showing flow of methodology development for examining the occurrence and distribution of microbial bioherms in Great Salt Lake, Utah.

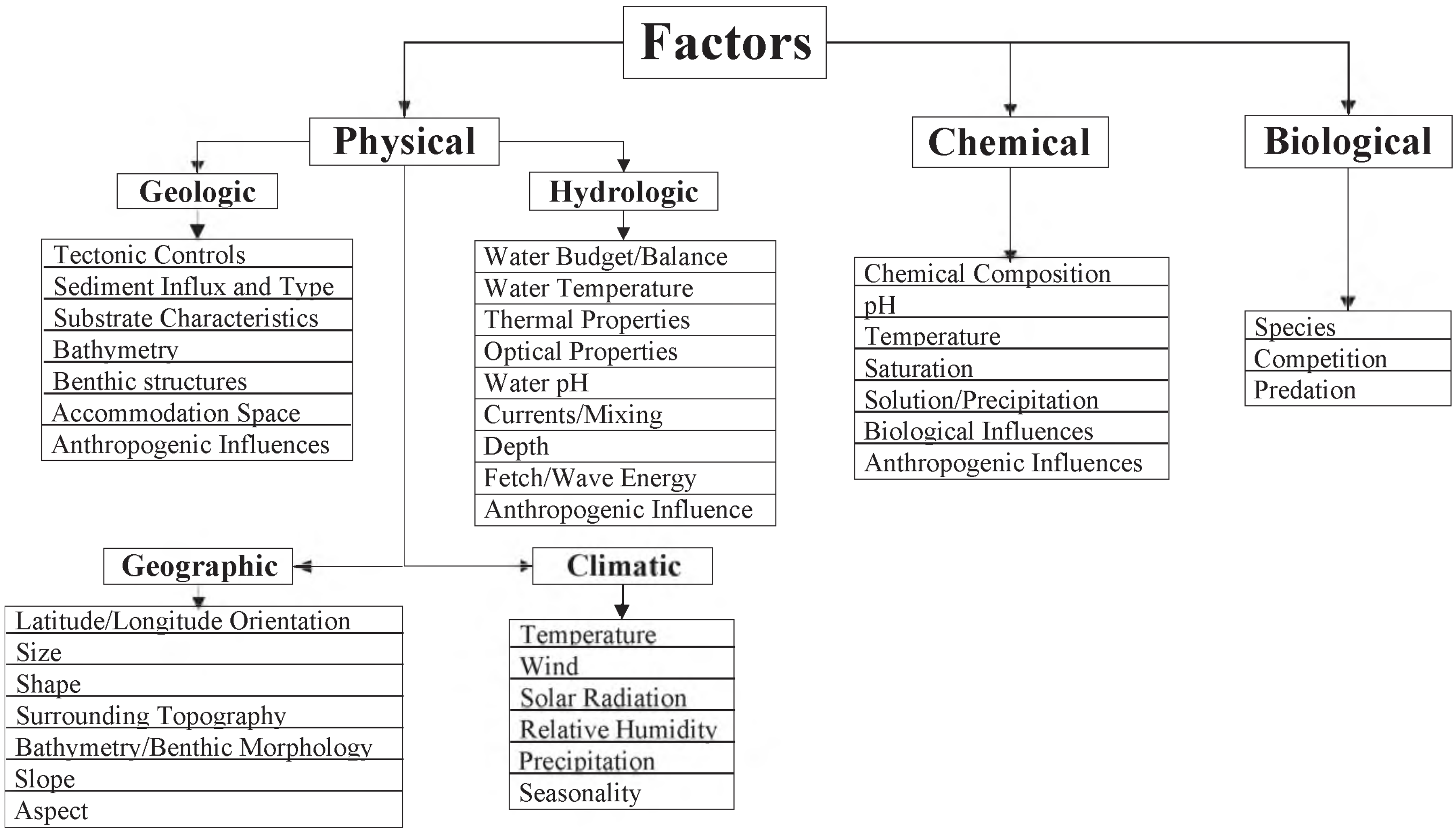

Figure 12. Factors related to the occurrence and distribution of microbial bioherms in Great Salt Lake, Utah.

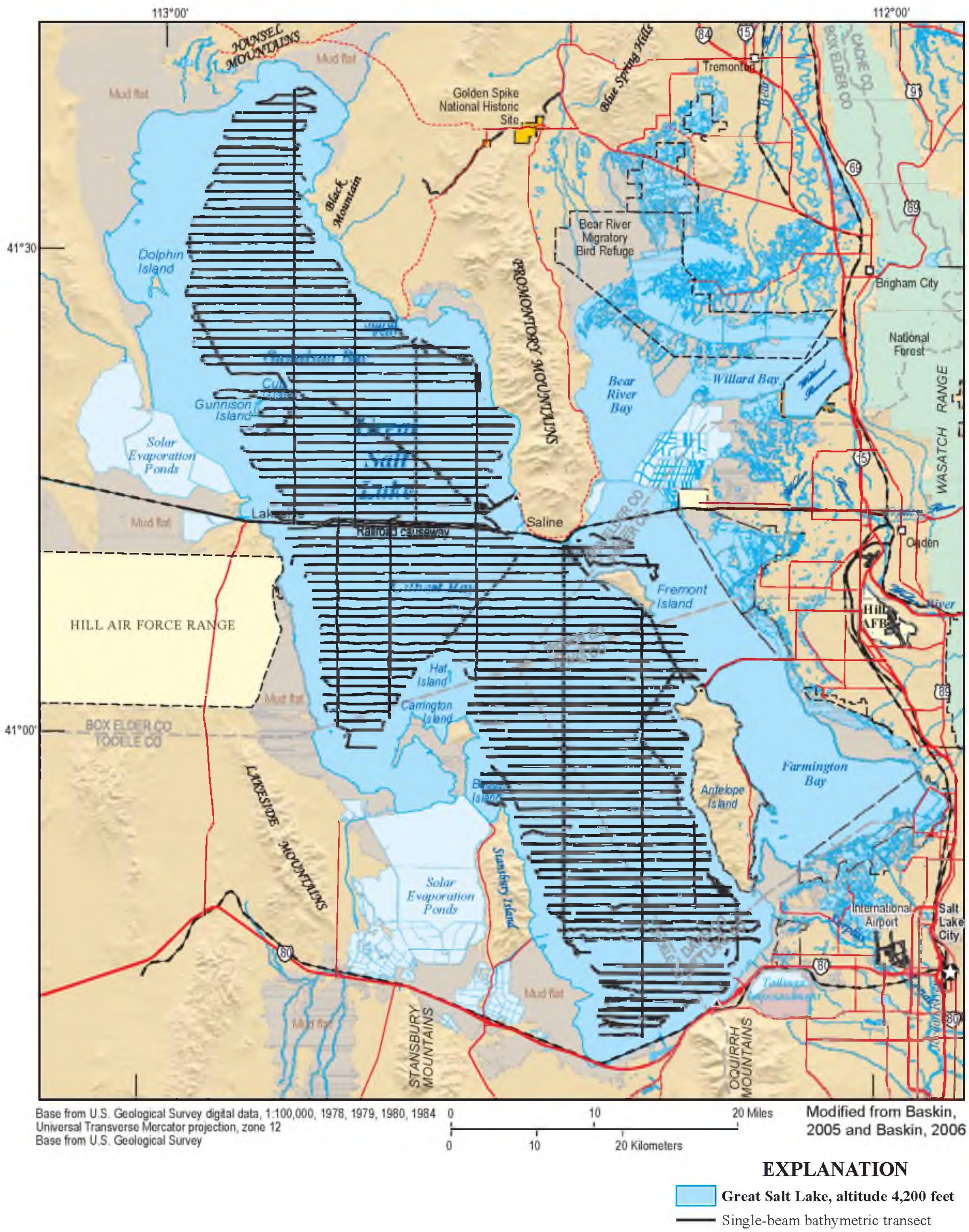

Figure 13. Location of single-beam transects used during this investigation, Great Salt Lake, Utah.

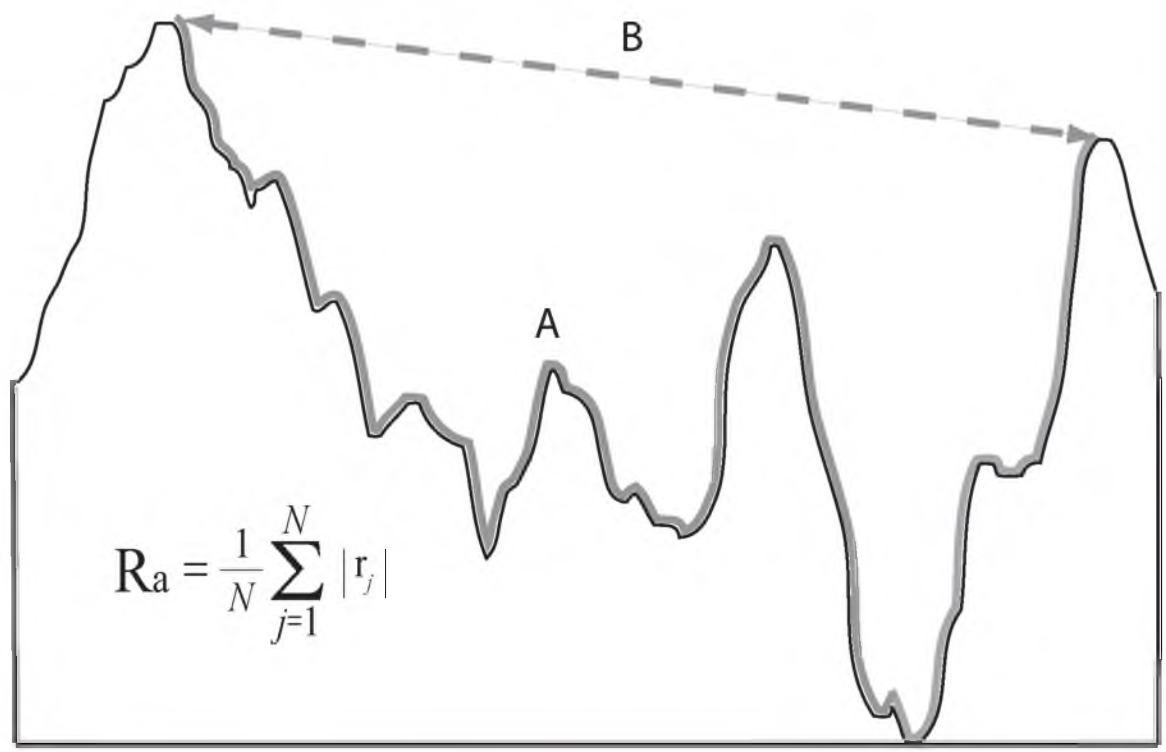

Figure 14. Simplified relation between measured distance along benthos (A) and straight line distance (B) used in rugosity calculations for Great Salt Lake, Utah.

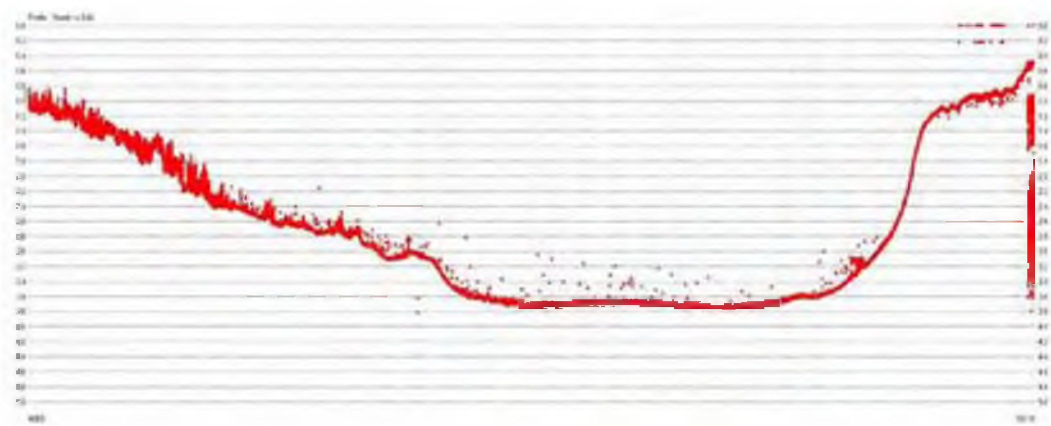

Figure 15. Unprocessed digital bathymetric data obtained during recent bathymetric survey showing variations in the acoustic roughness of the benthic surface of Great Salt Lake, Utah (vertical scale gradations 0.5 feet).

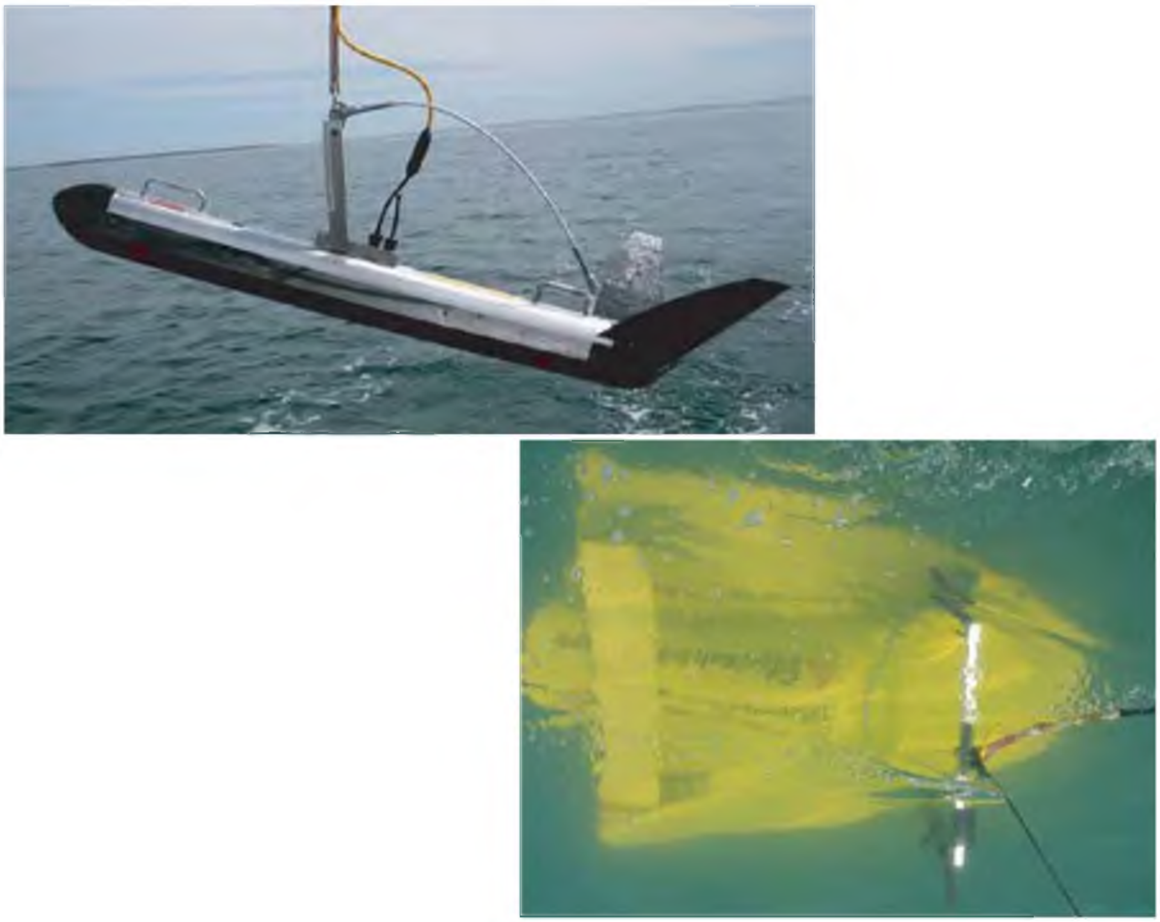

Figure 16. Photographs of side scan sonar and CHIRP towfish used for this investigation.

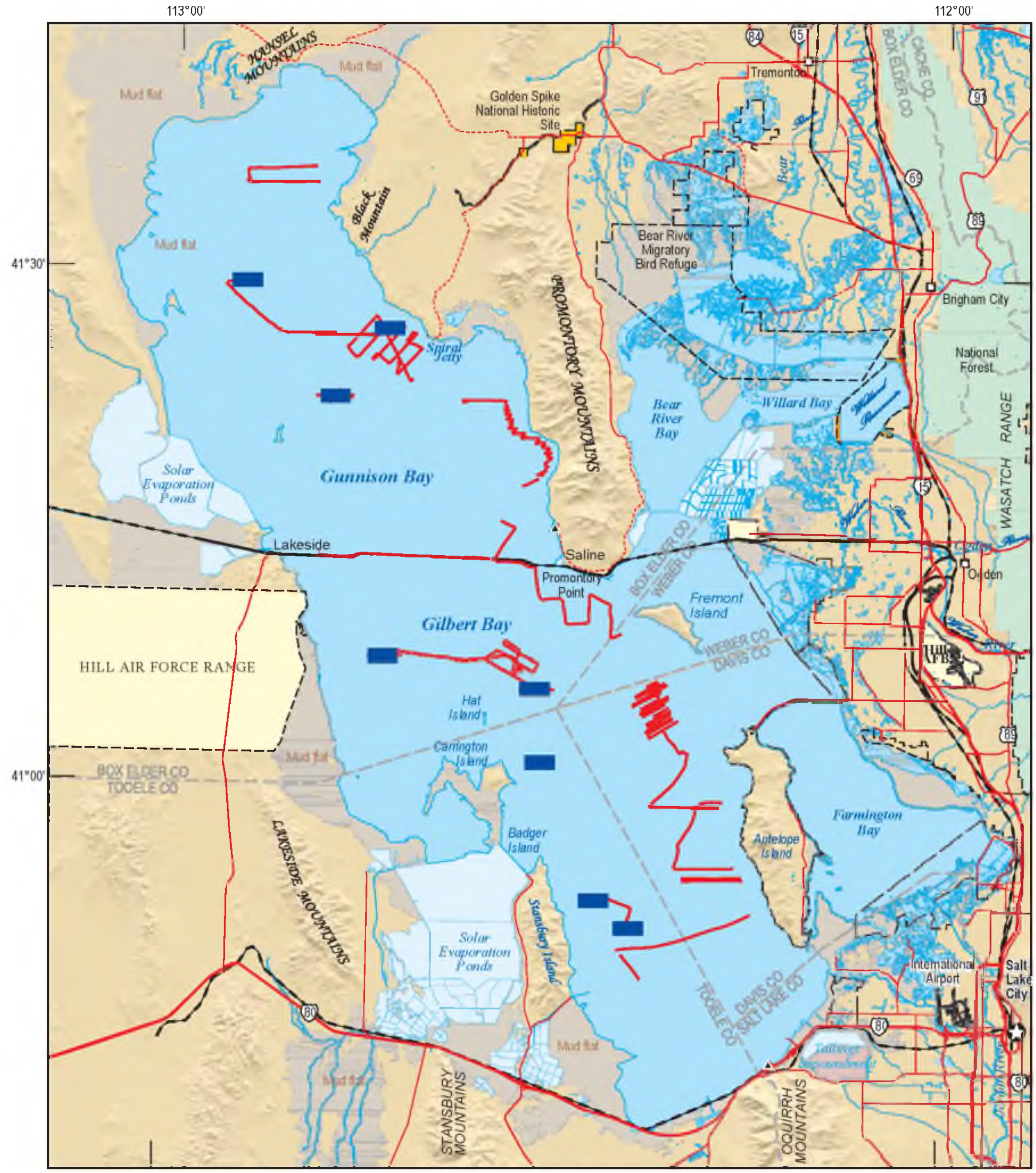

Base from U.S. Geological Survey digital data, 1:100,000, 1978, 1979, 1980, 1984
Universal Transverse Mercator projection, zone 12
Base from U.S. Geological Survey

0 10 20 Miles
0 10 20 Kilometers

EXPLANATION

- Great Salt Lake, altitude 4,200 feet
- Verification data block
- Side scan sonar and CHIRP transect

Figure 17. Location of verification areas, and side scan sonar and CHIRP geophysical transects acquired during this investigation, Great Salt Lake, Utah.

CHAPTER 4

ANALYSIS OF DATA

4.1 Introduction

In order to quantify the patterns of microbial bioherm occurrence and compare those patterns to factors that may be influencing their distributions, both spatial statistical analyses and conventional a-spatial statistical analyses were applied to the various datasets. A custom-designed computer program was developed to quantify changes in acoustic rugosity. ArcGIS™ (ESRI, 2010) software was used for spatial management and analysis of the spatial components of data collected or included in this investigation.

4.2 Analysis of Single Beam Data

Mapping the occurrences of microbial bioherms in Great Salt Lake, Utah, was primarily based on the analysis of single beam sonar acoustic rugosity calculated from digital bathymetric data. Original digital bathymetric data are stored in a proprietary HyPack™ format (HyPack, 2013) and required significant manual edits to remove multiple reflections (Fig. 18) and within water-column noise. Data-quality issues such as spurious reflections from suspended objects or gas in the water column, intermediate reflections from chemo- or thermoclines, or nonbenthic reflections from manmade objects also were removed during the editing process. To retain nonmodified acoustic characteristics of the benthic zone, no smoothing or averaging of points was applied during reprocessing of the original data. The reprocessed acoustic data were exported to ASCII data tables and used for calculation of acoustic rugosity.

Rugosity data were initially graphed along individual transects to examine the range of rugosity values and to visually compare rugosity with visually identified increases in lake-bottom rugosity. This effort provided a direct visual comparison between mathematically derived rugosity values and interpretation of increased variation in benthic rugosity derived from analogue bathymetric data. This comparison supported the conceptual aspects of the method and provided a preliminary range of values that could be used to discriminate microbial bioherms from nonbioherm areas.

Quality-assurance procedures employed during the Great Salt Lake bathymetric surveys provided a dataset that can be used for examining small-scale changes in the rugosity of the substrate. As with spatial resolution issues in terrestrial environments, the scale of variation within a target dataset must be able to be discriminated by the method of measurement. Acoustic bathymetric data were gathered at a resolution appropriate to define rugosity changes associated with observed 1–2 meter diameter bioherm structures using a 3–5 points per meter spatial resolution along transects and with submeter geographic position control. These procedures included a high data acquisition rate (10 Hz), limited vessel speed (<8 kts), narrow beam angle of the transducer (2.8 degrees), and other associated quality-control measures.

4.2.1 Quantification of Substrate Rugosity

To gain insight into the patterns of bioherm occurrence in Great Salt Lake, rugosity variations and associated spatial locations were calculated for subsets of sonar-based acoustic returns along the acoustic bathymetric survey transects. Although the calculation of rugosity itself is aspatial, it uses distances along paired surfaces to derive roughness.

Benthic rugosity was calculated for subsets of digital single-beam acoustic data along more than 1,690 kilometers of transects for the south part of Great Salt Lake and more than 1,200 kilometers for the north part of the lake. Geographic reference information was calculated for each transect segment by deriving an average position from each subset of data along all transects. The average position was assigned to the appropriate calculated rugosity, thus maintaining the spatial component of the data. Retention of the geospatial component of rugosity variation allows for examination of not only the rugosity of a surface but the change in rugosity across a surface and the spatial distribution of roughness. The methodology also reports adjacent maximum and minimum benthic altitudes and allows for calculation of statistics on the physical heights and locations of benthic formations. This analytical procedure was programmed in Python for applying and testing the effects of varying transect subset length on rugosity values.

In addition to the use of rugosity as a surrogate for bioherm occurrence, high frequency, high-amplitude changes at the sediment-water interface also were examined using aspatial statistics, box plots (i.e., box and whisker plots) (Tukey, 1977), and spatial analysis techniques. These analyses involved both an area-based selection of rugosity that examined differences in rugosity values for subsets of spatially distributed data, and an examination of randomness in the rugosity data using a global Moran's *I* statistic (Moran, 1950) and local Getis-Ord Gi* statistic (Getis and Ord, 1992).

4.2.2 Analysis of Polygonal Subsets for Rugosity

Aspatial statistics of rugosity values provided 1) a straightforward method of comparing differences in substrate rugosity; 2) a rapid method to identify outliers that may adversely affect statistical analyses; and 3) a method to rapidly assess dataset minimums, maximums, median, mean, and other aspects of calculated rugosity.

Rugosity values from the 50-sample dataset were grouped into 10 classes based on a geometric interval and plotted on a base map of Great Salt Lake using their calculated average position. Nineteen individual polygons with relatively uniform rugosity were identified for the south part of the lake and 15 for the north. Each selection was based on the uniformity of values in a 10-class geometric interval classification. Rugosity values in each polygon were extracted from the original datasets for analysis. Rugosity values for each polygon were analyzed to identify differences between the datasets and to determine a threshold that could be used to define probable areas of microbial bioherm occurrence.

4.2.3 Global Moran's *I* Spatial Statistic

To test for patterns in the lake-wide distribution of microbial bioherms in Great Salt Lake, a simple global statistical measure of clustering, Moran's *I* (Moran, 1950), was utilized. The Moran's *I* statistic utilizes the value of a feature, in this case – rugosity, instead of simply a location. Moran's *I* merely provides a test of randomness in the distribution. It neither differentiates between clustering of high or low roughness values nor provides information on the locations of nonrandom distributions. The output of the Global Moran's *I* statistic is a standard score (commonly called a Z-score) for the entire dataset that represents deviation from the mean for a standard normal distribution. A high Z-score indicates clustering. A Z-score near zero indicates no apparent clustering, i.e., a random distribution. A local spatial statistic, such as Getis-Ord Gi* statistic (Getis and Ord, 1992), would need to be used to identify locations of nonrandom distributions within the datasets.

4.2.4 Local Getis-Ord Gi* Statistic

To further quantify the characteristics of the bioherm distribution in Great Salt Lake, a local statistical measure of clustering, "Getis-Ord Gi*," was applied to the data (Getis and Ord, 1992). This method compares a subset of rugosity values in the dataset with the rugosity values of the entire dataset and was applied to supplement and test the results from the global Moran's *I* analysis. This method provides the spatial locations of high and low rugosity value clusters. Unlike similar spatial statistics (Gi, Quadrat, Ripley's K), which are based solely on the spatial attributes of data, the "Gi*" statistic allows data values (in this case, rugosity) to be included in the calculation. The Gi* statistic identified those clusters of points with rugosity values higher or lower in magnitude than expected given randomly distributed rugosity values. Similar to the Moran's *I* output, the Gi* function uses a standard score (Z-score) that represents deviation from the mean for a standard normal distribution. For each calculated rugosity, a Z-score is calculated to examine the spatial distribution of deviations in rugosity. Because the statistic compares a subset of rugosity values against the mean of the entire dataset, a high Z-score indicates that a calculated rugosity value is spatially associated with other high-rugosity neighbors. The opposite also is true: low rugosity values are spatially associated with other low-rugosity neighbors. The higher or lower the Z-score, the stronger the association. A Z-score near zero indicates no apparent concentration of high or low values, i.e., a random distribution.

4.3 Confirmation of Bioherm Occurrence and Distribution

4.3.1 Use of Side Scan Sonar Data

Typically utilized in oceanographic applications, side scan sonar use provided a series of challenges when used for scientific applications in the closed basin, hypersaline environment of Great Salt Lake. The high-density water (due to the high dissolved-solids content) allowed for better acoustic coupling between the instrument and the water column but created path-refraction errors and subsequent distortion of the acoustic imagery. In addition to changes in sound velocity, the change in density through the water column changed the sound refraction coefficients as depth and density increased. Although the ranging errors had minimal effect on the substrate classification, off-nadir feature locations were erroneous and had to be corrected during postprocessing of the side scan sonar data.

Side scan sonar data were processed using HyPack, Inc., software (HyPack, 2013). Geographic control was supplied by a WAAS-supplemented GPS receiver simultaneously supplying location and navigation data for both the side scan sonar and CHIRP subbottom geophysical acquisition computers.

Side scan sonar imagery supplies an acoustic record of the basic morphological characteristics of benthic features and their location relative to the sonar towfish (Fig. 19). Identification of microbial bioherms and other benthic features along with variations in benthic sediment type were obtained from measurement and interpretation of the side scan sonar data. Coregistration of the side scan sonar imagery with the bathymetric data and rugosity characterization allowed for confirmation of microbial bioherm occurrence in areas of increased rugosity. Substrate classification information was extracted from both unmosaicked and mosaicked data.

Georegistration of side scan sonar data allows for the determination of morphological characteristics of the bioherms including size, shape, and orientation and their location in the lake. Miscellaneous measurements of bioherm size and shape were conducted for determining the maximum size of individual bioherms. However, determining the morphological characteristics of the majority of bioherms in Great Salt Lake, or even those imaged during this study, was beyond the scope of this investigation.

4.3.2 Use of CHIRP Geophysical Data

The subsurface of Great Salt Lake should be, in the absence of tectonically induced modification, a relatively flat, layered sedimentary basin. To test this conjecture, a Compressed High Intensity Radar Pulse (CHIRP) system was used to infer depositional and structural changes in the sediments beneath Great Salt Lake and examine possible structural and sedimentological influences on microbial bioherm occurrence and spatial distribution. Although uniformity of composition can be inferred from the characteristics of the CHIRP seismic signal returns, successful use of the CHIRP system relies on the existence of acoustic differences between the layers, not the properties of the sediments themselves.

CHIRP geophysical data were used in this effort to examine the types, patterns, and degrees of structural deformation beneath areas of microbial bioherm occurrence; determine the general characteristics of sediments beneath and adjacent to bioherms; identify acoustic signatures that could indicate possible buried bioherms; and provide information that could be used to examine structural influences on bioherm occurrence.

Stratigraphic interpretation of the subbottom was from examination of the geometric expression of seismic reflections. Limited inferences of sediment characteristics were based on the acoustic transparency of the sediments, orientation and strength of reflectors, and previously published reconstructive histories of Great Salt Lake. Identification of basic structural features included faults, folds, monoclines, horsts, grabens, and other evidence of tectonic deformation. Depositional features included varying thicknesses of acoustically similar sediments and distinct sedimentary buildups within the general depositional facies of the lake (Fig. 20).

4.4 Analysis of Spatial Variations within the Population

In an attempt to examine within-population distribution differences, two randomly selected points were generated for each transect segment to identify locations where subsamples of the larger rugosity-defined microbial bioherm distributions would be examined. More than half of the randomly selected points did not intersect an identifiable occurrence of microbial bioherms. This likely was due to the verification survey design where each survey block contained areas of suspected bioherm occurrence and nonoccurrence. Identifying individual bioherms in georectified side scan sonar data was problematic due to variations in bioherm size, scope of interconnectivity, possible burial by sediment, acoustic shadows masking adjacent bioherms, and distortions of the data from georectification efforts and varying sound velocities. These factors prevented a random resampling of distributions within the larger surveyed population. To examine variations in localized populations, specific locations were selected nonrandomly to ensure that a representative range of distribution types were included in the study.

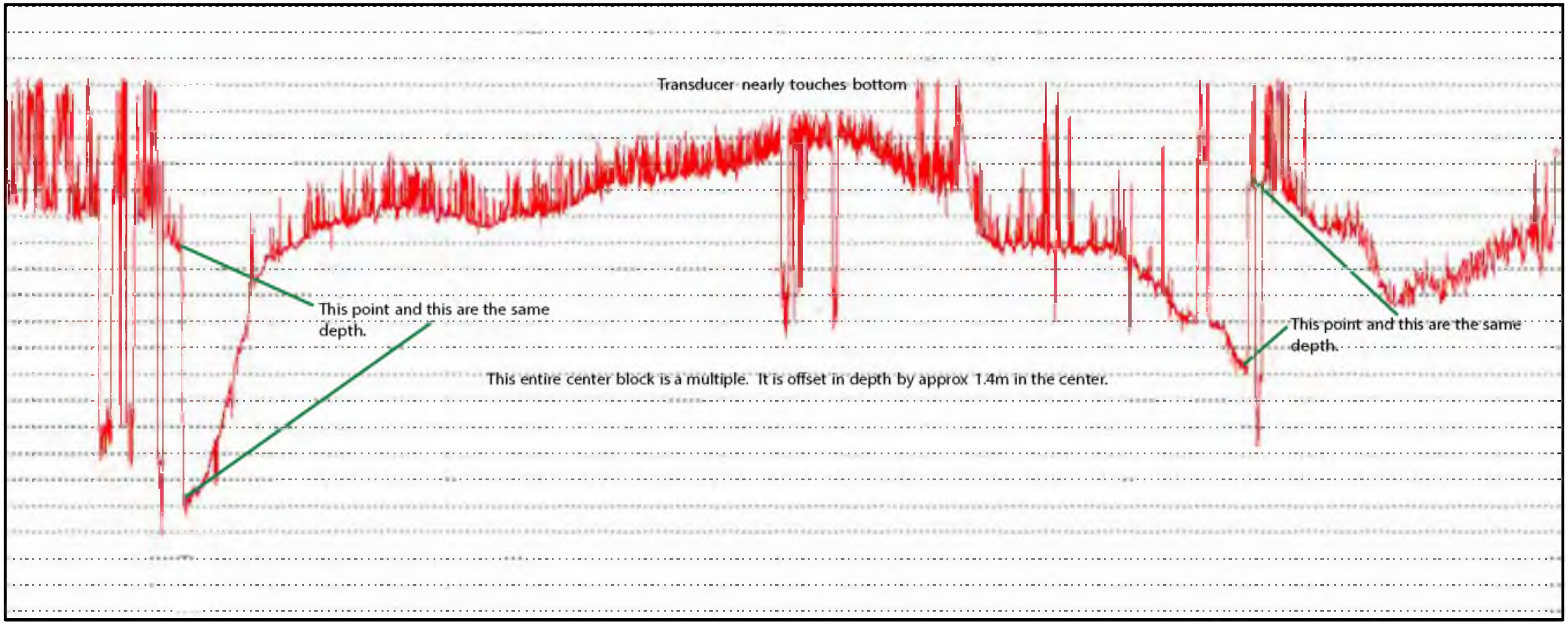

Figure 18. Example of "multiple" acoustic reflection in shallow area north of Fremont Island, Great Salt Lake, Utah.

Figure 19. Side scan sonar image showing microbial bioherms (lighter, high acoustic reflectivity) occurring with fine-grained sediments (darker, low acoustic reflectivity) in Great Salt Lake, Utah. Distortion due to the varying high salinity is apparent in the image as are high intensity returns along nadir where the two sides on the sonar imagery are joined.

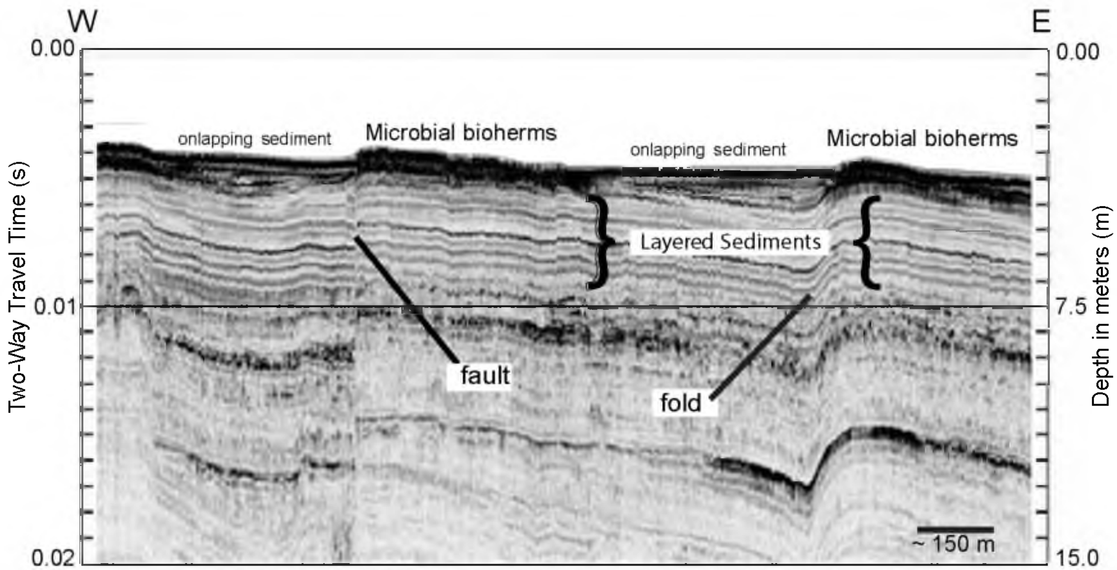

Figure 20. CHIRP subbottom image showing typical structural and depositional features imaged by the CHIRP system, Great Salt Lake, Utah.

CHAPTER 5

ANALYTICAL RESULTS IN AN ENVIRONMENTAL FACTORS CONTEXT

5.1 Introduction

Marine-based acoustic remote sensing techniques coupled with results from spatial and aspatial statistics and in situ verification of substrate type were utilized to examine the geographic patterns of occurrence for microbial bioherms in Great Salt Lake, Utah. Comparison of bioherm occurrence with relevant environmental factors provided evidence of the relations between physical processes and distributions. Systematic examination of these patterns was used to infer environmental processes that either inhibit or promote bioherm initiation and growth. Integration of GIS technologies with the remotely sensed acoustic data provided mapping and analysis tools for examining and classifying locations and patterns of microbial bioherm occurrence.

Data from a single-beam fathometer, side scan sonar, and CHIRP subbottom profiler were integrated with Geographic Information System technologies during this research to provide limited geographically registered, three-dimensional representations of microbial bioherm occurrence and spatial distribution. Verification of bioherm presence/absence was achieved by visual inspection using in situ underwater and shoreward observations of bioherms above or at the water surface, videography, and benthic substrate sampling. This methodology ensured that acoustically derived interpretations and classifications of the benthic zone and substrate were confirmed through additional lines of evidence, thereby minimizing possible misinterpretation of the acoustic data.

Living microbial bioherms, ranging from individual forms to coalesced, nearly solid reef-like structures, occupy an area of about 700 km^2 in the south part of Great Salt Lake. The areal estimate of microbial occurrence along the shallow margins of the north part of Great Salt Lake is greater than 300 km^2. The estimate of microbial bioherm extent in the north part of the lake is limited to shallow regions where the environmental conditions provide sufficient wave-base energy and currents to transport precipitating salt crystals lakeward to deeper water, exposing the bioherms for observation and study. However, thick salt deposits in the deeper areas and acoustically defined roughness in subbottom geophysical data suggest that widespread occurrences of microbial bioherms existed before the onset of extensive salt deposition in the north part of the lake.

The precauseway (pre-1960s) extent of living microbial bioherms in Great Salt Lake likely significantly exceeded the approximately 1,000 km^2 extent verified during this investigation. This estimate is more than four times the 1938 estimate of Eardley (approximately 259 km^2), and the actual areal extent of microbial bioherm occurrence in Great Salt Lake is likely to be larger. Smaller bioherms, less clustered bioherm occurrences, and bioherms that occur shoreward of the surveyed areas have been excluded from this estimate due to survey depth limitations greater than about 2 meters. Deposits of recent sediment in the south part of the lake also may mask additional bioherm occurrences, especially in high sediment inflow areas along the eastern margins of the south part of the lake.

Microbial bioherms in Great Salt Lake are exposed on the lakebed along the shallow margins of the lake but appear to be absent in the deeper regions. Environmental conditions related to this extinction may include the loss of solar energy for photosynthesis, the absence of a stable initiation surface, the possible presence of a highly saline chemocline at depth, or the presence and deposition of fine-grained sediments (including salt crystals) in the profundal areas of the lake. Fine grained sediment deposition in the deeper areas of the lake is likely to have prevented initiation of the bioherms or "drowned" any communities that had previously been able to initiate growth.

Populations of microbial bioherms in Great Salt Lake range from dispersed single, individual forms to highly clustered reef-like formations oriented parallel to structural controls. Individual bioherms range in size from centimeters to over 2 meters in diameter and bioherm heights have been measured at more than 1.5 meters above surrounding substrates. Transitions between nonbioherm areas to areas where bioherms exist range from gradual to abrupt.

5.2 Single Beam Results

Quantification of rugosity variations and associated geographic location are necessary in addressing questions 1 and 2 of this research, as found in Section 3.2. Subsets of data from the original acoustic bathymetric survey provide information on where substrate conditions change and the requisite information for calculation of rugosity. Higher rugosity values were indicative of microbial bioherm occurrence and were defined using spatial and aspatial statistics. Variations in substrate rugosity were used to locate transitions between lower rugosity, nonbioherm-populated substrates and higher rugosity, bioherm-populated substrates.

5.2.1 Calculations of Rugosity

Calculations of rugosity for each of the original transects used during this study were performed on 50, 100, 250, and 500-point windowed sets of data using the custom rugosity program developed for this investigation (Figs. 21, 22). At an average of 3–5 points per meter, this equated to approximately 10–15, 20–33, 50–63, and 100–166 meter subset intervals with mean lengths of 14, 29, 72, and 143 meters, respectively. Calculated rugosity varied as expected, with abrupt increases in calculated rugosity in areas where high-frequency, high-amplitude changes occurred at the sediment-water interface. Comparison of the acoustic profiles with calculated rugosity also confirmed that rugosity was not a function of lake-bottom altitude or depth below water surface (Fig. 23).

Results from the 50-sample rugosity calculations (Figs. 24, 25) were used to define an area of probable occurrence of microbial bioherms for use in subsequent calculations and comparisons against the 100, 250, and 500-sample distributions. The 50-sample rugosity calculation provided the most accurate positional information and was ultimately used in determining the transition between highly rugose and lesser rugose areas and production of the general occurrence/nonoccurrence rugosity classification map.

For the south part of Great Salt Lake, the 50-sample dataset had average calculated rugosity values of 0.021 with a variance of 0.0016 (Table 1). In the corresponding 500-sample dataset, calculated rugosity values were 0.045 with a variance of 0.0060. In the north part of Great Salt Lake, the 50-sample dataset had average calculated rugosity values of 0.014 with a variance of 0.0005. In the corresponding 500-

sample dataset, calculated rugosity values were 0.035 with a variance of 0.0061 (Table 2). Increases in calculated rugosity and variance from the 50-sample to 500-sample datasets are a result of the increased number of samples used in each calculation.

5.2.2 Analysis of Polygonal Subsets for Substrate Classification

Rugosity values for each of 19 individual polygon datasets from the south part of Great Salt Lake and 15 individual polygon datasets from the north were analyzed to identify differences between the datasets and to determine a threshold that could be used to separate high rugosity areas (as suspected bioherm occurrences) from low rugosity areas (suspected fine-grained sediments, i.e., not bioherms). Rugosity values from each 50-sample dataset were grouped into 10 classes based on a geometrical interval and plotted using their calculated average position. Polygons with relatively uniform rugosity were extracted from the original data as "training" sets for classification of the larger datasets (Figs. 26, 27).

Rugosity value counts in each polygon varied from 181 to 3,560 in the south part of the lake and from 52 to 10,958 in the north part of the lake. Polygons ranged in size from 3.0 to 33.7 km^2 in the south part of the lake and from < 1 to 78.5 km^2 in the north part. Basic statistics (count, minimum, maximum, sum, mean, standard deviation, skewness, interquartile range, and a single frequency distribution) were calculated for each of the datasets. Box plots based on those calculations were generated and depicted dataset range, 1st, 5th, 25th, 75th, 95th, and 99th percentiles, mean, and median. Interquartile range was identified in the box plots by boxing the data range. Outlier values were retained in the box plots as they played an important role in delineating microbial bioherm occurrence (Figs. 28, 29).

Mean rugosity was higher than the median for all 19 polygon-based datasets in the south part of the lake, indicating a positive skewness. This skewness resulted from positive outliers in the data; in some cases, extensive numbers and larger values of outliers were present. Outliers are directly associated with those datasets that contained larger statistical dispersions of data. Higher numbers of outliers, larger values in the outliers, larger statistical dispersions, higher variance of rugosity, and higher mean and median values of rugosity are all conceptually associated with bioherm occurrence. Datasets with a lesser quantity of outliers and lesser range of outlier values, smaller statistical dispersions, and lesser mean and median values are associated with areas of lesser-rugosity substrates (Fig. 28 and Table 1). For the north part of the lake, mean rugosity was higher than the median for 12 of the 15 polygon-based datasets, indicting a predominately but not uniform positive skewness in the data (Fig. 29 and Table 2).

To define probable bioherm occurrence using the aspatial statistical methods described above, the sampled polygons were classified into 3 groups based on the variance of rugosity within each polygon. The average mean variance for the upper third of each set of polygons was used to define the threshold for having a high probability of bioherm occurrence. Six mean rugosity values were used to define probable bioherm location in the south part of the lake, and five mean rugosity values were used from the north part of the lake.

For the south part of Great Salt Lake, the average of the statistical means and standard deviations for the subsets with the six highest variance values (polygons 2, 4, 5, 7, 10, 11) resulted in a mean rugosity value of 0.04734 and mean standard deviation value of 0.044. Average of the statistical means and standard deviations for the subsets with the six lowest variance values resulted in a mean rugosity value of 0.0061 and mean standard deviation value of 0.0027. Values greater than the mean high rugosity of 0.047 were used as a surrogate for microbial bioherm occurrence.

For the north part of Great Salt Lake, average of the statistical means and standard deviations for the subsets with the five highest variance values (polygons 2, 3, 4, 11, 14) resulted in a mean rugosity value of 0.071 and mean standard deviation value of 0.062. Average of the statistical means and standard deviations for the subsets with the six lowest variance values resulted in a mean rugosity value of 0.0063 and mean standard deviation value of 0.0027. Values greater than the mean high rugosity of 0.071 were used as a surrogate for microbial bioherm occurrence in the north part of Great Salt Lake.

The difference between the probable bioherm occurrence threshold in the south part of the lake (0.047) and the north (0.071) suggest a change in bioherm characteristics across the rock-filled causeway, an environmental change in substrate conditions related to the causeway, or a difference in the ability of the method to measure substrate roughness on either side of the causeway.

Original analog and digital bathymetric transect records were examined to help explain the difference in mean rugosity between the north and south parts of the lake. Additionally, areas of mapped rugosity showing linear assemblages of high-rugosity values but no neighboring similar values were cross-checked against the original sonar data to identify areas where vessel movement or other bioherm-related features could induce a nonbioherm caused rugosity into the datasets. For the south part of the lake, wave-induced vessel movement, anthropogenic modifications to the lake, and nonbioherm substrate features (suspected spring mounds and travertine deposits) were identified as inducing nonbioherm rugosity (Fig. 30). In the north part of Great Salt Lake, anthropogenic modifications and extensive secondary acoustic reflections were identified as inducing a nonbioherm rugosity (Fig. 31).

Areas where the cause of induced rugosity could be identified were removed from the datasets and not used in the final calculation of probable microbial bioherm occurrence (Figs. 32, 33). Areas of significant secondary acoustic reflections in the north part of the lake were edited to remove as many of the secondary reflections as possible without directly modifying the roughness characteristics at the sediment/water interface. Removal of the secondary reflections created a false rugosity surface that may or may not have any relation to the actual sediment/water interface rugosity.

5.2.3 Global Moran's *I* Spatial Statistic

Two of the basic assumptions in aspatial statistics are that each value in a dataset is independent of each other and that any value within the minimum and maximum values of a population is equally likely to occur in a random sample of that population. In spatial statistics, spatial autocorrelation, where geographic features that are near each other are likely to be more similar that distant features (commonly referred to as the "First Law of Geography" or "Tobler's Law") violates the independence requirement of aspatial statistics. To address the assumption of independence in the rugosity data from Great Salt Lake and measure the strength of the relation of spatially adjacent rugosity values to lake-wide rugosity values, a spatial autocorrelation analysis was applied to the calculations of rugosity.

To test for patterns in the lake-wide distribution of microbial bioherms in Great Salt Lake, a simple global statistical measure of clustering, Moran's *I* (Moran, 1950), was utilized. The Moran's *I* statistic utilizes the value of a feature, in this case – rugosity, instead of just location to determine if there is a pattern of occurrence within the study area. It compares the values of calculated roughness of neighboring features to the mean value of calculated roughness for the entire dataset. If the difference in roughness between neighboring points is different than the mean difference in roughness between all the points in the dataset, the data are considered nonrandomly distributed. If the difference in roughness between neighboring points is the same as the difference in roughness between all the points in the dataset, the data are considered to be randomly distributed. An observed positive Moran's Index value indicates a clustering of values while a negative Moran's Index value indicates a dispersed pattern. A nonrandom spatial distribution of microbial bioherms in Great Salt Lake would suggest that at least one factor, such as depth, aspect, or salinity, influences distribution of the forms.

Calculated rugosity values from the 50-sample, 250-sample, and 500-sample datasets were used in the Moran's *I* spatial statistic to test the randomness of data from both the south part of the lake and the north part of the lake. The sampling neighborhood for all datasets was calculated as those rugosity values within a Euclidean fixed distance of 500 m.

Results from the Global Moran's *I* spatial statistic showed statistically significant clustering of rugosity within the analyzed 50 sample, 250 sample, and 500 sample datasets. Moran's Index values for the south part of the lake were 0.54, 0.29, and 0.47, respectively, with positive Z-scores of 517, 15, and 74: Z-scores that show there is less than a 1 percent probability that the observed spatial distribution of substrate rugosity in the south part of the lake could be the result of random chance. Moran's Index values for the north part of the lake were 0.34, 0.34, and 0.49, respectively, with positive Z-scores of 729, 146, and 101: Z-scores that show there is less than a 1 percent probability that the observed spatial distribution of substrate rugosity in the north part of the lake could be the result of random chance.

5.2.4 Local Getis-Ord Gi* Statistic

Results from the Gi* calculation showed statistically significant clustering of large rugosity values along the margins of the lake in areas coincident with the box plot results. The sampling neighborhood for all datasets was calculated as those rugosity values within a Euclidean fixed distance of 500 m. Z-values for the south part of the lake for the 250-sample interval dataset ranged from -4.83 to 29.28. For the 250-sample interval dataset, 5,613 Z-scores (20 percent) were greater than 1.96 standard deviations away from the mean (95 percent confidence level). Z-values for the 500-sample interval dataset ranged from -3.83 to 20.48. For the 500-sample interval dataset, 2,404 Z-scores (17 percent) were greater than 1.96 standard deviations away from the mean (95 percent confidence level). Z-values for the north part of the lake for the 250-sample interval dataset ranged from -2.29 to 35.4. For the 250-sample interval dataset, 1,480 Z-scores (8 percent) were greater than 1.96 standard deviations away from the mean (95 percent confidence level). Z-values for the 500-sample interval dataset ranged from -1.79 to 23.26. For the 500-sample interval dataset, 605 Z-scores (7 percent) were greater than 1.96 standard deviations away from the mean (95 percent confidence level). These values indicate, at a 95 percent or greater confidence level, that there is a statistically significant degree of clustering in the calculated rugosity values. The results of the local Getis-Ord Gi* analysis support the findings from the global Moran's *I* statistic: there is less than a 1 percent probability that the observed spatial distribution of substrate rugosity could be the result of random chance.

5.3 Mapping Bioherm Occurrence

Results from the analysis of rugosity were used in the GIS to define the probable location of microbial bioherms in Great Salt Lake. The classification of rugosity for each area provided probable locations for bioherm occurrence and the location of transitions between rugose and nonrugose areas of the substrate. The classification resulted in a series of 1-km-spaced transect-based transitions that were subsequently joined using smoothed point buffers. Buffers were used to define the linear boundary between adjacent transects as contour-based methods produced a stair-step effect due to the closely spaced along-transect rugosity values (50-sample) and the distance between transects (1 km). Buffers of 1,000 m were created around each rugosity value greater than 0.047 for the south part of the lake and greater than 0.071 for the north. Those buffers were dissolved to remove overlapping areas, and the polygon boundary was smoothed using a Bezier interpolation algorithm. The resultant smoothed polygons were rebuffered and internally clipped to remove a 500 m edge area from the larger polygon. As a surrogate for microbial bioherm occurrence, this process defined the calculated edge of probable bioherm populations in Great Salt Lake (Figs. 34, 35).

Due to shallow depths along the margins of both the south and north parts of the lake and acoustic noise effects in the north part of the lake, gaps occurred in the identification of microbial bioherm occurrence in some areas of the lake. Additional information was used to extend the probable location of bioherms in Great Salt Lake to areas where there were known occurrences of microbial bioherms that either were not included in the extent of the original surveys or where acoustic noise affected the classification of the substrate. Aerial photography, satellite imagery, notes from surveys, and personal observations were used to fill gaps in unclassified areas of known bioherm occurrence. Quantitative extent of probable microbial bioherm extent in the south part of the lake was calculated at 521 km^2 using the rugosity based method. The qualitatively determined extent added an additional 25 percent to the total area.

The majority of nonclassified area added to the estimate of probable extent occurred along the western edge of the north part of the lake where bioherms were observed during the bathymetric surveys. Salt deposits and acoustic noise effects are prominent in the acoustic data from that area and appear to mask previously observed bioherm occurrences. Shoreward extension of bioherm occurrence in the northwest area of the lake was limited to approximately 1 km to prevent excessive biasing of the aerial extent of bioherm occurrence. Quantitative extent was calculated at 134 km^2, with the qualitative extent more than doubling the probable extent of bioherm occurrence in the north part of the lake to over 300 km^2. Areas quantitatively classified as microbial bioherms and those areas qualitatively determined are noted in Figs. 36 and 37.

5.4 Bioherm Occurrence and Spatial Distribution

Verification of acoustically based classifications of substrate type is a critical component of this research. The surrogate relation between acoustic roughness and bioherm occurrence must be well defined to avoid classification errors and subsequent miscalculation of spatial distribution. A total of approximately 580 km of verification transects were surveyed during this effort including 350 km from the south part of the lake and the remaining 230 km from the north part of the lake. Side scan sonar and

CHIRP geophysical data were simultaneously collected along all verification transects.

Microbial bioherms occur as structures with positive relief and vary from dispersed to laterally connected coalesced forms throughout shallow areas of the lake (Fig. 38). Results from the global Moran's *I* and local Getis-Ord Gi* analysis show statistically significant clustering of calculated rugosity values and, by inference, microbial bioherms. Clustering of bioherm populations, to the point of forming continuous reef-like deposits shoreward of each occurrence (Fig. 39), indicate that changes in depth, or some environmental variable related to depth, such as light availability, wave base or current-related energy, or a combination of depth-related factors, has effect on bioherm initiation, growth, survivability, and preservation. As depth increases, bioherm populations become increasingly sparse, reaching a depth extinction zone beneath which occurrences of bioherms, if they exist, are no longer identifiable. These changes occur over a horizontal distance ranging from tens of meters to over a kilometer and within 1 meter to a few meters vertically.

Quantification of changing population distributions along the observed gradient was not possible as identification of all individual bioherms within clustered populations was not possible. In some areas, a pavement of continuous intergrowth bioherms was apparent in the side scan sonar imagery. Complications in identifying individual bioherms within clustered populations included variations in bioherm size, degree of interconnectivity, possible burial by sediment, acoustic shadows masking adjacent bioherms, and similar issues. Distortions due to georectification, probable variations in sound velocity within the lake, and onlapping sediment that masks bioherm occurrence also inhibited quantification of distributions within the larger surveyed populations.

Statistically dispersed populations were quantified in areas down-gradient of clustered shallow-water occurrences due to the separation and acoustic reflectivity of individual bioherms in those areas.

The extinction of microbial bioherms below a certain depth may indicate a persistent or recurring pycnocline (chemo or thermo) preventing their initial development, survival, or preservation, or a lack of appropriate environmental conditions for their formation (Fig. 40). This extinction depth could be related to wave or current energy, sediment deposition in the profundal zone, light extinction at depth, or the lack of suitable initiation surfaces. Although a persistent hypersaline layer currently forms in the south part of the lake, its occurrence is tied to differences in lake elevation between the restricted north part of the lake and the south part of the lake and contributions of high-salinity water migrating through the rock-filled causeway into the south basin. Data are not available that indicate a persistent precauseway pycnocline. However, one could have existed. The accumulation of halite and other evaporative minerals in the deeper sections of the north part of the lake prevented identification of changes in microbial bioherm occurrence along a shallow to deeper gradient except in areas where wave energy and currents inhibited salt accumulation. These areas were limited to shallow, near-shore occurrences.

5.5 Faults, Folds, and Bioherm Distribution

To determine if there is a relation between bioherm occurrence and the general structural trend of Great Salt Lake, CHIRP subbottom profiler data, acquired simultaneously and positionally coregistered with the side scan sonar data, were examined for stratigraphic characteristics that are coincident with changes in bioherm distributions.

Directly addressing research question 2, as provided in Section 3.2, integration of data from the side scan sonar and CHIRP systems revealed that the distribution of microbial bioherms in the south part of Great Salt Lake are closely associated with folding and faulting of subbottom sediments. Within-population variability of microbial bioherms ranged from intergrowth forms generally associated with abrupt transition areas to statistically dispersed distributions on the lakeward side of the deposits. The occurrence of reef-like populations along the fault-related topographic highs suggest that growth of the microbial bioherms located adjacent to the fault initiated before other bioherms deeper in the water column or that the environmental conditions at the topographic highs were more favorable for the bioherm-forming microbial communities. Increased light availability, greater wave-base energy, the availability of more initiation sites, lack of sediment deposition, increased availability of nutrients or carbonate or a combination of these factors all could contribute to the apparent success of the larger, closely spaced bioherms found in these locations. Transitions down gradient from clustered microbial carbonates on the topographic highs to fine-grained sediments along the edge of the profundal zone are associated with topographically related environmental factors such as depth increase/reduction in solar energy, wave/current effects, and deposition of sediments. Areas absent of microbial bioherms are primarily in pelagic zones or along the margins of the lake where depth-related environmental factors or clastic deposition has prevented their formation or effectively masked their occurrence.

5.6 Microbial Bioherm Features

In the surveyed areas of the south part of the lake, patterns of bioherm occurrence are directly related to topographic offsets resulting from tectonic activity. Faults and folds are apparent in the CHIRP profiles and coincide with the topographic offsets and abrupt edges of the linear microbial distributions (Figs. 41, 42). At the base of the footwall ramp, bioherm distributions generally grade into fine-grained sediment and, in some cases, appear to be completely buried by onlapping sediment. Observations of changes in bioherm size and density from the shallow to deeper water gradient suggest that it is not the faulting itself that controls the location of the bioherms but the changes in associated environmental conditions along that gradient. In more pelagic environments decreased light availability, less wave-base energy, fewer initiation surfaces, increases in fine-grained sediment deposition, decreases in the availability of nutrients or carbonate, or a combination of these factors could account for decreasing bioherm populations and more dispersed populations.

In areas of repeating linear bioherm populations aligned parallel to the small-scale topographic offsets, modern sediment infills the fault-controlled intervening lows. Preferential sediment accumulation between the tectonically controlled topographic highs is likely due to winnowing and reworking of fine-grained sediment from the highs and redeposition in the topographic lows as wave-base energy diminishes with depth. Despite the fact that the topographic lows experience less wave-base energy, the sediment is still reworked as bedforms are observed within these regions. Bioherm distributions examined in this study all appear to be above wave base as bedforms are apparent in deeper unconsolidated sediments adjacent to the bioherms. The relation between structural topographic highs associated with microbial bioherm occurrence and corresponding onlapping sediments trapped in hanging wall lows is consistent with observations from ancient microbialite deposits (Johnson and Grotzinger, 2006), which suggests lateral growth of microbialites is inhibited by sedimentation. The reduction in light availability, "drowning" of the microbial communities responsible for bioherm growth, or the lack of appropriate initiation locations could all contribute to the lack of extensive bioherms in these areas and the observed patterns of microbial bioherm occurrence in the lake.

Deeper stratigraphic horizons directly underlying the microbial bioherms are imaged in the CHIRP data as concordant, acoustically diaphanous strata with minimal lateral thickness variability, a pattern consistent with profundal lacustrine deposition.

5.7 Effects of Salinity Changes

Data were collected to investigate if anthropogenically induced changes to Great Salt Lake have affected the microbial bioherms from areas south and north of the rock-filled railroad causeway where salinities currently average about 15 percent and about 27 percent, respectively. These data were collected to address the issues raised by research question 3, as found in Section 3.2

Observations, videography, and samples of microbial bioherms from the south part of Great Salt Lake, in modern conditions of salinity averaging about 15 percent, show that the exterior of the bioherms are highly rugose and dark green in color, the color being a result of an abundant surface-based phototrophic community. Macroinvertebrate grazers are in abundance on the surface of the bioherms and in the surrounding water. Interstitial regions between the bioherm nodules contain organic debris (e.g., dead brine shrimp and brine fly larvae), weathered bioclastic detritus, oolitic sands, and clays. Deposits of calcareous detritus with wave-induced ripple patterns, located immediately adjacent to microbial deposits in the south part of the lake, infer recent formation, weathering, erosion, and localized deposition of material sourced from the adjacent bioherms (Fig. 43). Dissolved oxygen profiles acquired above the bioherms in the south part show an increase in dissolved oxygen near the lake floor, indicating photosynthetic primary production associated with the bioherms.

In marked contrast to the shallow-water bioherms and associated detritus observed in the south part of the lake, shallow-water bioherms in the north part of the lake are white and not populated by either surface-based phototrophic communities or macro-invertebrate grazers. Bioherms in the north part of the lake have a lower surface roughness and are surrounded by fine sands and mud. Deposits of calcareous detritus adjacent to the bioherms are conspicuously absent. Increases in dissolved oxygen were not observed near the bioherms, indicating that photosynthetic primary production was not occurring at a similar rate as in the south part of the lake. Conditions in the north part of Great Salt Lake, averaging about 27 percent salinity, appear to have exceeded the environmental range of survival for bioherm-forming microbial communities (Fig. 44).

The high salinity in the north part of the lake has resulted in the death of the microbial bioherm-forming community structure. Although the bioherms in the north part of the lake appear to be moribund, bacterial communities likely remain or a different bacterial community may exist on the previously productive bioherms.

In the northern part of the lake, videography and samples show that thick deposits of cm-sized salt crystals cover inferred bioherms in the deeper waters. The depth at which bioherm morphology is obscured in the geophysical data is consistent with the depth where thick salt deposits (>25 cm) are observed at the dive sites. Thick layers of salt crystals accumulate in deeper water in the north part of Great Salt Lake and obscure bioherm morphology. Salt crystals precipitate at the surface of the lake (Fig. 45) or directly in the water column, sink, and form a layer of salt on the lake floor. Thick layers of salt are inhibited from forming in shallow regions as wave-base energy and currents transport the salt crystals lakeward to deeper water.

Underwater videography acquired by divers during the verification of bioherm occurrence documents the biological associations between brine shrimp, brine fly larvae, brine flies and the bioherm microbial community and structures both in the south and north parts of Great Salt Lake. In the south part of Great Salt Lake, brine fly larvae and brine shrimp occur coincident with the microbial bioherms and calcareous detritus immediately adjacent to the bioherms. Underwater videography acquired in the north part of Great Salt Lake imaged extensive deposits of cm-sized salt crystals at the sediment–water interface, obscuring bioherm morphology. Microbial communities, brine shrimp, brine fly larvae, and brine flies were visually absent from the benthos in the north part of Great Salt Lake.

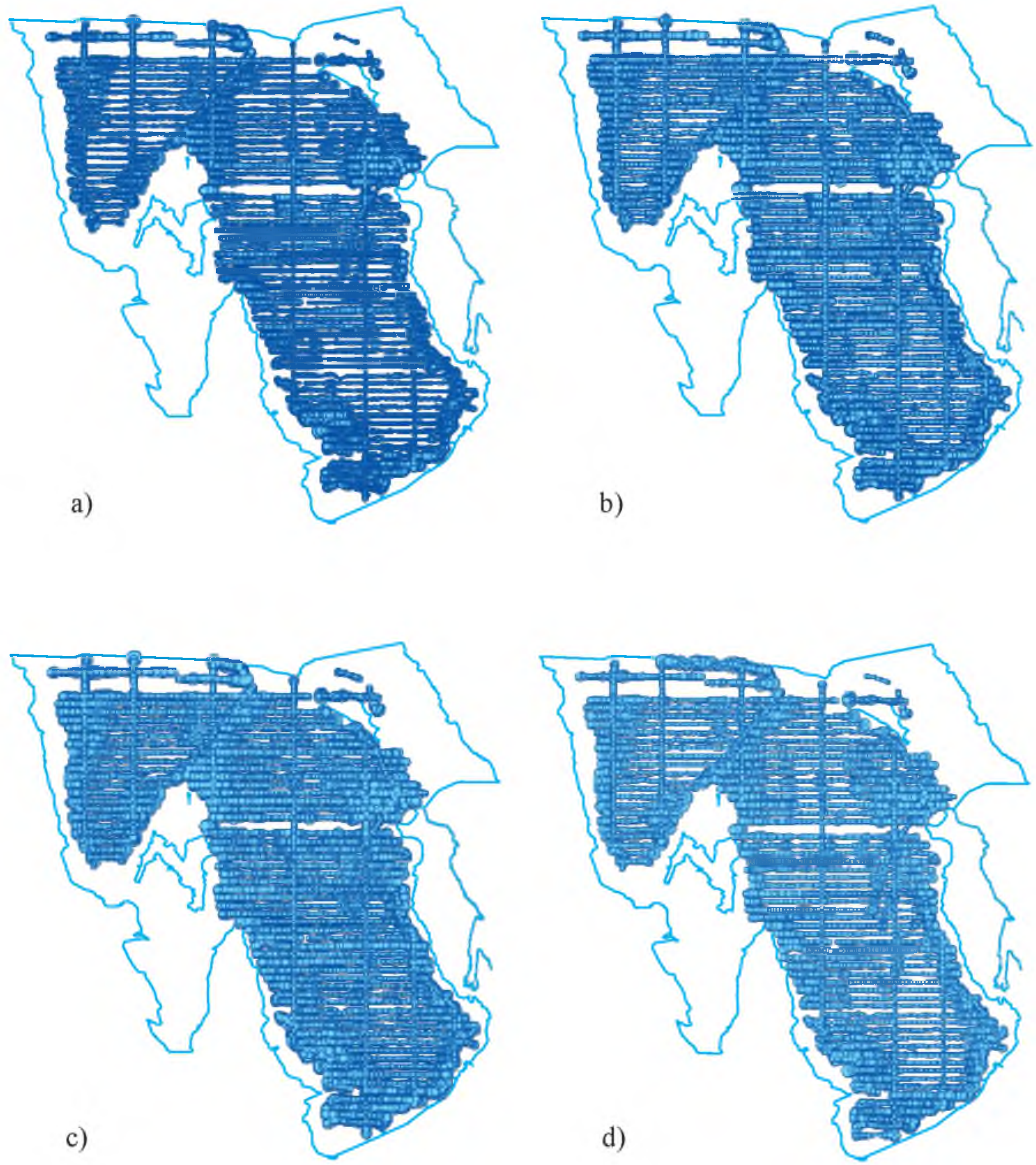

Figure 21. Calculated rugosity values for 50, 100, 250, and 500-sample intervals, south part of Great Salt Lake, Utah. Larger diameter circles indicate larger calculated rugosity. Rugosity based on a) 50-sample interval, b) 100-sample interval, c) 250-sample interval, and d) 500-sample interval.

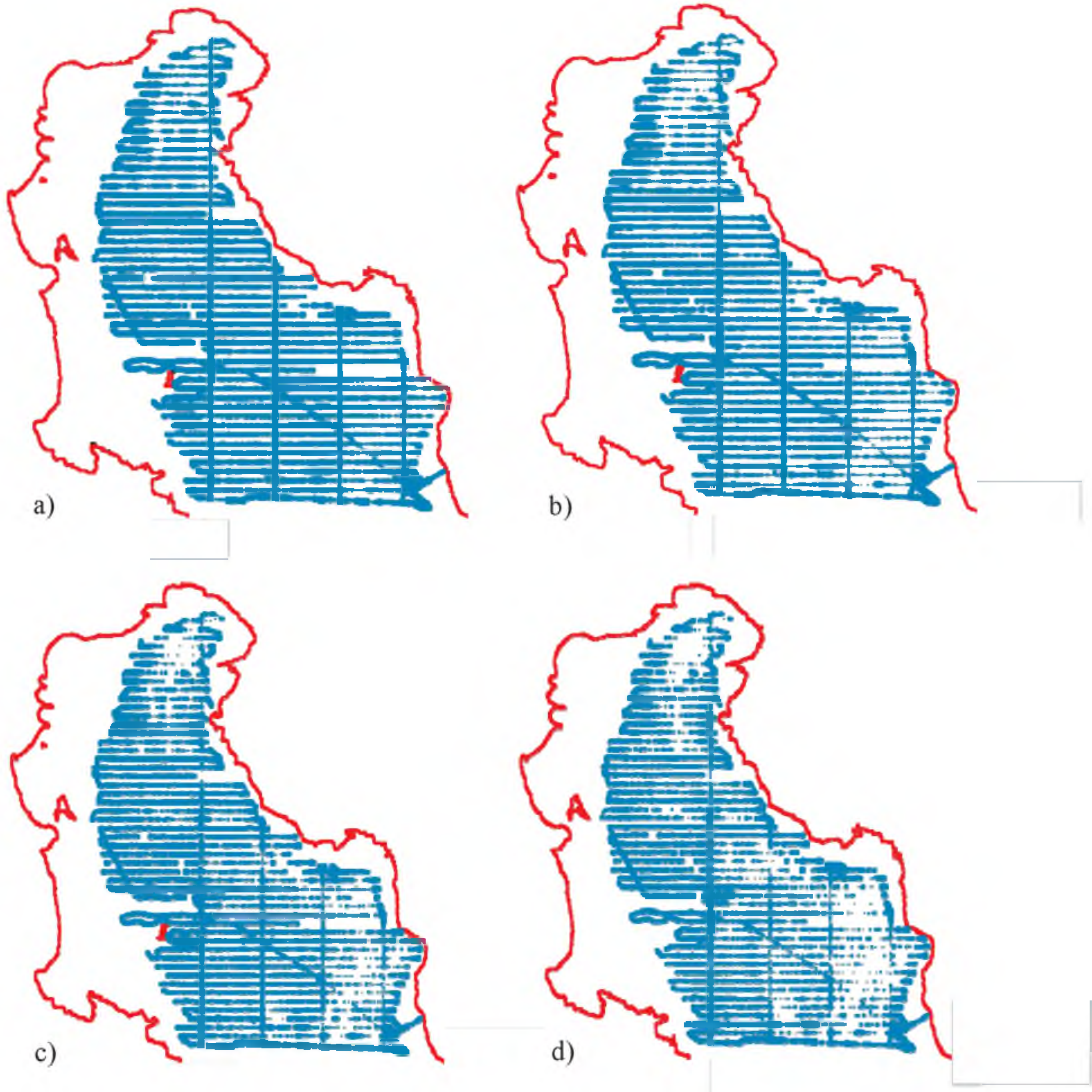

Figure 22. Calculated rugosity values for 50, 100, 250, and 500-sample intervals, north part of Great Salt Lake, Utah. Larger diameter circles indicate larger calculated rugosity. Rugosity based on a) 50-sample interval, b) 100-sample interval, c) 250-sample interval, and d) 500-sample interval.

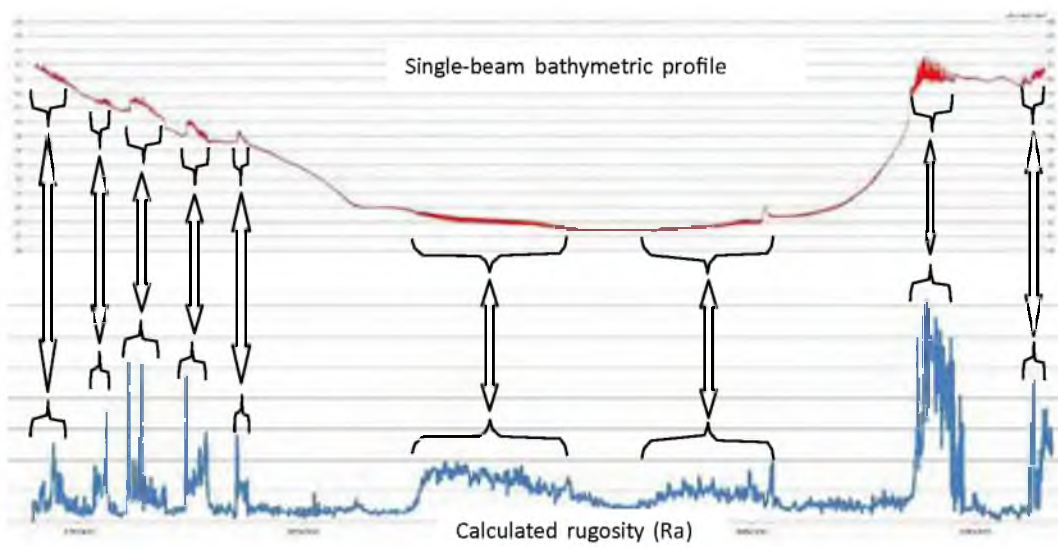

Figure 23. Comparison between mathematically derived rugosity values and the analog interpretation of increased variation in benthic rugosity derived from bathymetric data, Great Salt Lake, Utah.

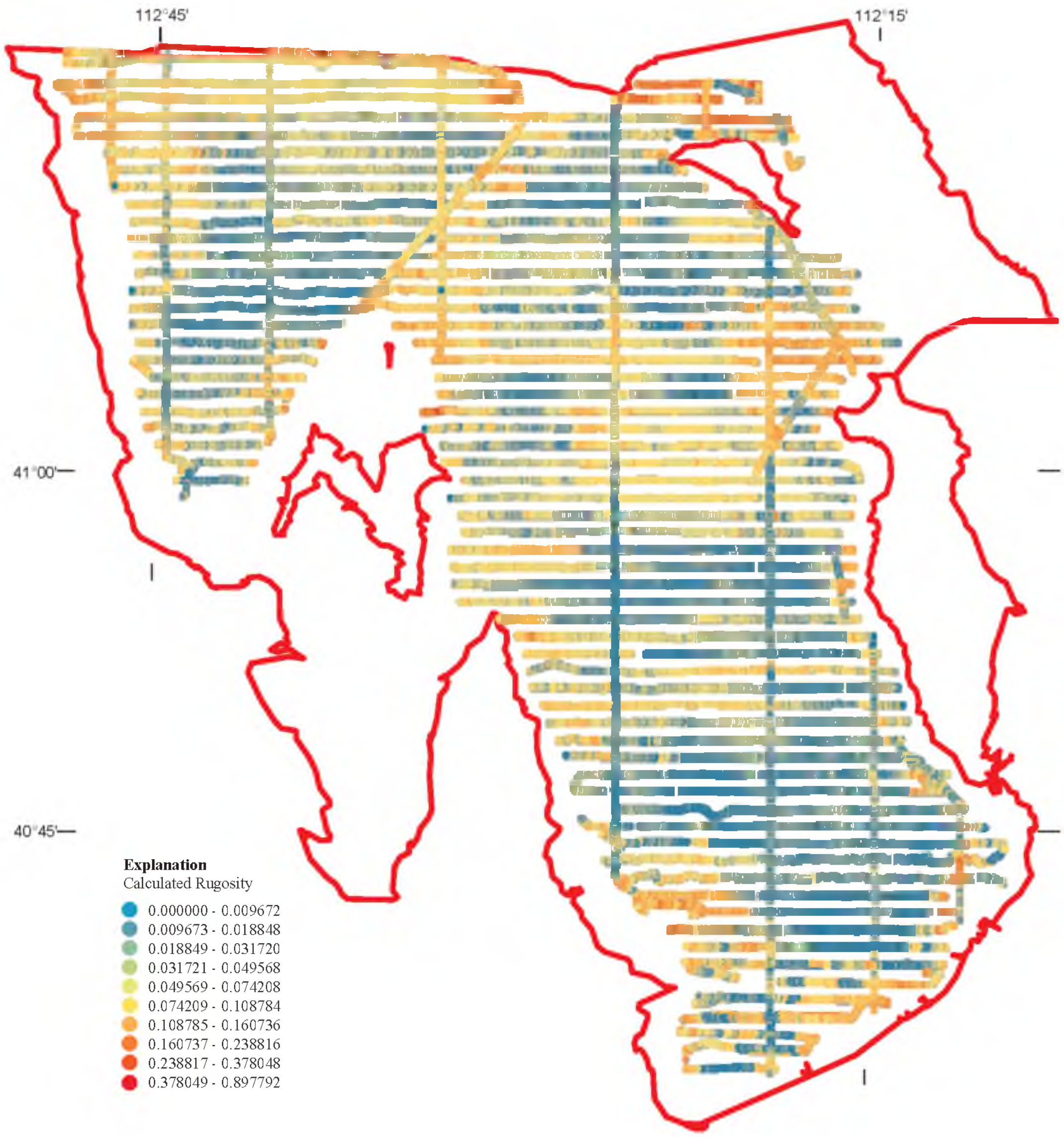

Figure 24. Distribution of calculated rugosity for 50-sample transect subsets, south part of Great Salt Lake, Utah. Data displayed as 10-class geometric interval.

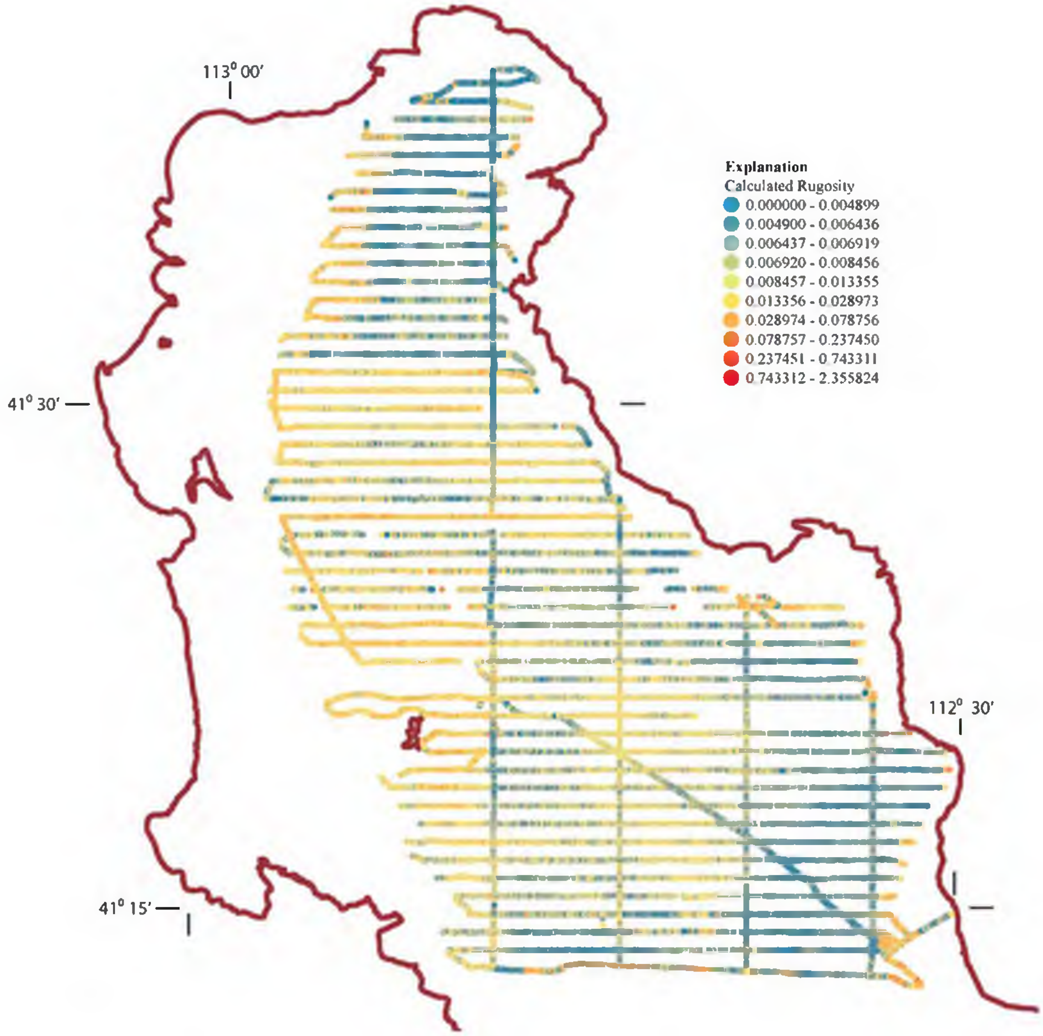

Figure 25. Distribution of calculated rugosity for the 50-sample transect subsets, north part of Great Salt Lake, Utah. Background data displayed as 50-sample rugosity, 10-class geometric intervals.

Table 1. Summary statistics for calculated benthic rugosity, south part of Great Salt Lake, Utah. Statistics include results from 50-sample; 100-sample; 250-sample; and 500-sample interval calculations. Increases in many of the statistical values are a function of the increased number of samples used in the calculation of rugosity and the higher variance within the increasingly larger sample sets.

Statistic	50 Point Rugosity	100 Point Rugosity	250 Point Rugosity	500 Point Rugosity
Mean	0.0211	0.0249	0.0333	0.0449
Standard Error	0.0001	0.0002	0.0004	0.0007
Median	0.0099	0.0117	0.0159	0.0226
Mode	0.0050	0.0048	0.0077	0.0168
Standard Deviation	0.0394	0.0460	0.0608	0.0778
Sample Variance	0.0016	0.0021	0.0037	0.0060
Kurtosis	161.6115	136.0889	123.6876	97.2717
Skewness	9.2951	8.6616	8.4778	7.6350
Range	1.3807	1.6217	1.8801	1.9741
Minimum	0.0000	0.0000	0.0000	0.0001
Maximum	1.3807	1.6217	1.8801	1.9741

Table 2. Summary statistics for calculated benthic rugosity, north part of Great Salt Lake, Utah. Statistics include results from 50-sample; 100-sample; 250-sample; and 500-sample interval calculations. Increases in many of the statistical values are a function of the increased number of samples used in the calculation of rugosity and the higher variance within the increasingly larger sample sets.

Statistic	50 Point Rugosity	100 Point Rugosity	250 Point Rugosity	500 Point Rugosity
Mean	0.0203	0.0237	0.0307	0.0400
Standard Error	0.0001	0.0002	0.0004	0.0008
Median	0.0108	0.0127	0.0160	0.0206
Mode	0.0050	0.0054	0.0075	0.0166
Standard Deviation	0.0310	0.0373	0.0529	0.0761
Sample Variance	0.0010	0.0014	0.0028	0.0058
Kurtosis	111.5138	278.9292	305.9980	488.6738
Skewness	6.8747	9.7349	11.7928	14.8343
Range	1.3418	2.0888	2.2333	3.4733
Minimum	0.0000	0.0000	0.0000	0.0000
Maximum	1.3418	2.0888	2.2333	3.4733

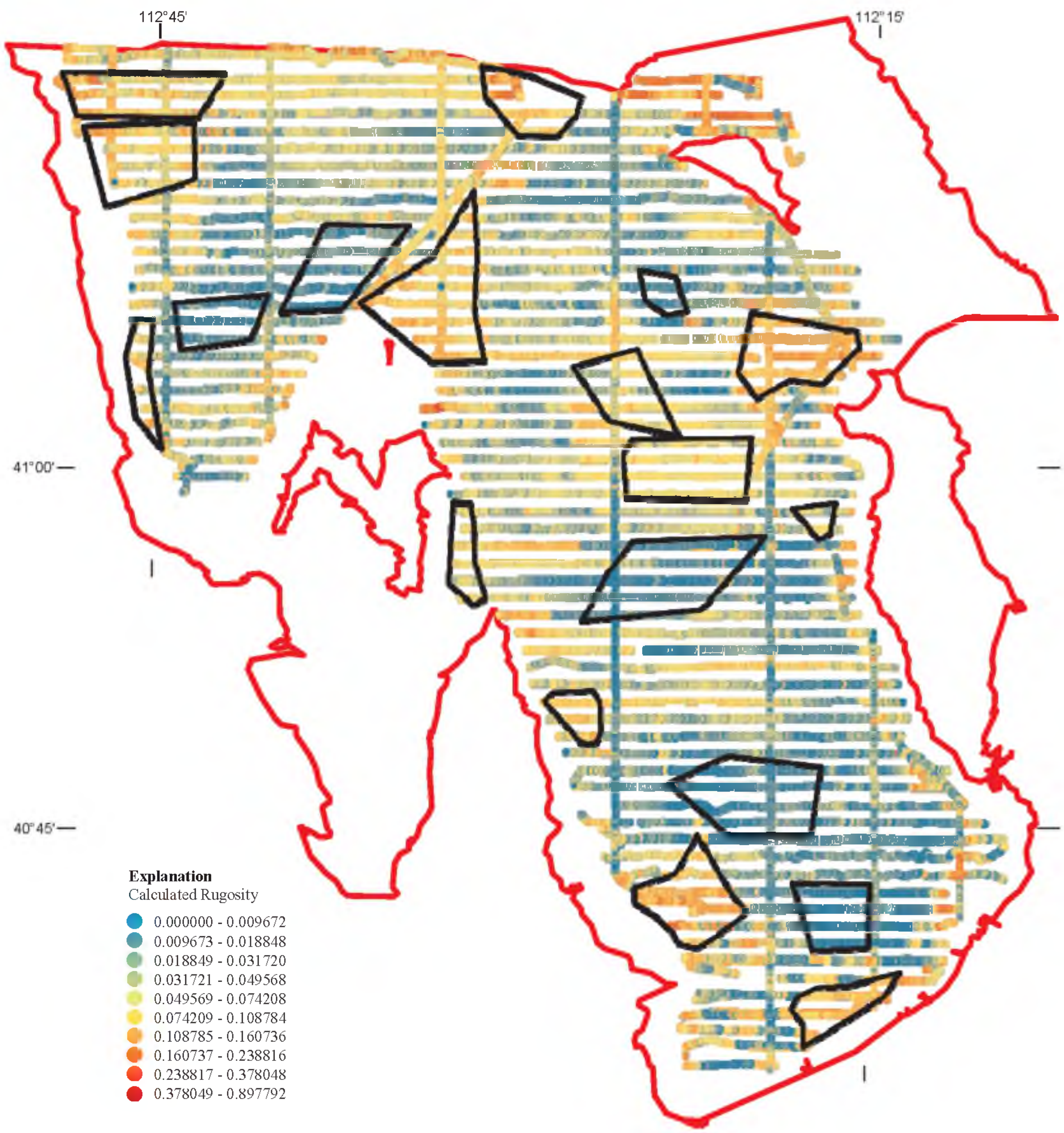

Figure 26. Location of selected polygonal areas with relatively uniform rugosity, south part of Great Salt Lake, Utah. Background data displayed as 50-sample rugosity, 10-class geometric intervals.

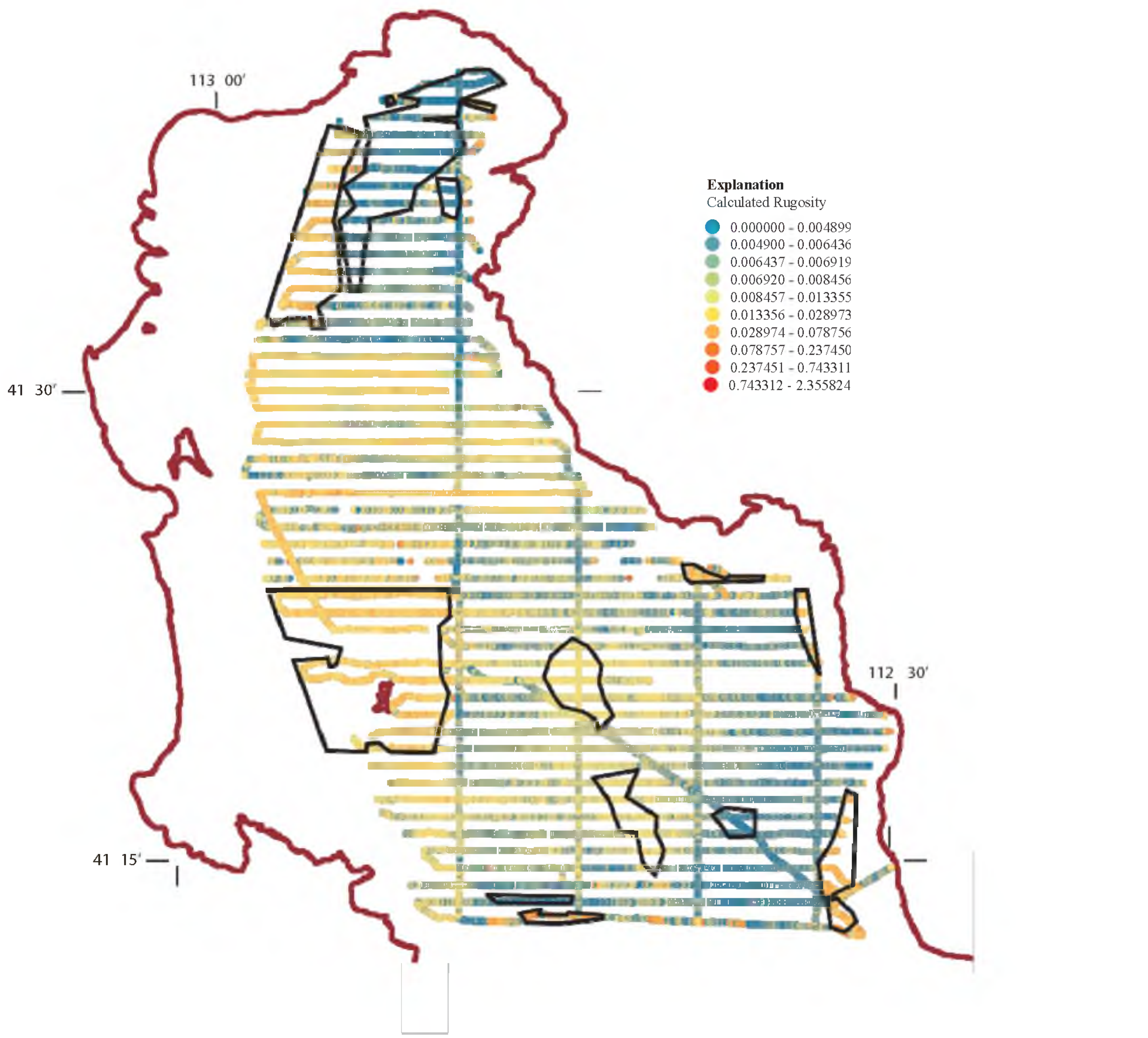

Figure 27. Location of selected polygonal areas with relatively uniform rugosity, north part of Great Salt Lake, Utah. Background data displayed as 50-sample rugosity, 10-class geometric intervals.

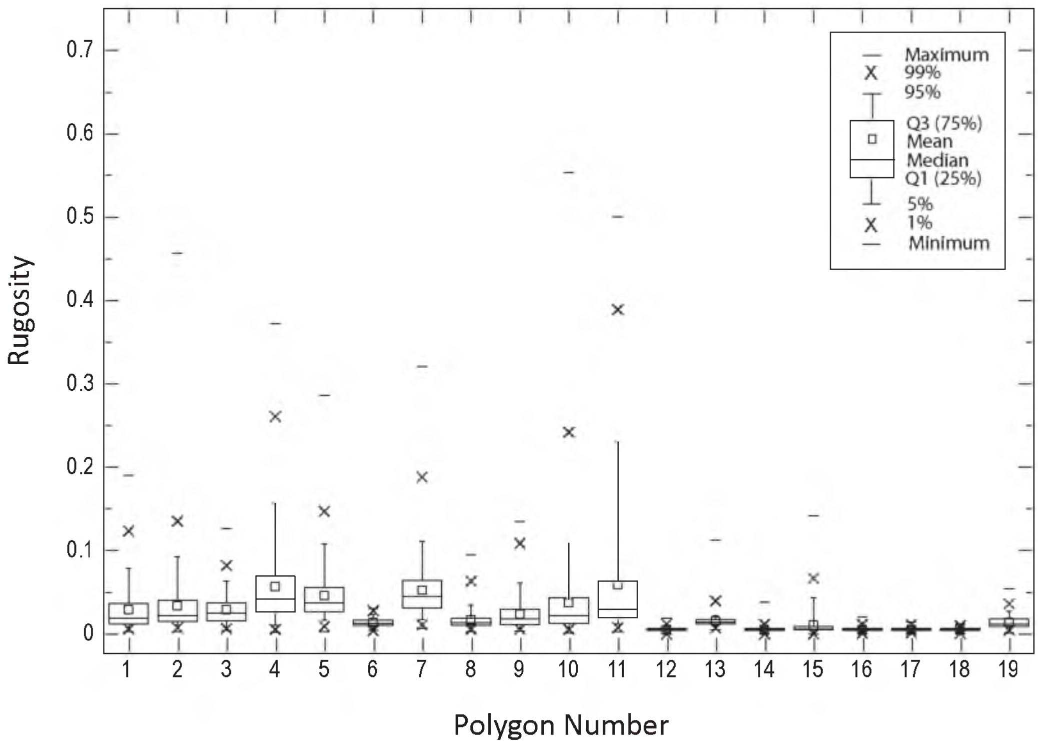

Figure 28. Box plots showing calculated rugosity minimum, maximum, mean, standard deviation, skewness, and interquartile range for each of 19 polygonal areas, south part of Great Salt Lake, Utah.

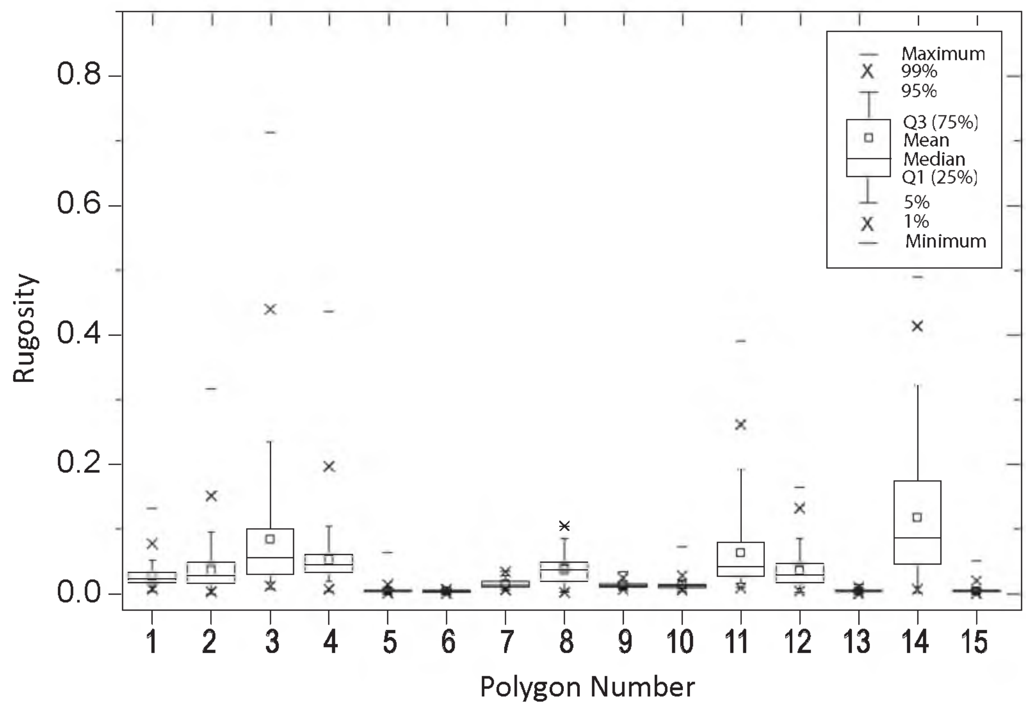

Figure 29. Box plots showing calculated rugosity minimum, maximum, mean, standard deviation, skewness, and interquartile range for each of 15 polygonal areas, north part of Great Salt Lake, Utah.

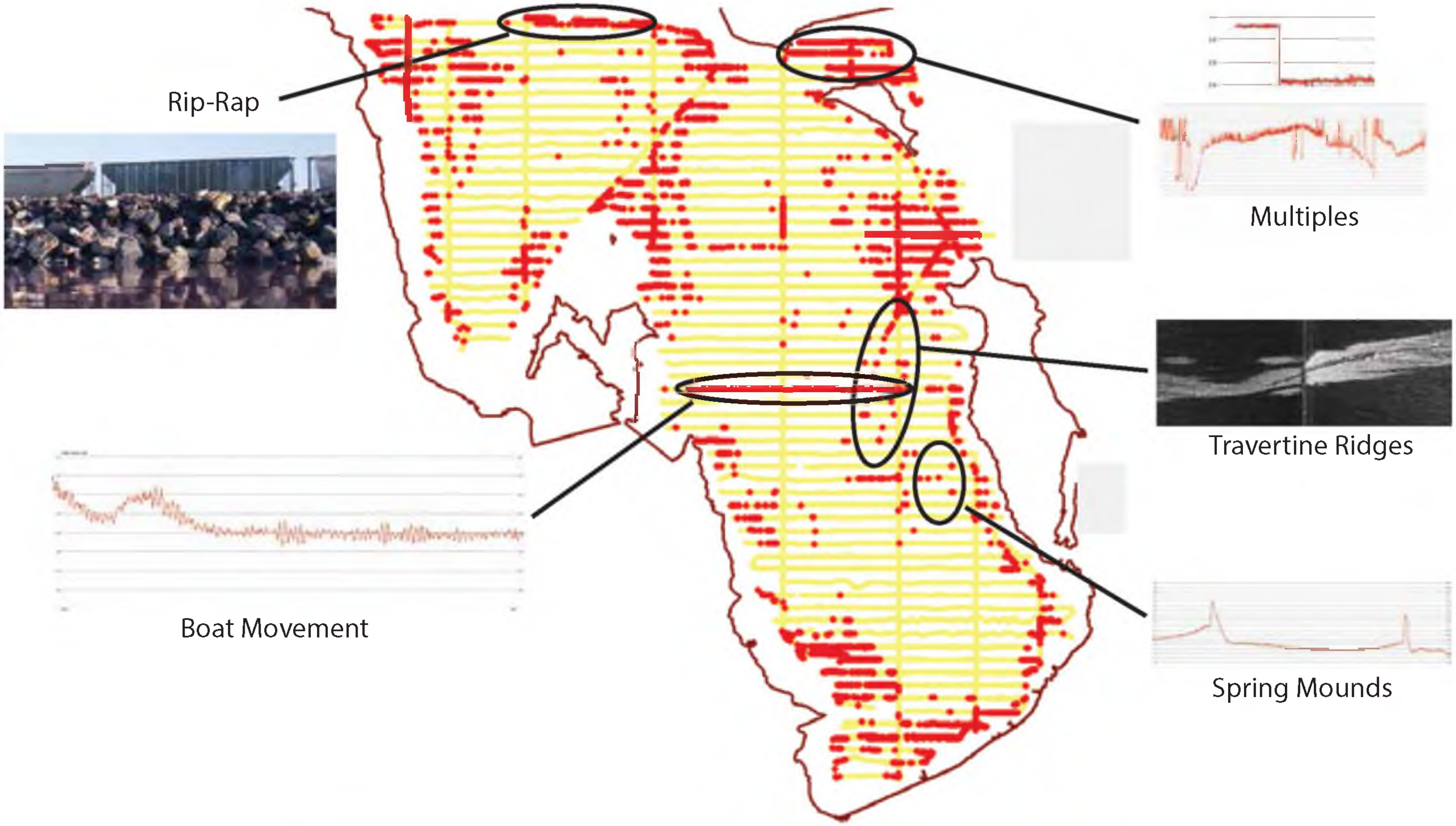

Figure 30. Selected examples of calculated rugosity greater than 0.047 caused by nonbioherm features (circled), south part of Great Salt Lake, Utah. Acoustic outliers were identified by examination of the original analog and digital records, compared to known conditions in the lake, and removed from the dataset before defining the probable extent of microbial bioherm occurrence. Imagery from subsequent side scan sonar investigations identified the causes of increased rugosity at the sediment-water interface.

Figure 31. Selected examples of calculated rugosity greater than 0.071 caused by nonbioherm features (circled), north part of Great Salt Lake, Utah. Acoustic outliers were identified by examination of the original analog and digital records, compared to known conditions in the lake, and removed from the dataset before defining the probable extent of microbial bioherm occurrence. Imagery from subsequent side scan sonar investigations identified the cause of increased rugosity at the sediment-water interface.

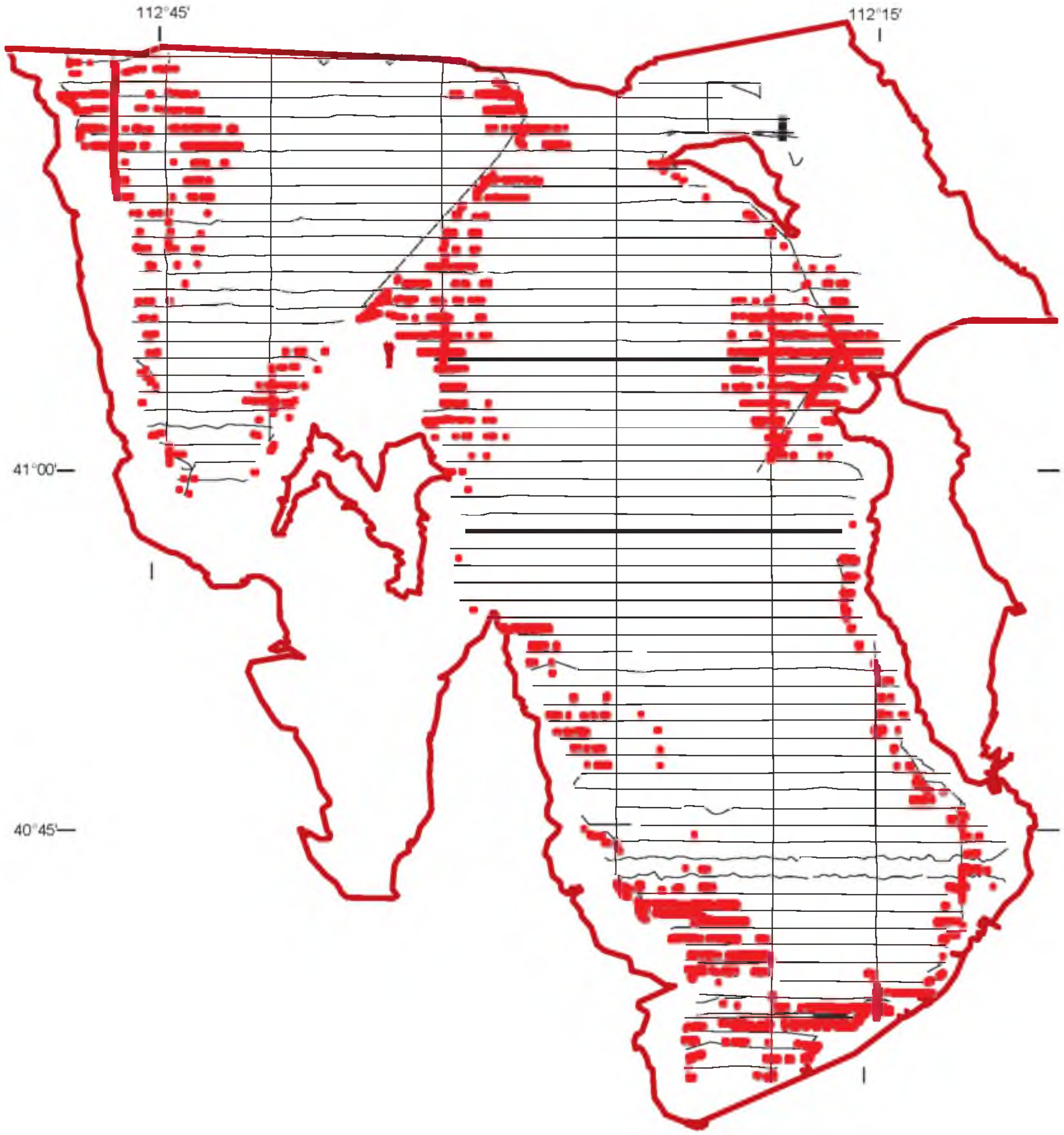

Figure 32. Rugosity values greater than 0.047, south part of Great Salt Lake, Utah. Increases in rugosity greater than 0.047 were used to map the probable occurrence of microbial bioherms in the south part of Great Salt Lake. Lower rugosity values generally occur in pelagic areas of the lake while higher rugosity values generally occur along the margins of the lake in shallower waters. Calculated values associated with known nonbioherm induced acoustic rugosity were previously removed.

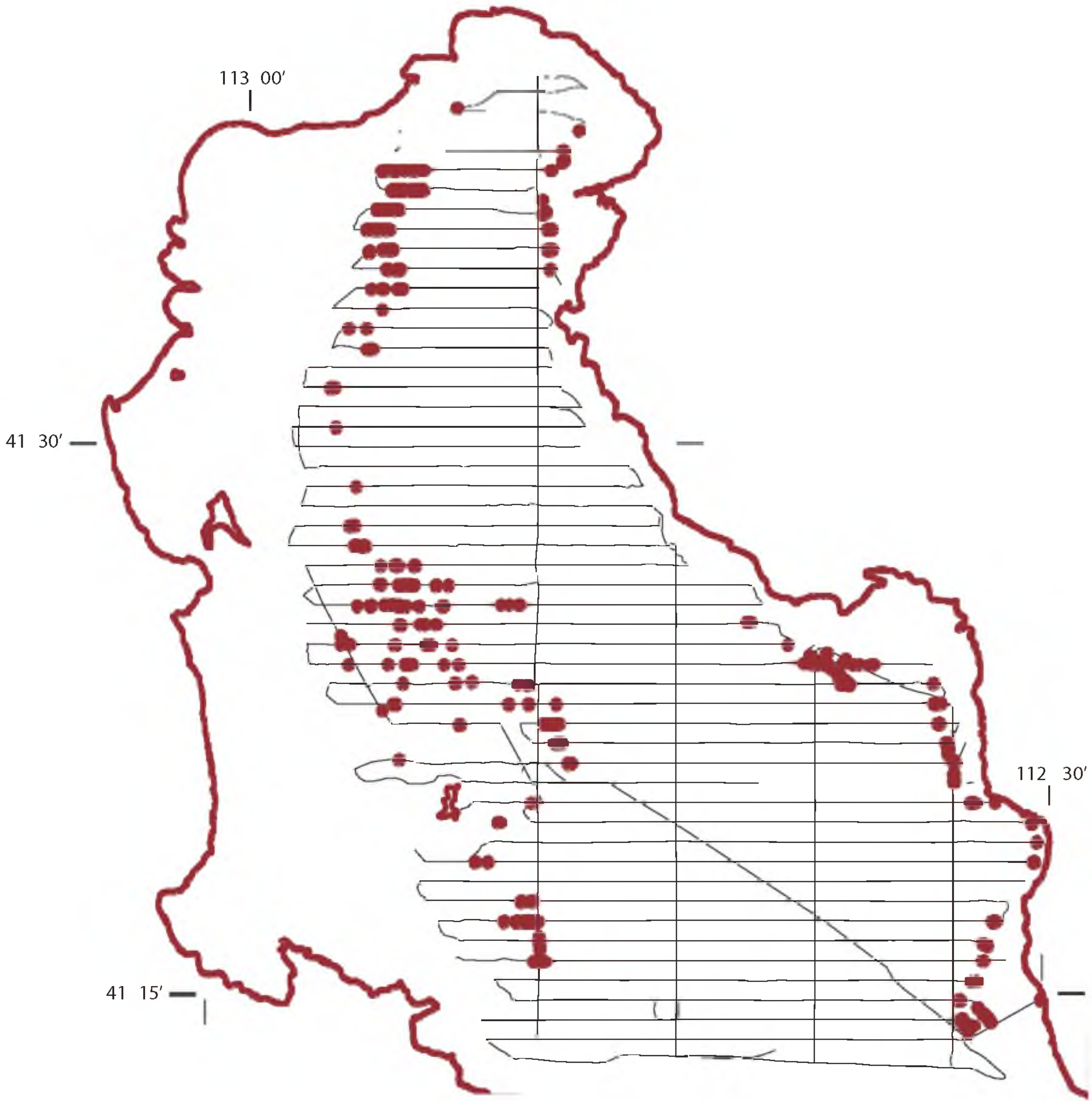

Figure 33. Rugosity values greater than 0.071, north part of Great Salt Lake, Utah. Increases in rugosity greater than 0.071 were used to map the probable occurrence of microbial bioherms in the north part of Great Salt Lake. Lower rugosity values generally occur in pelagic areas of the lake while higher rugosity values generally occur along the margins of the lake in shallower waters. Calculated values associated with known nonbioherm induced acoustic rugosity were previously removed.

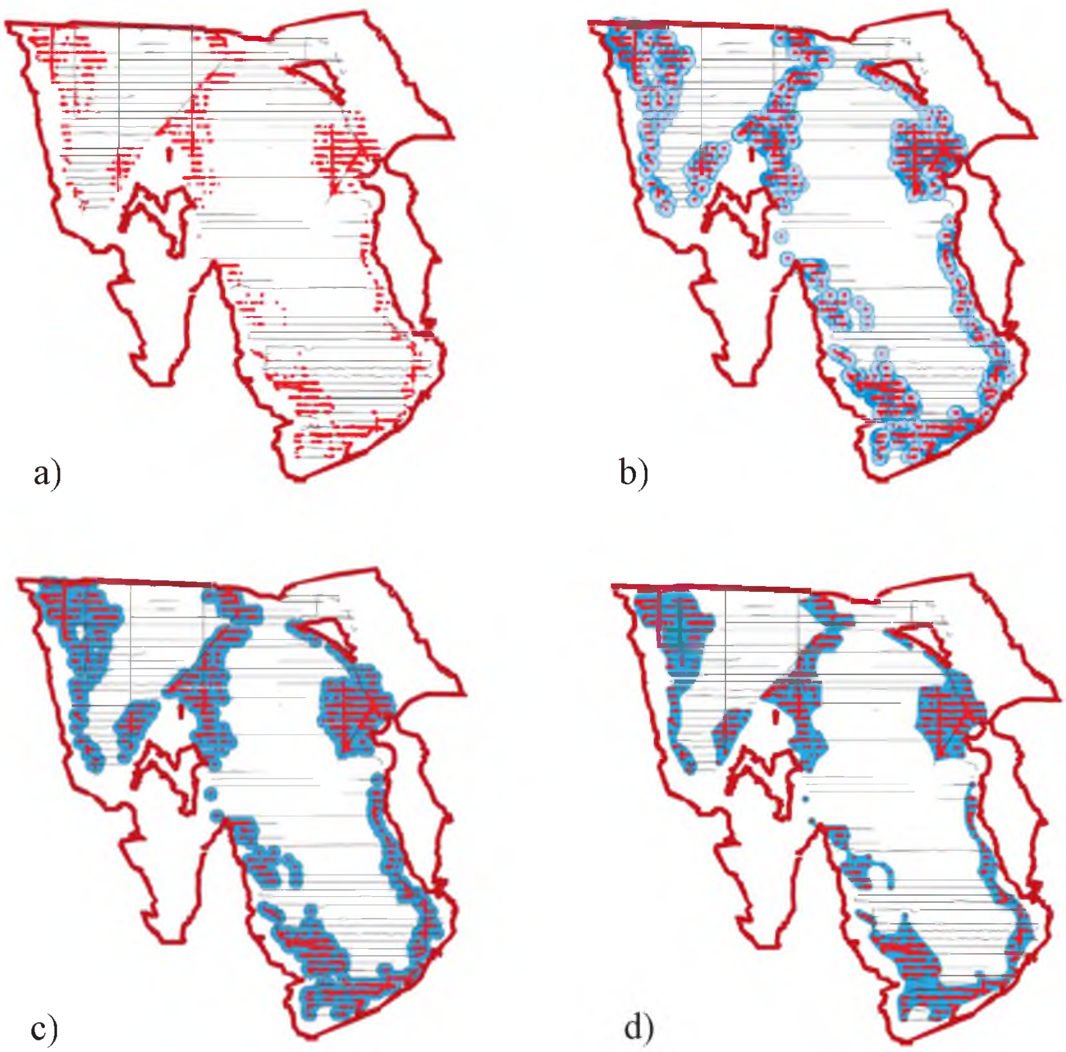

Figure 34. Process for defining the probable distribution of microbial bioherms in the south part of Great Salt Lake, Utah, using calculated rugosity values greater than 0.047. The process included a) limiting rugosity values to GT 0.047, b) creating a 1,000 m buffer around each rugosity value, c) dissolving buffer overlaps and smoothing resultant polygons, and d) creating a 500 m buffer and subtracting that buffer area from the smoothed polygons.

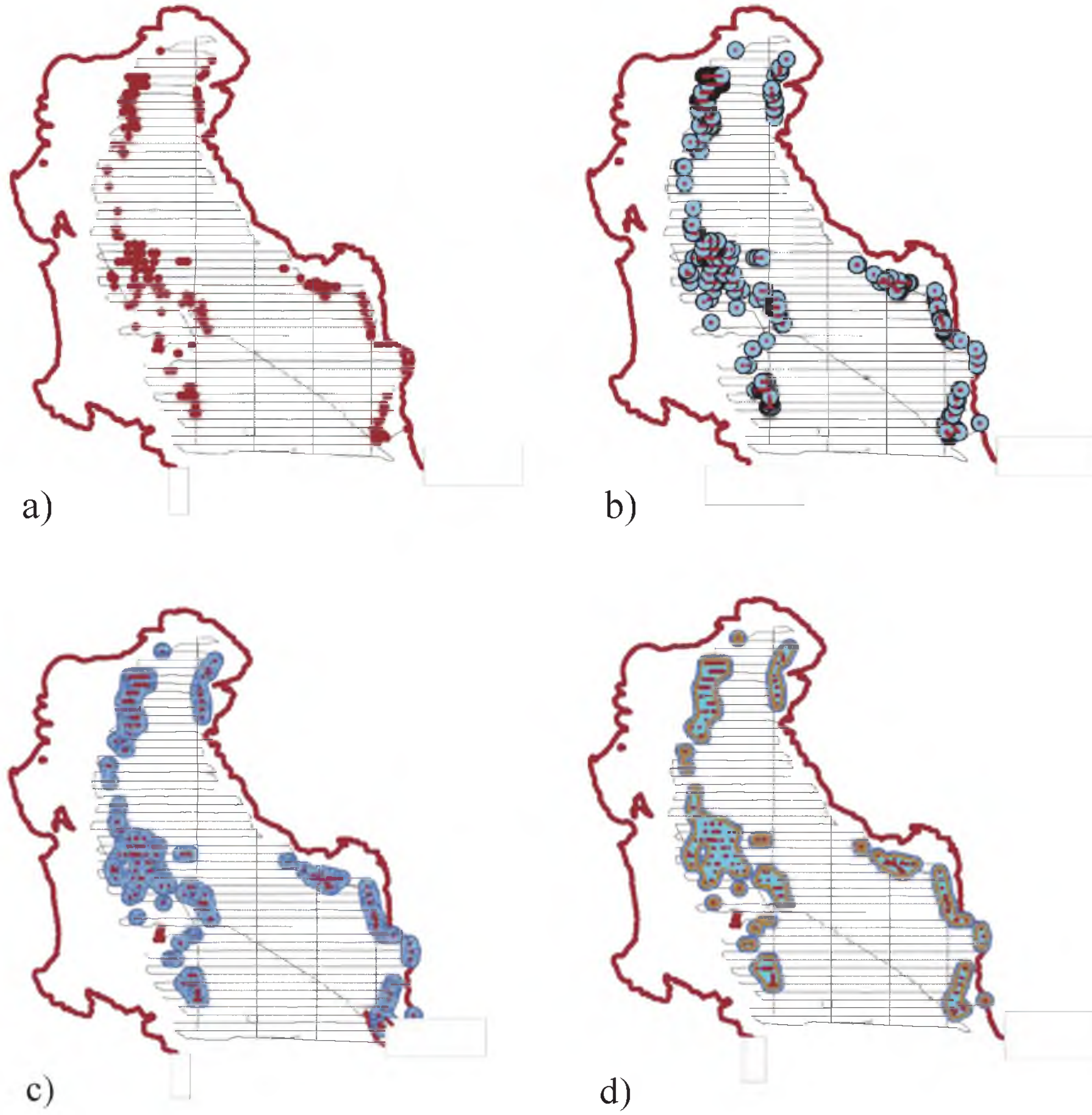

Figure 35. Process for defining the probable distribution of microbial bioherms in the north part of Great Salt Lake, Utah, using calculated rugosity values greater than 0.071. The process included a) limiting rugosity values to GT 0.071, b) creating a 1,000 m buffer around each rugosity value, c) dissolving buffer overlaps and smoothing resultant polygons, and d) creating a 500 m buffer and subtracting that buffer area from the smoothed polygons.

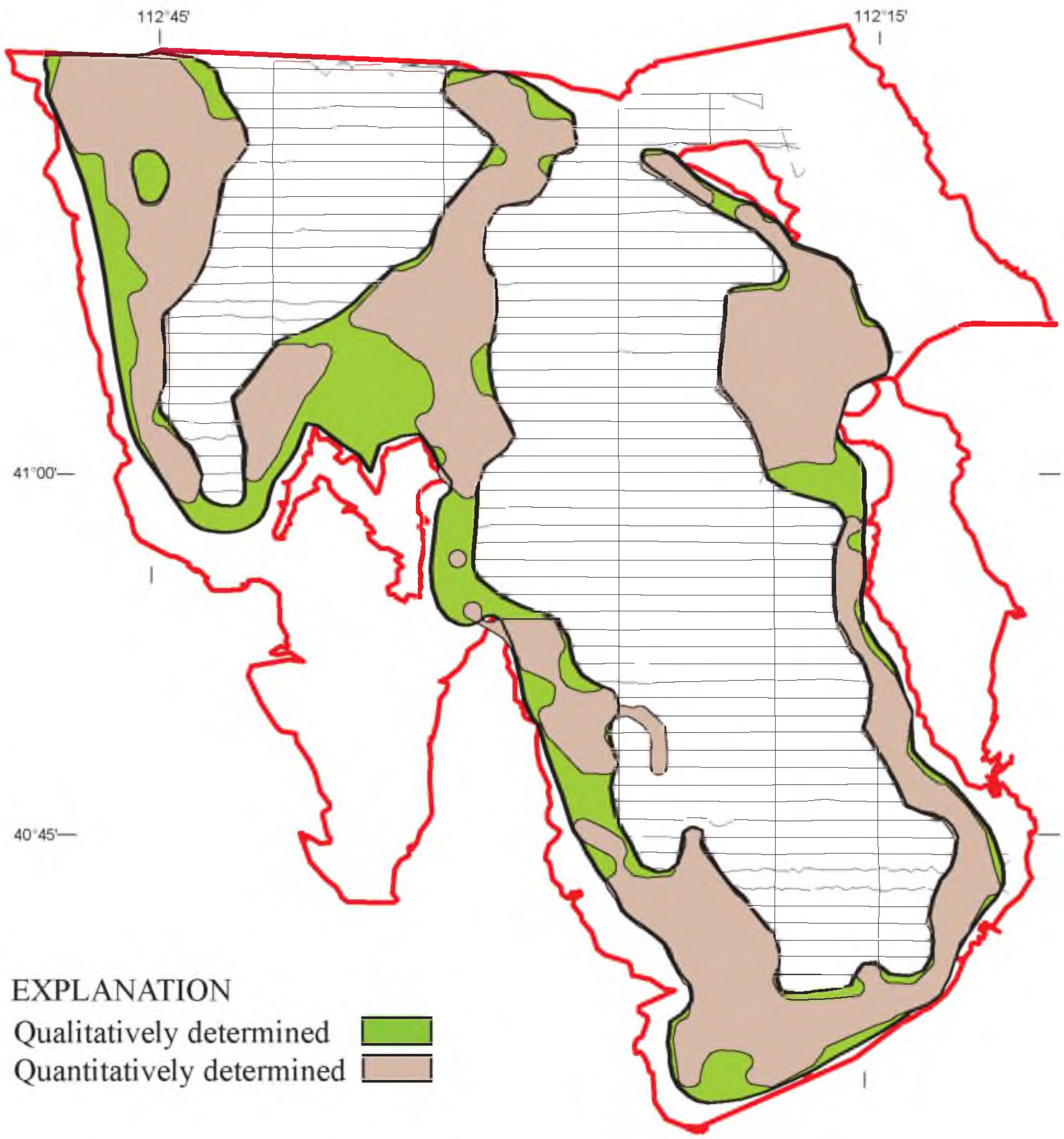

Figure 36. Locations of probable microbial bioherm occurrence derived from quantitative and qualitative methods, south part of Great Salt Lake, Utah.

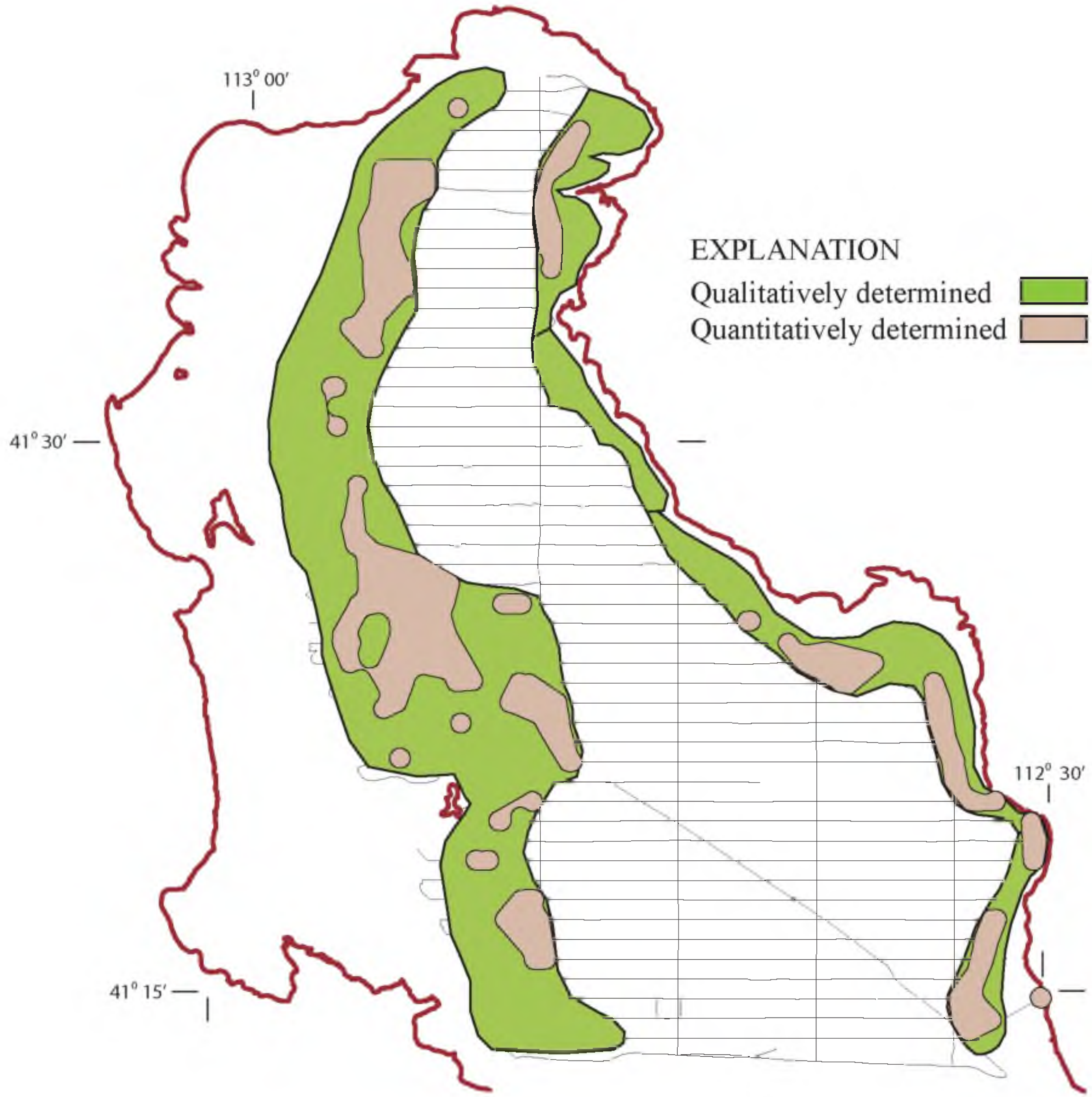

Figure 37. Locations of probable microbial bioherm occurrence derived from quantitative and qualitative methods, north part of Great Salt Lake, Utah.

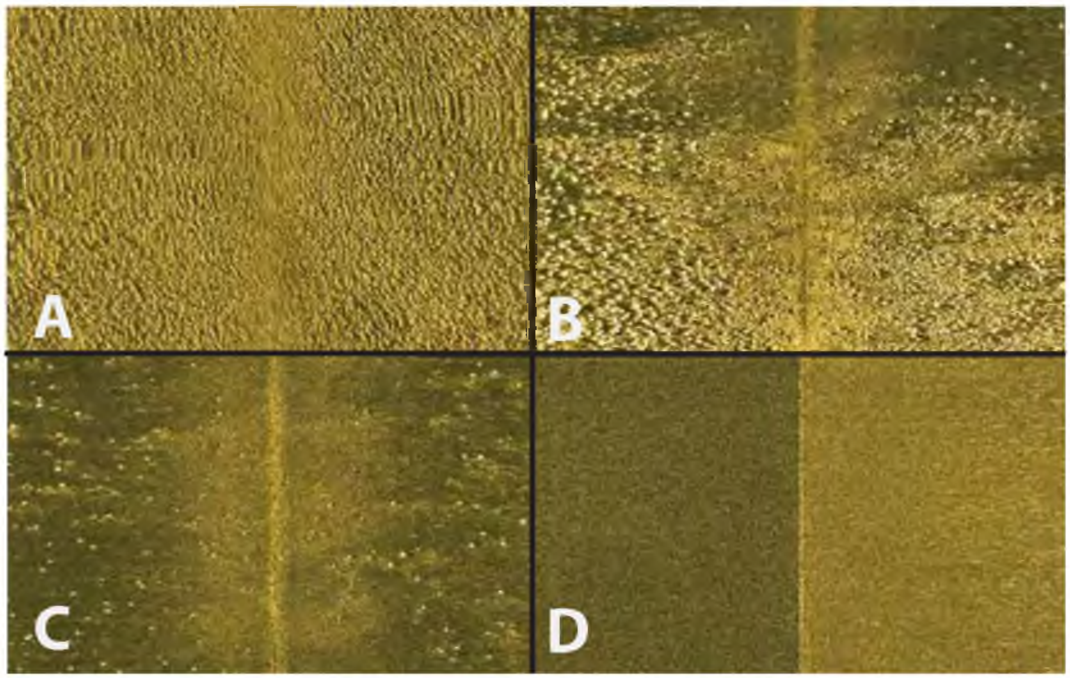

Figure 38. Side scan sonar image showing variations in the distribution of local populations of microbial bioherms, south part of Great Salt Lake, Utah (A) highly clustered microbial bioherm deposit; (B) transitional area from clustered bioherms to a dispersed bioherm distribution; (C) dispersed bioherm distribution; and (D) an area characterized by mud and fine sands.

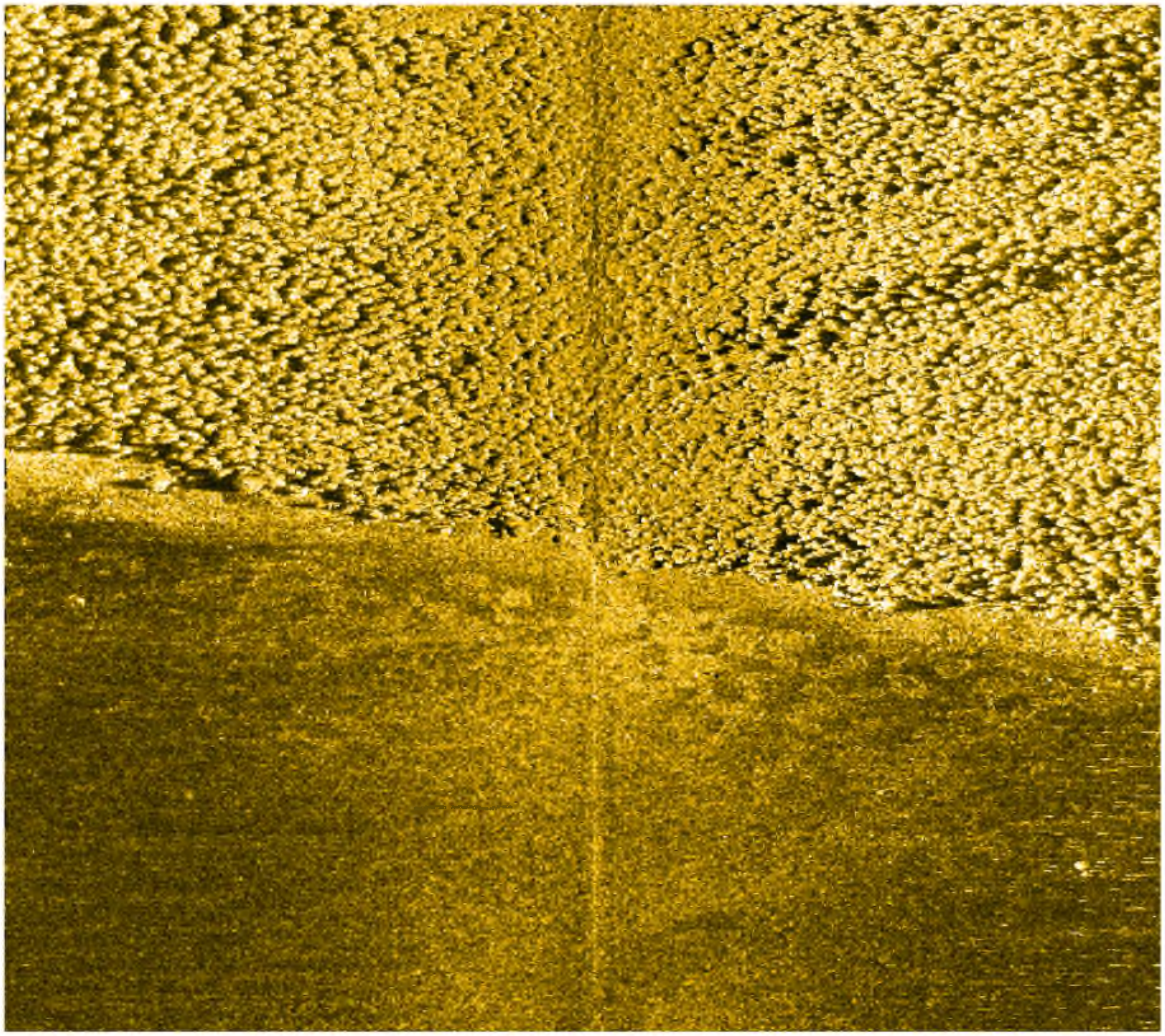

Figure 39. Side scan sonar image showing benthic reef-like microbial bioherm deposit in the south part of Great Salt Lake, Utah. Abrupt change between area of highly clustered microbial bioherms (light-colored area) and adjacent fine-grained sediments (darker area) is related to microtopographic structural control. CHIRP geophysical data acquired simultaneously with the side scan sonar imagery shows a fault-related offset at the mud/sand microbial bioherm interface.

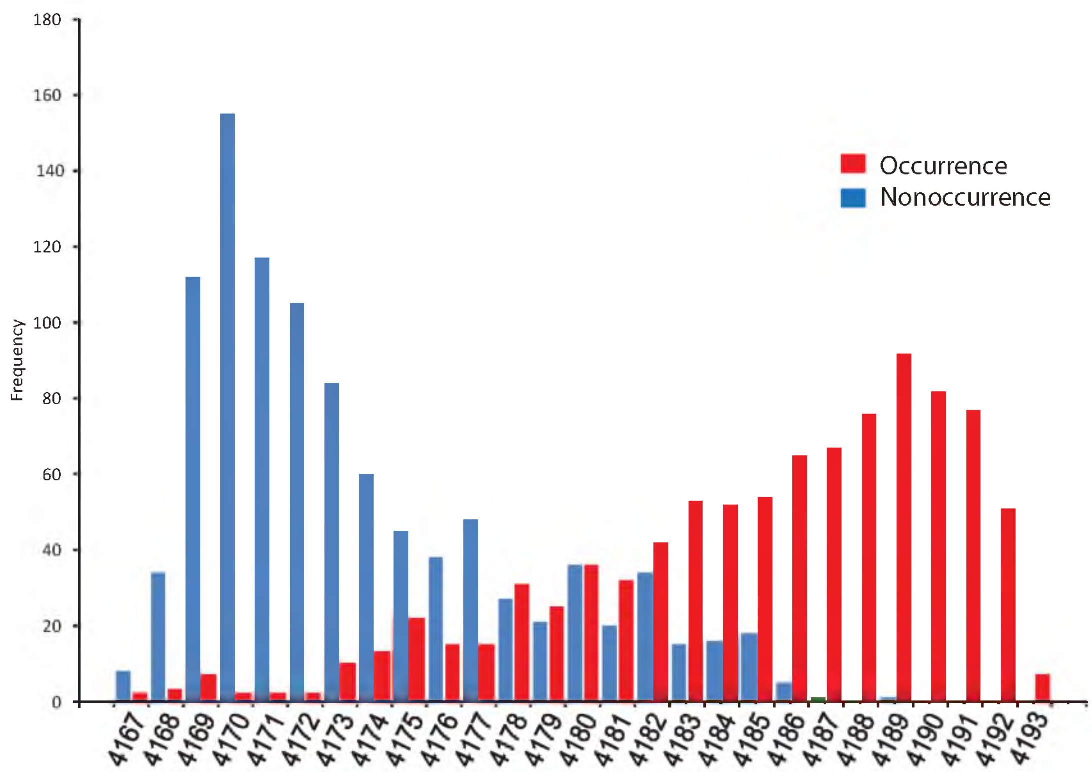

Figure 40. Depth distribution of randomly sampled lake-bottom altitudes from areas of microbial bioherm occurrence and nonoccurrence, south part of Great Salt Lake, Utah.

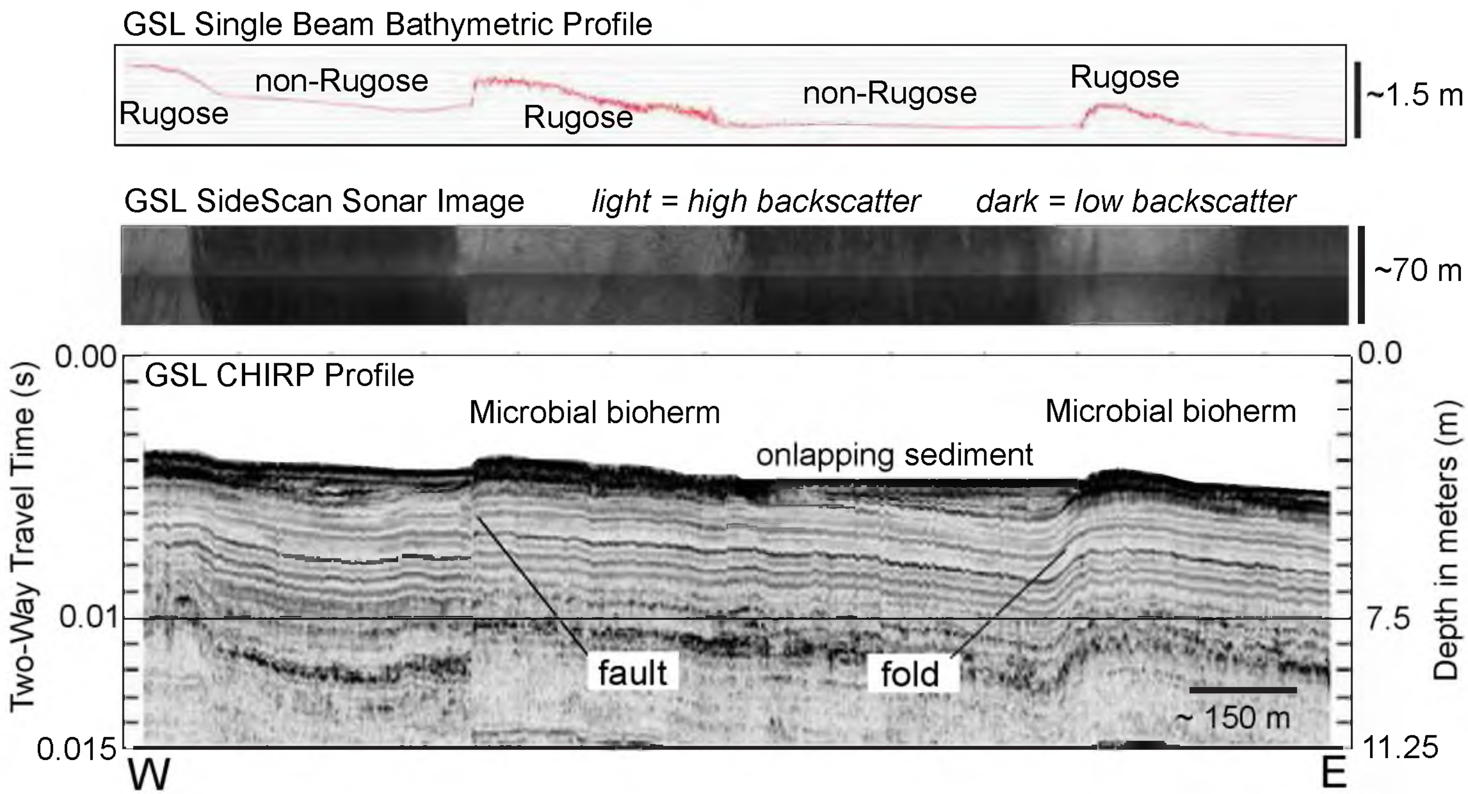

Figure 41. Relation between benthic rugosity, microbial bioherm occurrence and tectonically induced microtopographic offsets along the western margin of the main body of Great Salt Lake, Utah. (Top) Single-beam bathymetry showing variations in roughness and depth associated with microbial bioherm occurrence; (Middle) Side scan sonar mosaic across three microbial bioherm deposits, which are delineated by regions of high backscatter. The intervening lows are infilled with onlapping sediment and have lower backscatter; (Bottom) CHIRP seismic profile coregistered with side scan sonar image llustrates structural control on the topographic highs. Both the fault and fold show growth with depth.

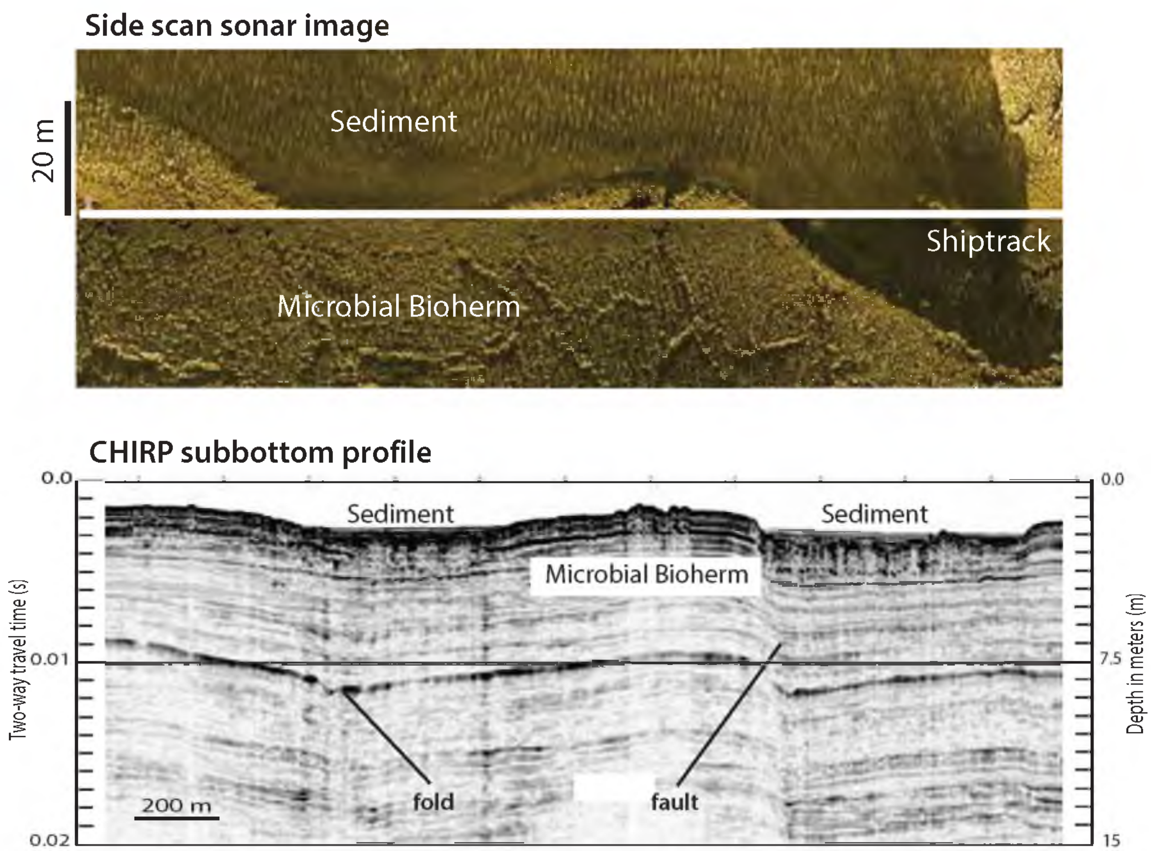

Figure 42. Relation between tectonically induced microtopographic offsets and microbial bioherm occurrence along the northern margin of the south part of Great Salt Lake, Utah.

Figure 43. Recent deposits of detritus derived from microbial bioherms. Location is along the western shore of Antelope Island, Great Salt Lake, Utah.

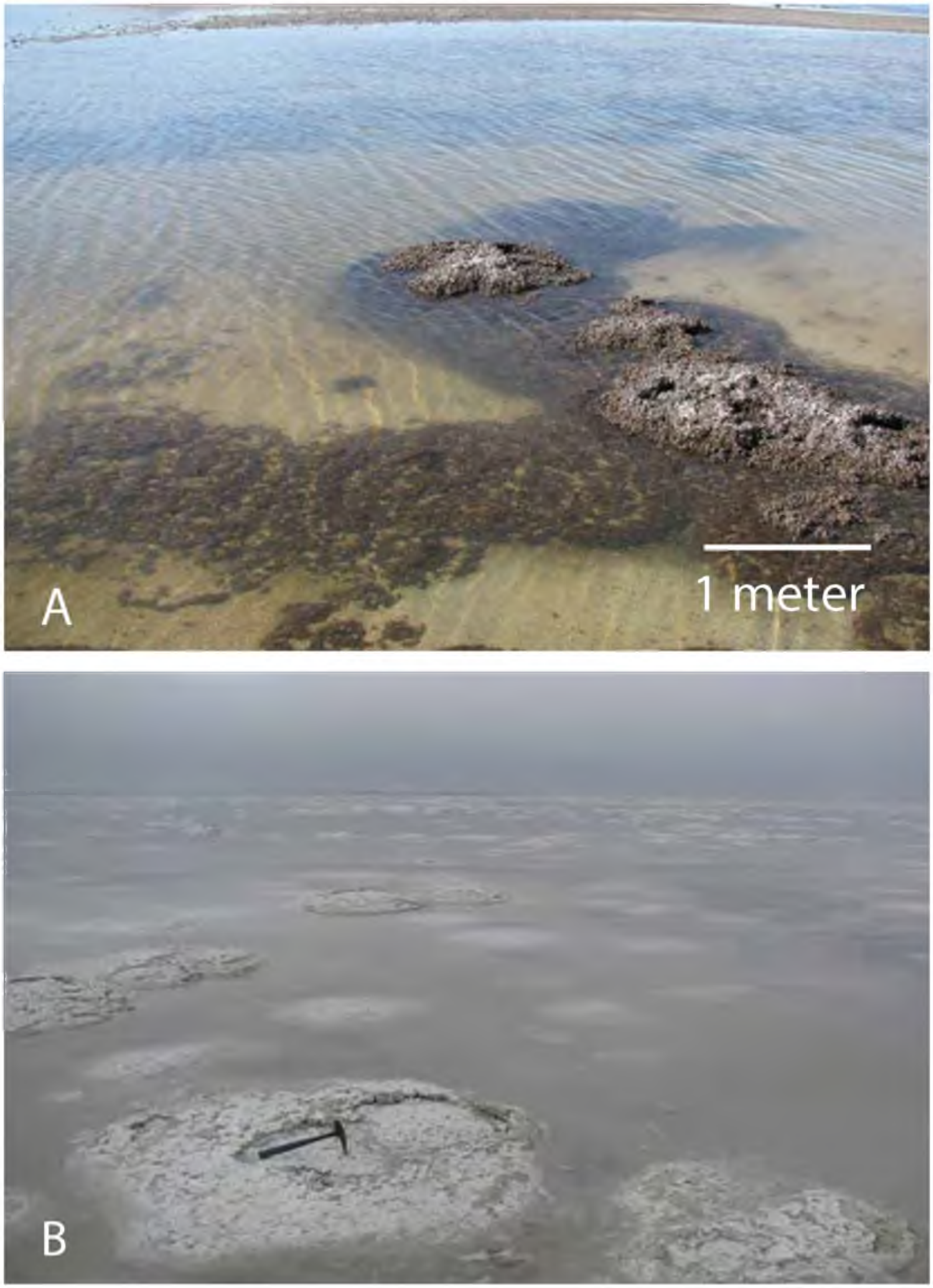

Figure 44. Microbial bioherms located in the south (A) and north (B) parts of Great Salt Lake, Utah.

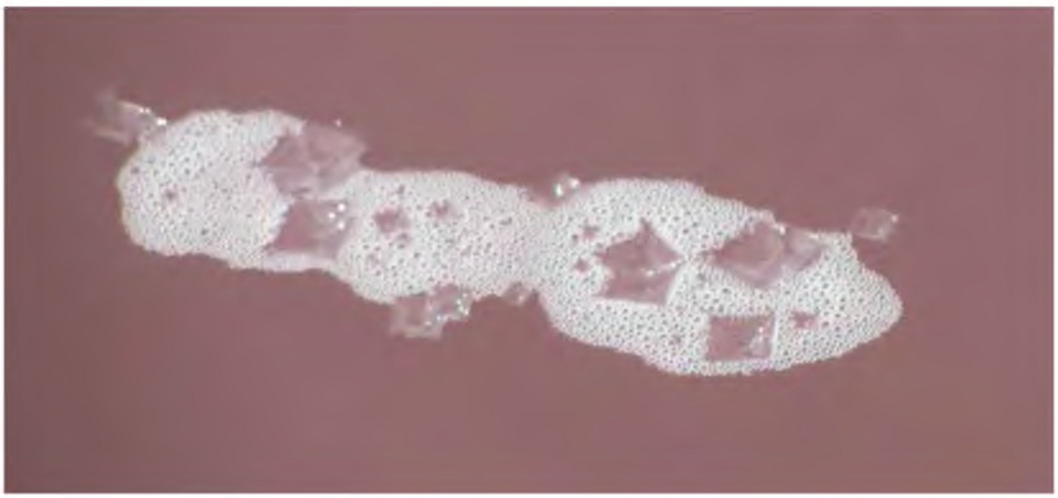

Figure 45. Hopper crystals of sodium chloride forming on the surface of the north part of Great Salt Lake, Utah. The crystals eventually overcome surface tension and sink, forming a layer of salt on the lake floor. In shallow areas, wave-base energy transports the salt crystals lakeward to deeper water, forming thick deposits of cm-sized salt crystals in the deeper waters of the north part of Great Salt Lake.

CHAPTER 6

CONCLUSIONS AND IMPLICATIONS

6.1 Summary of the Research

This research examined three basic questions concerning microbial bioherms in Great Salt Lake, Utah. Those questions asked if the bioherms were randomly distributed, if they were influenced by environmental conditions, and if changes in bioherm characteristics can be attributed to changes in the chemistry of Great Salt Lake and have been preserved.

6.2 Research Questions

Research Question 1 – Are microbial bioherms in Great Salt Lake, Utah, randomly distributed?

To define the occurrence and spatial distribution of microbial bioherms in Great Salt Lake, acoustic data from a previous survey of Great Salt Lake were reprocessed to preserve variations in depth and to provide a lake-wide probabilistic dataset that could be used for statistical examination of changes in substrate rugosity. By examining the pattern developed by acoustic returns from the previous acoustic survey and comparing those patterns with acoustic returns from known benthic environments, including known microbial bioherm occurrences, spatial distributions of microbial bioherms were mapped over the navigable extent of the lake. Thick deposits of cm-sized salt crystals obscured bioherm morphology in the north part of the lake and interfered with the estimation of bioherm extent in that area.

Spatial patterns in the lake-wide distribution of microbial bioherms in Great Salt Lake, were defined by using two statistical measures of clustering: Moran's *I* (Moran, 1950) and Getis-Ord Gi* (Getis and Ord, 1992). Results from the global Moran's *I* and local Getis-Ord Gi* spatial statistics showed significant clustering in the population, even when rugosity values derived from different sample sizes were analyzed. Z-scores (a measure of the deviation from the mean for a standard normal distribution) from both analyses show there is less than a 1 percent probability that the observed spatial distribution of substrate rugosity could be the result of random chance.

The methodology employed during this research provides sufficient evidence to reject the assertion that microbial bioherms in Great Salt Lake are randomly distributed. As such, the nonrandom spatial distribution of microbial bioherms in Great Salt Lake would suggest that at least one factor, such as depth, aspect, or salinity, influence distribution of the population.

Research Question 2 – Do environmental factors influence the distribution of microbial bioherms in Great Salt Lake, Utah?

Examination of environmental factors that could influence the distribution of microbial bioherms in Great Salt Lake involved analysis of the geographic patterns of bioherm occurrence and comparing those patterns with quantifiable changes in environmental conditions in those same areas. Eight areas of the lake, identified as having a significant clustering of high rugosity values, were surveyed for verification of microbial bioherm occurrence using side scan sonar, CHIRP, videography/photography, and substrate sampling. Examination of multiple microbial bioherm distributions suggest that there is a direct relation between changes in environmental conditions and the occurrence and distribution of microbial carbonates.

Microbial bioherm populations in Great Salt Lake are prevalent in shallow waters along the margins of the lake and are oriented parallel to structural controls. Populations range from dispersed individual forms to highly clustered reef-like formations generally occurring along a deeper to shallower water gradient. Areas absent of microbial bioherms are primarily located in pelagic zones or along the margins of the lake where depth-related factors or clastic deposition has prevented their formation or effectively masked their occurrence.

Of significant interest, CHIRP geophysical data show that distributions of microbial bioherms in Great Salt Lake are closely associated with folding and faulting of subbottom sediments. The relation between structural microtopographic highs associated with bioherm occurrence and corresponding onlapping sediments trapped in hanging wall lows is well documented in those areas where side scan sonar and CHIRP geophysical data exist and likely is repeated throughout the lake.

The abrupt occurrence of bioherms in areas of small positive topographic relief indicates an acute sensitivity to environmental gradients. Based on the observed relation between small-scale tectonic features and pervasive bioherm distributions along the shallow margins of the lake, it appears that depth-related factors play a prominent role in bioherm distribution. Alignment of microbial bioherm distributions parallel to strike lines of underlying faults indicates a strong tectonic influence.

Environmental factors influence the geographic distribution of microbial bioherms in Great Salt Lake and include, but are not limited to, factors related to tectonics (depth, light penetration, sedimentation, substrate type, and/or wave-base energy) and, as shown below, salinity.

Research Question 3 – Are the influences of changing environmental conditions preserved in the microbial bioherms found in Great Salt Lake, Utah?

Modern alterations of Great Salt Lake have changed the physical, hydrologic, biologic, and chemical characteristics of lake waters by subdividing the lake into two hydrologically distinct water bodies. One basin is hydrologically connected to the south part of the lake (Gilbert Bay) and the other is a separate, isolated, inflow-limited system (Gunnison Bay). Segmentation of the lake effectively limits the supply of fresh water and sediment available to the north part and affects the chemistry of the water, wave-base conditions, circulation patterns, and the biological communities found in the south and north areas of Great Salt Lake.

Comparison of observations, videography records, and samples of microbial bioherms from the south and north parts of Great Salt Lake show distinct differences in bioherm conditions and their surrounding physical and biological environments. Differences between bioherm exposures in the south and north parts of the lake include roughness, color, microbial communities, surrounding biota, interstitial materials, and surrounding sedimentary deposits. Dissolved-oxygen profiles acquired above the bioherms in the south part show an increase in dissolved oxygen near the lake floor while dissolved-oxygen profiles acquired above the bioherms in the north part do not. Conditions in the north part of Great Salt Lake, averaging about 27 percent salinity, appear to have exceeded the environmental range of survival for bioherm-forming microbial communities.

Observations and measurements of microbial bioherms in Great Salt Lake provide substantial evidence that changes in environmental conditions are preserved in the physical and biological characteristics of the population. Differences in the physical and biological characteristics of microbial bioherms between the north and south parts of Great Salt Lake are clearly apparent and measurable and result from recent anthropogenic modifications that place constraints on the movement, mixing, and energy regime of the precauseway Great Salt Lake.

6.3 Summary of Research Conclusions

6.3.1 Advances in Knowledge

This research developed methodologies for studying the occurrence and distribution of microbial bioherms and successfully integrated acoustic single-beam, side scan sonar, and CHIRP subbottom geophysical data with physical, chemical, and biological data in examining the occurrence, spatial distribution, and controls on microbial bioherms in Great Salt Lake, Utah. This research produced a number of theoretical, methodological, and technical contributions that are summarized in Table 3 and below.

1. This effort provides the first systematic study researching the lake-wide spatial distribution of microbial bioherms in Great Salt Lake, Utah.
2. Evidence acquired during this investigation supports previously published claims that the distribution of microbial bioherms primarily occur along the shallow margins of the lake.

3. This research quantified the intimate relationship between small-scale tectonic features and microbial bioherm distributions in Great Salt Lake. Bioherm occurrence is associated with structurally controlled, positive, microtopographical changes in the benthos.
4. This research supports the theoretical basis of a shallow water environment for development of prehistoric microbialite-rich carbonate deposits by documenting the sensitivity of microbial bioherm occurrence associated with small-scale topographic changes.
5. Geophysical data collected during this investigation substantiates the theory that conditions favorable for microbial bioherm development previously occurred in Great Salt Lake and confirms that some microbial bioherms have been recently buried by sediment.
6. Geophysical data collected during this investigation substantiates that anthropogenic modifications in the physical characteristics of Great Salt Lake have resulted in substantial environmental changes in Great Salt Lake and in the burial of microbial bioherms by halite and other evaporite minerals in the north part of the lake.
7. Geophysical data acquired for this investigation identified multiple, previously unknown faults and folds in the sediments beneath Great Salt Lake and provide details of offsets and relative timing of fault movement.
8. Comparison of the environmental conditions immediately surrounding the bioherms in the south part of Great Salt Lake with environmental conditions in the north part of Great Salt Lake substantiates the hypothesis that the chemistry of

lacustrine waters is critical in the survival of bioherm-forming microbial communities.

9. Fault, folds, and other tectonic features associated with bioherm occurrence extend through concordant acoustically transparent deposits likely associated with pelagic deposition from Pleistocene Lake Bonneville. These data support recent (post-Bonneville) formation of the bioherms in Great Salt Lake.
10. Analysis of CHIRP subbottom data supports the premise that the sudden regression of Lake Bonneville resulted in faulting and folding of the sediments beneath Great Salt Lake interrupting the concordant sediments of Lake Bonneville and indicating post-Bonneville isostatic rebound.
11. Examination of faults and their vertical extension through the sediments of Great Salt Lake provide a maximum age for the small-offset faults discovered as part of this research, sediment accumulation rates in the area of the faults, and age-limits on the initiation of modern benthic microbial deposits in Great Salt Lake.
12. This research identified a method for examining variations in acoustically defined benthic roughness and successfully applied the method in the identification of probable areas of microbial bioherm occurrence in Great Salt Lake, Utah.

6.3.2 Implications of the Research

Great Salt Lake is part of the world avian ecosystem and a vital component of the Western Hemisphere Shorebird Reserve Network. The lake and its marshes provide a resting and staging area for between 2 to 5 million shorebirds, as many as 1.7 million eared grebes, and hundreds of thousands of waterfowl during spring and fall migration. These bird populations rely on Great Salt Lake and the abundance of food found in and around its waters as they migrate.

Microbial bioherms are suspected to play a critical role in production of the food resources for avian populations, brine shrimp, brine flies, and other aspects of the ecosystem of Great Salt Lake, yet detailed information about the extent and function of the microbially dominated benthos has heretofore not been available. Previous research on the modern environment of Great Salt Lake has focused on many of the major limnological and ecological variables related to Great Salt Lake (surface altitude, water transparency, dissolved nutrients, cyanophtyes/chlorophyll a concentration, salinity, bathymetry, avian resources, aquatic biology, etc.). Until only recently, the possible contributions and interaction of the microbial communities that populate the benthos were overlooked, widely ignored, or purposefully avoided. Microbial bioherms and similar biogenic carbonates form a stable base for adherence of benthic biological forms such as brine fly larvae and the base for critical primary production during periods of water-column overgrazing by brine shrimp. Baseline information about the occurrence, distribution, morphology, biology, and development of microbial structures is critical in understanding the role of this benthic community on the ecology and health of the Great Salt Lake, the long-term hydrologic history of the lake, and the effects of anthropogenic influences on the environment of the lake. Knowing the extent and location of the microbial bioherms allows researchers and managers to estimate primary productivity and food availability for aquatic and avian populations. Changes in climate, increases in water diversions for human use, and the introduction of waste materials from human activities adjacent to the lake threaten the stability of the lake and the organisms depending on it for their survival. Loss of the microbial bioherms through changes in the environment or by the introduction of biocidal compounds would be catastrophic.

Great Salt Lake provides a glimpse into what the Earth was like for 3 billion of its 4.6 billion year existence and serves as a modern analogue to ancient environments developed, or being developed elsewhere, as oil and gas reservoirs. Environmental conditions in Great Salt Lake are suspected to mimic those found in the Proterozoic: an environment ripe for microbialite initiation and growth. As such, Great Salt Lake provides one of very few settings where the distribution of microbial carbonates can be accurately mapped both in order to develop predictive facies models and as a means of providing quantitative spatial distribution data and spatial distribution controls for hydrocarbon reservoir mapping.

The extent of microbial bioherms in Great Salt Lake, and the possibility of defining the environmental conditions under which the bioherms initiated, formed, and thrive, provide a unique analogue for understanding the possible controls on microbial bioherm distributions of ancient earth. The microbial substrates in Great Salt Lake are invaluable for comparison with ancient microbial deposits because of their spatial extent, varying morphologies and internal fabrics, microbial communities, and the relatively well defined environmental conditions in which they have formed and live. The extensive distribution of bioherms formed under widely varying environmental conditions provides researchers in other locales where microbial bioherms exist the opportunity to extend their understanding of environmental controls on microbial bioherm formation. Results from this research show preferential bioherm development on tectonically controlled structures and abrupt facies changes perpendicular to structure. These results can be tested against subsurface datasets from ancient microbial reservoirs, allowing researchers to assess if subseismic scale faulting is influencing reservoir orientation and quality and providing a significant benefit to those exploring for resources in microbially dominated carbonate reservoirs.

6.4 Comments on Microbial Bioherm Age

Microbial populations on carbonate substrates do not necessarily mean that the microbial communities are actively forming bioherms. The stable nature of the irregular surface of a bioherm along with the general shallow-water occurrence provides an opportunistic foundation for benthic microbial growth, especially cyanophytes, despite the fact that the interior of the bioherms may be relic. Two locations where bioherms are exposed in lacustrine environments (Lake Tanganyika and Lake Turkana) have extensive bioherm populations with exterior microbial growth. However, age dates from the exterior surface of these bioherms show their interior to be relic (Cohen and others, 1997a,b; McCall, 2010, respectively). Many locations that have microbial bioherm populations, including Great Salt Lake, are assumed to be actively depositing calcium carbonate. Nevertheless, the necessary investigations for determining active deposition (chemical and biological) have not yet been successful, and workable methods are not noted in the literature to date.

The results of radiometric age-dating of the exterior surface of the microbial bioherms were inconclusive (F. Corsetti, personal commun., Sept. 2013). Nonetheless, ooid samples collected from Great Salt Lake have significant excess ^{210}Pb, suggesting that carbonate-fixing microbial communities are currently active and accreting carbonates in Great Salt Lake. Clumped isotope paleothermometry work by Corsetti and others (2013) shows that the waters of Great Salt Lake are supersaturated with calcium carbonate throughout the year and become significantly more saturated during the summer months. Corsetti's research suggests that ooid formation occurs primarily during the warmer months when temperatures approach 25 °C or above and when the normal carbonate supersaturation state of the lake water is significantly more saturated. Supersaturation of calcium carbonate in the waters of Great Salt Lake provides bioherm-forming microbial communities with the basic building blocks for bioherm formation.

Examination of faults and their vertical extension through the sediments of Great Salt Lake provides the following: a maximum age for the small-offset faults discovered as part of this research, sediment accumulation rates in the area of the faults, and age-limits on the initiation of modern benthic microbial deposits. These observations suggest that faulting and microbial bioherm growth is recent, occurring after Pleistocene-age Lake Bonneville receded. This interpretation directly supports the observations of Gilbert (1890), Crittenden, (1963), and Bills, and May (1987), showing that small-scale faults and folds interrupt the concordant sediments of Lake Bonneville and are indications of isostatic rebound, again occurring after Pleistocene-age Lake Bonneville receded. The overprint of faults and folds on concordant, acoustically diaphanous strata with minimal variability in lateral thickness, when located directly under microbial bioherm occurrences, suggests that tectonic activity occurred after a prolonged period of fine-grained sediment deposition, likely a profundal environment related to Lake Bonneville.

Interpretations of underwater videography and digital photography also suggest that carbonate-fixing microbial communities are active in Great Salt Lake. Videography records and digital photography from the south part of Great Salt Lake show highly rugose bioherms covered with an abundant microbial community. Immediately adjacent to the bioherms are deposits of aragonitic debris with wave-induced ripple patterns. The aragonitic debris has the same physical characteristics as the small forms that comprise the surface of the adjacent bioherms, suggesting that the source of the debris to be the bioherms. One can infer recent formation, weathering, erosion, and localized deposition of the aragonitic material sourced from the adjacent bioherms. The presence of wave-induced ripple patterns in the sediments suggest that if the deposits were relic, abrasion, attrition, or chemical weathering would have long destroyed the relatively fragile aragonitic material or it would have been buried under recent sediments. The high surface roughness, large surface-area to volume ratio, and the delicate nature of the detrital aragonitic fabric is indicative of recent formation. The presence of similar aragonitic detritus at the water/sediment interface along the eastern margins of Great Salt Lake, an area of high sediment influx, also provide evidence of recent biogenic carbonate formation.

In stark contrast to the microbial bioherms and patterned peloidal detritus observed in the south part of the lake, bioherms in the north part of the lake are surrounded by mud and fine sand. Deposits of aragonitic detritus adjacent to the bioherms are conspicuously absent as are the abundant phototrophic communities that populate bioherms in the south part of the lake.

6.5 Future Directions

Beneath the grey-, green-, and pink-colored waters of Great Salt Lake lies the world's largest experimental research laboratory for the study of microbial bioherms. Hidden from view except to the most resourceful and diligent, this laboratory has been in development for tens of thousands of years and has housed innumerable experiments, mixing the effects of tectonic activity, catchment properties, hydrology, and climate in a large wide-form crucible. Recent man-made modifications to the basin and structure of the lake have further enhanced the study of certain environmental impacts on the lives of the microbial bioherm-forming communities and thereby created a secondary, experimental subset of harsh conditions proven to stress the very fabric of their existence.

Access to and use of the laboratory is limited, challenging, and costly. Similar to the harsh conditions that stress the microbial communities, the Great Salt Lake's environment also presents logistical and environmental extremes for her students, extremes that are well beyond the scope of typical scientific explorations. Nevertheless, the rewards for this research reveal a wide-range of physical, chemical, and biological variations, written within the voluminous layers of sediment beneath the lake, which present a unique and stunning three-dimensional record of life and death.

This dissertation should foster major advancements in the study of microbial bioherms in Great Salt Lake. Although only a small area of the lake was surveyed to verify the results of the rugosity classification and examine the details of bioherm occurrence, the data-collection methodology allows for the integration of the verification data in three-dimensional modeling applications and provides future opportunities to examine the relations between environmental factors and the initiation, growth, and preservation of microbial bioherms.

This research has identified and tested multiple methods for examining the physical and process-based framework for microbial bioherm evolution and occurrence in Great Salt Lake. Identifying the necessary conditions for microbial bioherm initiation, growth, and preservation necessarily involves the study of environmental conditions over time and space. The integration of knowledge from multiple disciplines, utilization of spatial and aspatial statistics, and application of GIS technologies provides a wide range of research opportunities using spatially distributed multidiscipline data. Application of ancillary data from Great Salt Lake in three-dimensional software applications demonstrates a few of the possibilities (Figs. 46, 47).

6.6 Conclusions

Microbial bioherms and other morphologies of microbial carbonates are some of the earliest evidence of life on Earth. This research developed an innovative methodology for gathering, examining, and interpreting both qualitative and quantitative data regarding the occurrence and spatial distribution of microbial bioherms in Great Salt Lake and the environmental factors that influence those distributions. The methodology integrated multiple technologies, the general physical and chemical characteristics of Great Salt Lake, and spatial and aspatial analyses to address the objectives of the research.

This research reveals that microbial bioherm occurrences and spatial distributions in Great Salt Lake are nonrandom and a result of physical and chemical changes within the lake. Subtle changes in depth and sedimentation resulting from recent tectonic deformation directly affect microbial bioherm occurrence and spatial distributions throughout Great Salt Lake. In addition, construction of a rock-filled causeway that divided the Great Salt Lake has resulted in salinity increases that exceed the salinity threshold for viability of bioherm-forming microbial communities. The death of these microbial communities provides ample evidence of a chemical threshold for bioherm formation in hypersaline waters and the sometimes unexpected effects of man's modification of a natural ecosystem.

The identification of factors that influence microbial bioherm occurrence and spatial distribution in Great Salt Lake, combined with the effects of anthropogenic modifications to that system, provide an ideal scenario for studying environmental and anthropogenic controls on the occurrence, spatial distributions, and survivability of microbial bioherms within a midlatitude shallow lacustrine environment. In addition to providing valuable information for studying the effects of the benthic microbial community on the ecology and health of the Great Salt Lake, the study of microbial bioherm distributions in Great Salt Lake also may provide insights into the physical and chemical controls that existed during the formation of large fossil microbialite communities and in assessing the range of salinities and associated environmental conditions for microbial life during early Earth history.

Table 3. Summary of research conclusions.

Research Question	Research Supports?
Microbial bioherms in Great Salt Lake are randomly distributed.	
• Previous research documents or mentions random distributions	No
• Mapping of calculated rugosity from single beam data	No
• Examination of statistically derived differences in areas of uniform rugosity	No
• Global Moran's *I* spatial statistic	No
• Local Getis-Ord Gi* spatial statistic	No
• Statistical examination of side scan sonar data	No
Distributions of microbial bioherms are not affected by environmental factors.	
• Research shows that environment does not affect distributions	No
• Microbial bioherms in Great Salt Lake are randomly distributed	No
• Microbial bioherms in Great Salt Lake are uniformly distributed	No
• Microbial bioherms occur through all areas of Great Salt Lake	No
• Changes in bathymetry do not affect bioherm distributions	No
• Salinity differences do not affect the bioherms	No
Changes in environmental conditions are not apparent in the bioherms.	
• Salinity differences do not affect the bioherms	No
• Bioherms in different environmental conditions have the same characteristics	No
• Biological communities associated with bioherms remain constant in different environmental conditions	No

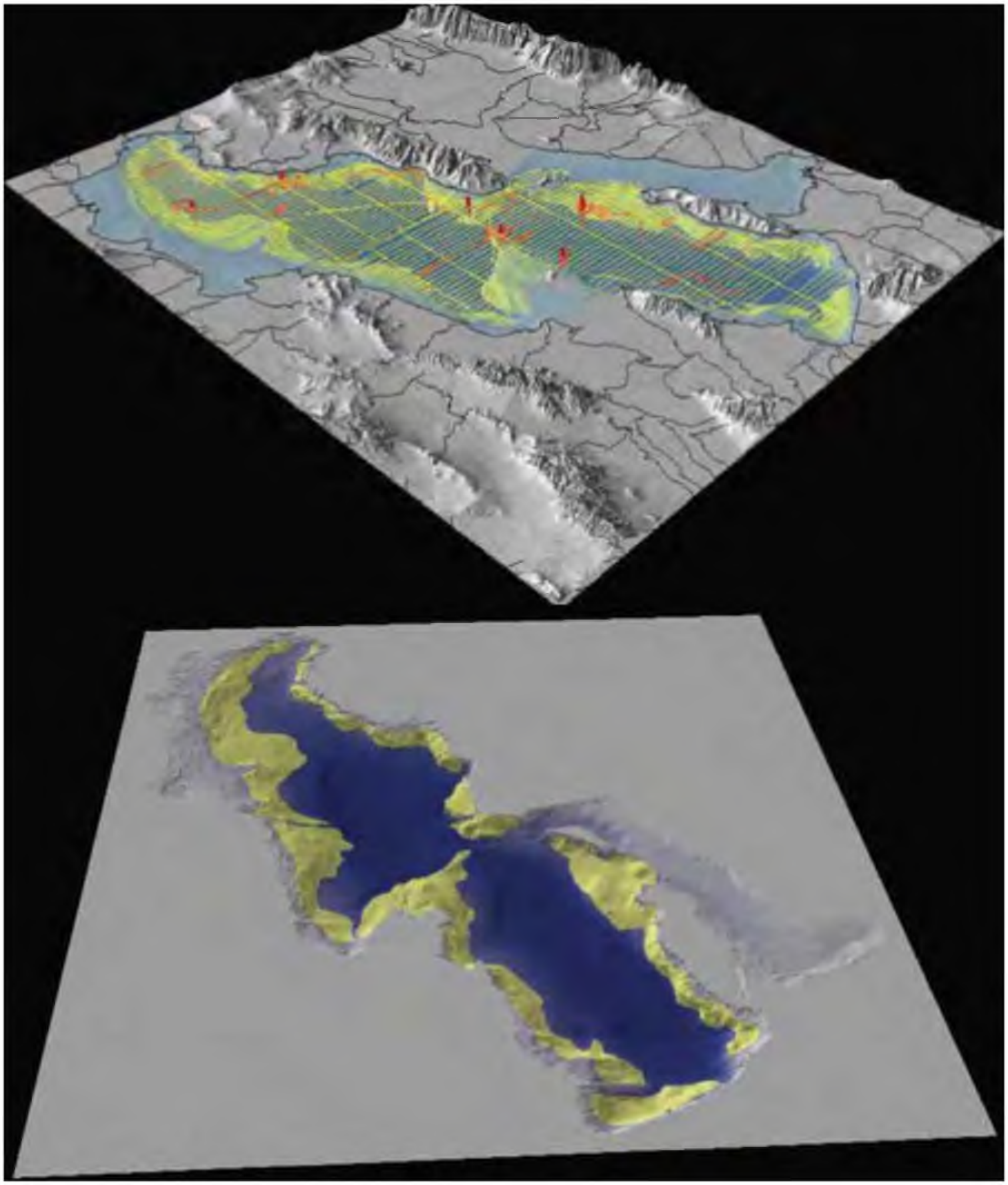

Figure 46. Three-dimensional (3-D) representations of Great Salt Lake and vicinity. Images show integrated digital elevation data, bathymetry, microbial bioherm occurrence, single beam sonar transects, CHIRP and side scan sonar transects, and point sampling locations. Images courtesy of University of Utah Department of Geography.

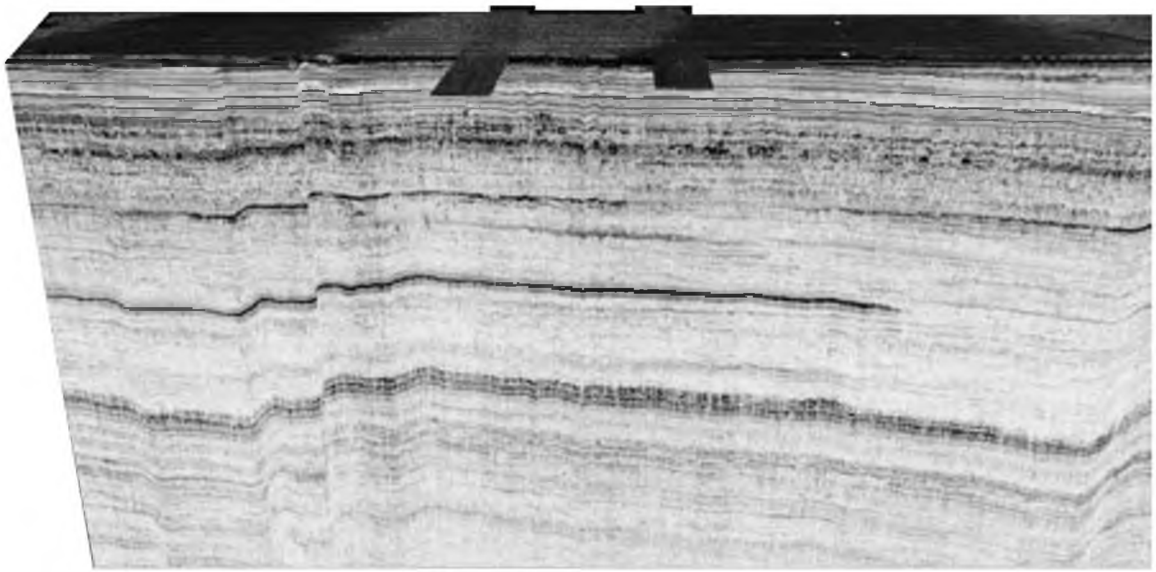

Figure 47. Three-dimensional representations of integrated side scan sonar image and CHIRP geophysical profile, Great Salt Lake, Utah. Image courtesy of Dr. Jillian Maloney, Scripps Institution of Oceanography, La Jolla, CA.

APPENDIX A

SINGLE-BEAM INSTRUMENTATION AND DATA COLLECTION

Single-beam fathometer data utilized to define the distribution of benthic microbial bioherms were gathered as part of an effort to define the bathymetry of Great Salt Lake. Data were collected over the navigable areas of Great Salt Lake during the fall of 2002, the first half of 2003, the spring of 2004, and in 2006, using an automated system consisting of a digital and analog (paper chart) single-beam fathometer coupled to a real-time, differentially corrected global positioning system (RTDGPS). Data were logged in real time to the same computer used for navigation control. Distance below the transducer was derived indirectly by measuring the time required for a sonar signal to travel from the transmitter to the bottom of the lake and back to a receiver. For the purposes of this investigation, raw depths below the transducer were used in calculations of rugosity.

For the bathymetric surveys, a total of about 2,900 kilometers of transects were collected. Position data were recorded at about a 1 hertz interval and depth data at about were recorded at a frequency of 10 hertz. Position information for each depth value was based on a linear interpolation between RTDGPS control locations. Vessel speed was limited to less than 9 knots to maximize the number of depth measurements gathered during the data-collection phase. As a result of these data collection parameters, about three to five depth measurements were recorded for every meter of survey line depending on actual vessel speed. About 7.6 million discrete depth measurements were initially collected along more than 1,690 kilometers of survey transects in the south part of the lake, and about 5.2 million depth measurements were collected along more than 1,230 kilometers of survey transects in the north part of the lake. Quality-control considerations limited the periods of data collection to times when the lake surface had no noticeable swell and waves generally were less than 0.15 meter. Because of the high sound velocity (a result of the higher density water) and limitations in the instrumentation, data collection was limited to areas deeper than about 1 meter. Details of the data collection and processing for the bathymetric surface can be found in Baskin (2005 and 2006).

APPENDIX B

SIDE SCAN SONAR INSTRUMENTATION AND DATA COLLECTION

Side scan sonar is a specialized (SOund NAvigation and Ranging) system primarily used for searching and detecting objects at or near the interface of water and sediment in marine environments. Like other sonars, a side scan transmits sound energy and analyzes the return signal (echo) that has bounced off the substrate or other objects. It is a "push-broom" instrument that ensonifies a swath perpendicular to its travel path using narrow beams of acoustic energy (sound) transmitted out from the sides of a towfish. Sound is reflected back from the bottom and from objects on the substrate to receivers in the towfish where the acoustic return from the lake bottom is amplified and recorded creating a linear array of acoustic backscatter returns oriented perpendicular to the transducer array. As the side scan sonar is moved along transects, repeated scans provide a series of cross-track slices that when stacked together provide an acoustic image of the lake floor. Amplitude of the returns is a function of the density of the substrate, the orientation of the reflecting surface, the roughness of the surface, and the distance to the target. High backscatter objects (typically displayed as lighter colors or white in the imagery) are typically hard surfaces, gravel, and topographic features facing the transducer array. Low backscatter objects (typically displayed as darker colors or black in the imagery) are typically flat-lying fine sediments, shadows from larger topographic features, or losses in signal due to gas or other sound-absorbing materials in the water column. The frequencies employed in side scan sonar do not penetrate the subsurface to any appreciable extent and the product of the sonar is an acoustic image of backscatter intensities. Position control for the resultant imagery is from integration of towfish location information (GPS position) with heading, pitch, and roll information internal to the towfish.

Range of the sonar is a function of the “listening” window for the particular instrument, the sonar transmit frequency, and the characteristics of the water in which the sonar is deployed. Resolution is a function of the frequencies that are used. High frequencies provide higher resolution, but the acoustic energy only travels a short distance. Lower frequencies provide lower resolution but the distance that the energy travels is greater.

The system used for this investigation was an Edgetech 4200 dual frequency side scan sonar system. Along track resolution for the 400 kHz data used in this report is cited at 0.6 m, and across-track resolution is cited at 2 cm. Additional specifications are available at http://www.edgetech.com/docs/4200-Brochure-122012.pdf

Side scan imagery was used during this investigation to verify the occurrence of microbial bioherms in areas of increased substrate rugosity and provide two dimensional imagery of the areas adjacent to areas of increased rugosity. These images were used to examine the distribution of the microbial forms and determine size and shape of individual microbial bioherms.

APPENDIX C

CHIRP INSTRUMENTATION AND DATA COLLECTION

The Compressed High Intensity Radar Pulse (CHIRP) system used for this investigation was a custom-built instrument designated as an Edgetech SB512SC on loan from the Scripps Institution of Oceanography. No written specifications were available for this unit; however, this unit differs from commercial units in that the signal digitization process and impedance matching are performed in an on-fish pressured bottle instead of at a top-side computer unit on the boat. The system is fairly immune from noise and system changes as there is little outside interference from electromagnetic sources and changes in signal quality due to variations in the physical configuration of the deployment or varying environmental conditions. Because the signal digitization process and impedance matching are performed in the bottle, the system configuration and impulse response function never change.

CHIRP systems use a signal of continuously varying frequency instead of using a single pulse. The CHIRP systems "sweep" frequencies through the duration of the outgoing pulse. This allows for increased transmit-pulse length to get more energy into the water and in forming of a unique acoustic signature based on the bandwidth and frequency spectrum of the pulse. The receiver looks for "echoes" from the pulse and produces an enhanced response when the system "recognizes" the transmitted frequencies. By analyzing frequency versus time patterns, spatial (based on speed of sound) resolutions shorter than the pulse length can be resolved.

The CHIRP towfish contains both the sound source and receiver. The CHIRP releases a set amount of acoustic energy into the water column and subsurface. Some of that energy is reflected when it encounters a change in acoustic impedance (such as the lake floor or sediment layers beneath the lake). Return echoes are received, and the strength and timing of the returns are recorded on a computer. A "trace" is generated showing the timing and strength of the echoes from each pulse of energy transmitted by the CHIRP. The outgoing pulse is generated at regularly timed intervals (for example, 0.5 s), and the echoes are recorded for specific intervals of time (for example, 30 ms).

Data are represented as two-dimensional vertical profiles through the subsurface with higher energy reflectors (higher acoustic impedance reflectors) appearing as darker features in the profiles. Instead of using a single pulse, the CHIRP system "sweeps" frequencies through the duration of the outgoing pulse providing the opportunity to impedance match the reflected signals. Frequency and power levels were tested and modified in the field to determine the frequency and power range for discrimination of subbottom structure and geology.

Data for this investigation were acquired at a swept frequency of 1–15KHz with a 500 ms shot interval. Raw data were converted from their original format into a SEGY format and processed using SIOSeis software (Henkart, 2003). Geographic control was provided using the WAAS-supplemented GPS signal that was shared with the side scan sonar. Adjustments for changes in the speed of sound due to changes in sediment characteristics were not included in the analyses and were held at a constant 1,500m/s.

The CHIRP on-fish pressurized bottle contains a circuit board that processes instructions from the topside unit and performs all the impedance matching from the power supply to the transducers. Two transducers on the towfish supply the outgoing CHIRP signal. The smaller of the two transducers produces a signal from 500 Hz to 6 kHz. The larger transducer produces a signal from 2 kHz to 16 kHz. The two transducers are phased with a slight delay between their outputs. As the low frequency output is decreasing, the high frequency transducer is ramping up. The two transducers together produce the outgoing signal. The system filters out frequencies below 700 Hz and above 15 kHz, effectively clipping the extremes of the transducers to insure a uniform signal and to reduce environmental noise. At the high end of the output range, decimeter resolution is attainable.

The towfish contains four hydrophone arrays in a near vertical orientation. The four arrays are summed and the known CHIRP signal (source characteristics) is deconvolved from the entire returned signal using impedance matching. What is left is the "earth filter," the signal that has been filtered by the earth and returned to the system. This signal is digitized in the bottle and transmitted to the topside unit for further processing. Assembly of the individual traces containing the remains of the deconvolved signal results in a two-dimensional vertical profile of changes in subbottom acoustic impedance changes along transects.

Communication between the topside unit and the processor contained inside the pressurized bottle is accomplished through a single coaxial cable that doubles as the 400 volt power cable. Communications are passed along the cable using ADSL protocol (asymmetric digital subscriber line) (Waring, 1991). Signal processing between commercial units and this unit is the same except for gain adjustments and CHIRP-specific data enhancements. In optimal conditions, the SB512SC CHIRP system can obtain interpretable data to approximately 100 m below the sediment/water interface.

APPENDIX D

LIMITATIONS IN USING RUGOSITY AS A BIOHERM SURROGATE

Admittedly, the use of rugosity (either relative or absolute) as a surrogate for actual microbial bioherm occurrence has limitations. Since rugosity is a comparison between the absolute values of the profile departure and its associated reference length, the ability to discriminate the location of sudden changes in substrate rugosity from the actual distribution of bioherms is subject to the length of the reference segment. If the reference length is long, the location information associated with the rugosity value cannot clearly identify the transition between differing substrate rugosities. As the reference length increases, positional uncertainty increases as positional accuracy inversely varies with reference length.

Accurately locating the transition between differing substrate rugosities was critical in the examination of controls on microbial bioherm occurrence. The sheer volume of data (over 12 million data points), the general occurrence of microbial bioherms along the ends of transects where the lake shallows, the required use of unfiltered data, and random noise as a result of boat movement all affected the analysis and mapping of microbial bioherm occurrence. Thus, as the accuracy of the rugosity location decreased, there was an increase in the difficulty of mapping and analyzing the spatial correlations between controls such as faults or a specific lake bottom elevation.

Generally speaking, because rugosity is calculated over a set distance, sudden or short-term changes in rugosity within the reference length may influence the rugosity value significantly, especially in those calculations involving shorter reference lengths. The influence of a sudden increase or decrease in rugosity of any given calculation will vary based on the amplitude and frequency of the change. Changes in transducer depth during data collection can appear as benthic rugosity changes and consequently limit the applicability of the method. Transducer depth is fixed in relation to the collecting vessel; however, vertical and rotational movement of the boat caused by wave or wind effects, personnel movement during data collection, and changes in boat speed can affect interpretation of the rugosity data. Nonbioherm materials on the lake bottom or in the water column, reflections from the deep hypersaline layer that existed in the lake during the surveys, or other causes of spurious reflections could affect the calculated rugosity. Thus, significant aberrations due to nonrugosity-related effects were systematically removed before the data was used for calculating rugosity. All transect intervals exhibiting increased rugosity were examined for multiples, boat-induced systematic variations in depth, and spurious single-point reflections outside the general altitudinal trend of the benthic surface.

Additional complications in mapping microbial bioherms in Great Salt Lake include the burial of the microbial forms by sediment, intergrowth of individual bioherms, and the interstitial deposition of reworked microbial fragments weathered from the larger forms. These complications masked the preburial native bioherm rugosity and inhibited rugosity-based mapping in certain areas of the lake. Complications in identifying buried microbial bioherm occurrences were especially prevalent in the north part of Great Salt Lake where salt crystals overlay deposits that exhibit similar high acoustic reflectance and roughness as exposed bioherm distributions. The underlying materials are suspected to be buried microbial bioherm deposits. However, an attempt to penetrate the salt layer in the north basin to confirm the existence of buried microbial bioherms was not successful due to the thickness of the salt and the difficultly in maintaining a negative buoyancy in the hypersaline brine. Salt deposits were observed to be onlapping microbial bioherm deposits along the shallow margins of the lake where wave and current transport of the salt prevents accumulation. Rugosity increases observed along the margins of the north part of the lake allowed mapping of the shallow-water forms but prevented determination of the precauseway extent of bioherm extent.

APPENDIX E

SUMMARY OF MAJOR MICROBIAL CARBONATE OCCURRENCES

Table 4. Summary of major microbial carbonate occurrences around the world.

Location	Prim. forms	Physical Extent	Environment?	Water Quality	Age	Competition. noted?	Water Source	Depth of occurrence.	Citation
1. Bahamas (USA) Highborne Cay Andros Island San Salvador Island Exuma Cays	Stromatolites (S), Mats (M)	Exuma Cay, 2.5 km long by average of 10 m wide. Fringing reef. Very small extents, fringing or shallow subtidal	Restricted circulation marine intertidal/shallow/ subtidal brackish coastline, Marine and hypersaline environments, Formed by trapping and binding of ooids.	Elevated salinity/ Marine	Modern	Yes but restricted to lower areas	Marine / marine restricted	50 m, most <10 m,	Bowlin, 2011, Gebelein, 1976 Reid, 1995 Pickney, 1997 Baumgartner, 2009
2. Pavilion Lake, Kelly Lake (Canada)	S	Pavilion Lake is 4.6 km^2, 5.7 km x 0.8 km, max. depth 65 m; Kelly Lake is ~1.5 km^2, max depth 40m, stromatolites ~1 m size	Ultraoligotrophic, (dolomite source?), Karst environment, glacial tills surrounding area lakes	Fresh, high clarity, low nutrients, especially P, high $CaCO_3$	11,000 ybp	None	Groundwater	5–55 m	Lim, 2009 Ferris, 1997 Brady, 2010
3. Great Salt Lake (USA)	S, Thrombolite (T)	>700 km^2 living large forms and over 1,000 km^2 pre1960's. Extent of smaller structures unknown	Lacustrine, saline and hypersaline, Intermittent sulfate-rich chemocline, long-term variability in water quality	Saline to hypersaline, Intermittent sulfate rich chemocline	<10,000 ybp est. to Modern?	None	Lacustrine, Surface water, concentrated by evaporation	0 through ~5 m	Baskin, 2011 This study
4. Shark Bay (Australia)	S, M	1.5 m tall, 1–3 m wide, 0.5 mm/year accumulation rate, All microbial structures and sediments ~ 700 km^2 area, Microbial buildups 110 km^2	Salinity twice seawater (~7 percent), no competition, no phototropic elongation but possible sediment elongation, mainly trapping and binding	Hypersaline, 5.5–7.0+ percent salinity	"Few Thousand", 6ka	None	Marine, restricted	~2 m, living to 3.5 m	OLeary, 2008 Jahnert, 2011 Reid, 1995 Steneck, 1998 Papineau, 2005
5. Coorong Lagoon (Australia)	S, M	<10 km^2 for lakes, "several square meters" for stromatolites	Very shallow lakes, ephemeral,	Hypersaline, High $CaCO_3$, high pH, 10 percent NaCl, varies. 0.8–15 percent salinity	300 +/- 250 years old	Yes, arthropods	Groundwater	1 m	Walter, 1973 Wright, 1999
6. Thetis Lake (Australia)	S, Films (F)	~0.3 km^2 by ~2 m deep lake, stromatolites along outer margin about 5 m wide	Sinkhole in limestone, Steep pycno- and chemoclines	Salinity and pH Similar to or greater than seawater, high $CaCO_3$		None	Groundwater, evaporated seawater	1 m	LaCono, 2011
7. Clifton Lake, Lake Richmond (Australia)	T	21.5 km long by max. 1.5 km wide, 17.8 km^2. thrombolites cover ~ 4 km^2	Series of saline to hypersaline lakes,	Seawater, hypersaline, low nutrients	1,950 ybp	Yes, crustaceans, shrimp, etc.	Marine	Max. 1.5 m	Regan, 2009

Table 4. Summary of major microbial carbonate occurrences around the world - continued.

8. Al-Khiran (Kuwait)	S, M	Sabka area, 30 km^2, stromatolite size 5–10 cm in diameter, tidal pools, sabka/salt marsh	Narrow band along edge of Sabka, protected from sea, increased salinity	4–12 percent salinity	Modern	None. Crabs but no stromatolite grazers	Groundwater and marine, restricted	Surface	Duane, 1999
9. Solar Lake (Israel)	M, F	Mats and films only	Shallow nearshore, generally stratified	Monomictic Hypersaline	Modern and 2,464 +/-155 ybp	None	Seawater, evaporated	Mats and Films only	Krumbein, 1977 Cohen, 1977
10. Laguna Figueroa (Mexico)	M	No detailed information available			Modern				Stoltz,1983
11. Laguna Mormona (Mexico)	M, S	Entire lagoon <40 km^2 "stromatolites in 1 km^2 area	Enclosed, elongate lagoon, "stromatolites" <2 cm thick	Hypersaline	Modern	None	Seawater, restricted	Mats 5 to 20 cm thick – Surface – 30 cm only	Horodyski, 1975 Horodyski, 1977
12. Lake Tanganyika (Burundi/Tanzania) Note: most East African Rift Lakes have some microbial growth/carbonate buildups	S	36,600 km^2, 1,470 m max. depth, 570 m mean depth,	Steep slopes, biogenic muds	High Mg/Ca, Close to saturation. Supersaturated with Calcite	2,000–750 ybp but recent deposition, Many are Relic	None	River/fresh	6–60 m	Cohen, 1997 Cohen, 1995 Casanova, 1994
13. Lake Turkana, Lake Bogoria (Kenya)	S, Bioherms (B)	7,500 km^2, 116 m max depth, semiarid, moderately saline	Algal bioherms currently inhibited by low calcium and high suspended sediment loads.	Moderately Saline	1,000–700 ybp, Relic	None	Spring, Surface water, Groundwater		McCall, 2010 Abell, 1982
14. Chetumal Bay (Belize)	S, Oncolites (O)	<100 m^2. Located close to fresh-water inflow, shallow lagoon along coast	1.5 km long stretch adjacent to Rio Hondo outflow. Shallow lagoon	Fresh to Brackish, Seasonal variability, high $CaCO_3$	2,300 ybp, Modern	None	Surface water, high $CaCO_3$	<1.5 m	Rasmussen, 1993
15. Lake Untersee (Antarctica)	M, S	11.4 km^2 total, Lake is >160 m deep, mats/stromatolites in all areas	Stromatolites ~ 50 cm tall, 10–60 cm diameter, stromatolites not lithified, no mineral precipitation	Fresh water, high pH (>10), low DIC, oligotrophic, low bicarbonate	10–15 kabp	None	Glacial	100 m	Anderson, 2011 Parker, 1981 Priscu, 2005
16. Lake Van (Turkey)	S	607 km^2, tufa/spring related	Form near shore where neutral, relatively calcium enriched, groundwater from sublacustrine springs meets the calcium poor, highly alkaline lake water	Highly alkaline 2.7 percent salinity, near seawater. Mixing of the two water masses induces local very high calcium carbonate supersaturation and hence precipitation, generating milky solutions in some near-shore areas.	Modern	None	Groundwater, Surface water	62 m	Lopez, 2005
17. Green Lake (USA)	B, M, T	Lake depth 50+ m, stromatolites are 2–3 m thick to18.5 m depth.	Meromictic, hardwater, marl lake, Some mention of light influence.	Permanent chemocline, surface fresh water, recent subaerial exposure and resubmergence	11,500 ybp to Modern	None, previously snails	Groundwater, Surface water	14–15 m depth	Thompson, 1990 Eggleson, 1976
18. Lagao Salgada, Rio de Janerio (Brazil);	M, S, O, T	Lagoon is 16 km^2, depth 1 m, mats <1 m thick, stromatolites 10–20 m diameter	Discontinuous patches of stromatolites, principally at the southwest and northwest borders	Highly saline to dry	Isotope 3,780 +/- 170 ybp	None	Marine, runoff – connected to sea by tidal channel	Surface	Srivastava, 1999 Combria, 2000
19. Laguna Bacalar Quintana Roo (Mexico)	S, M	Lake size 35 km long by 10 km wide and max. 20 m deep. Coccolitos and stromatolites	Karstic landscape, spring fed from cenotes,	Freshwater High HCO_3 concentration, low nutrient?	"thousands of years"	Black-striped mussels	Groundwater	Max. depth 15 m	Gischler, 2011 Gischler, 2009 Gibson, 2006
20. Socompa and Tolar Grande lagoons; Salta central Andes Mountains; Elevation 3,600 meters	S	Salinity 135+ ppm plus high nitrate levels; stromatolites along margins, 24 cm high by 80 cm wide	Elevation 3,600+ meters, isolated, shallow,	Saline to hypersaline, low P concentration	Modern	None	Groundwater, surface water, Some hydrothermal	Surface	Farias, 2011

Table 4. Summary of major microbial carbonate occurrences around the world - continued.

21. Cuatro Cienegas Mexico	O, M, T	Springs, pools, and streams, isolated	Cyanobacterial filaments bind loose particles of micrite, larger carbonate allochems, and clastic grains on stromatolite surfaces	Fresh, low P content,	Modern	Yes, snails	Stream/Freshwater	Surface	Elser, 2005 Breitbart, 2009
22. Lake Alchichica Mexico	S, M	< 0.8 km^2 total area of lake, microbialites only around rim, < 0.1 km^2 microbialites	2,300 m amsl, 60 m total depth, volcanic crater lake, high water visibility	Brackish, 6,000–8,000 mg/l dissolved solids	Modern to 1,100–2,800 ybp	None	Groundwater	Microbialites up to 14 m depth	Kazmierczak, 2011 Couradeau, 2011
23. Niuafo'ou Island Crater Lakes, Tonga	S, M	Pacific Volcanic Island, Caldera ~15 km^2, steep-sided	Steep-sided, occur along shorelines, largest is >1 m diameters up to 80 cm high.	Low salinity surface, H_2S anaerobic saline bottom layer, high alkalinity	Modern (mats) to 15,000 ybp some 370 ±20 ybp	None	Nonmarine, rainwater	Surface	Kazmierczak, 2006
24. Giant's Causeway, Ireland	S, F	<10 m^2, called stromatolite in citation, only single layer?	Marine single layer	Marine, ocean	Modern	None	Marine	Surface	Cooper, 2011
25. Lagoa Vermelha (Brazil)	M,S	1.9 km^2	Shallow marine lagoon	Hypersaline	Modern	None	Marine	Mean 2.0 m	Spadafora, 2010 Vasconcelo, 2006
26. Ruidera Pools, Spain	T, S	20 cm height mentioned	Series of pools precipitating tufa, Biogenic or chemical?	Fresh, frequent flooding, periodic drying	Modern	None	Surface water and springs	Surface	Santos, 2010 Foster, 2011
27. Lake Vermilion (USA)		Iron/manganese – no further consideration							
28. Bahia Conception, Baha Mexico	T, S	No apparent biogenic influence	Hot spring deposits	Si/Ca hot springs – 62 °C.	Modern	None	Hot springs	N/A	Canet, 2005
29. Manito Lake, Canada	S	Lake is 120 km^2, 10m mean depth, Stromatolite size is cm to >1 m diameter, bioherms "several" meters high, near shore and shoreline	Till and glaciofluvial sediments, Recent drop in water levels to 65 km^2	Saline to hypersaline	2,300 ybp to Modern	None	Primarily groundwater, some surface water inflow		Last, 2010
30. Walker Lake, NV, USA	S, T	Shoreline, mainly exposed, likely relic	12 x 5 mi., 76 ft water depth in lake. No evidence at depth	Fresh to saline	Modern? and Relic	None	Surface water, some spring inflow	Surface, generally exposed	Benson, 1992
31. Yellowstone National Park, USA	M, S	Generally in thermal areas	Associated with thermal activity	Warm to hot. Fresh to mildly brackish	Modern	None	Groundwater	Surface	Jahnke, 2004

LITERATURE CITED

Abell, P.I., Awramik, S.M., Osborne, R.H. and Tomellini, S., 1982, Plio-Pleistocene lacustrine stromatolites from Lake Turkana, Kenya; morphology, stratigraphy and stable isotopes: Sedimentary Geology, v. 32, p. 1–26.

Andersen, D. T., Sumner, D. Y., Hawes, I., Webster-Brown, J., and Mckay, C.P., 2011, Discovery of large conical stromatolites in Lake Untersee, Antarctica: Geobiology, v. 9, p. 280–293, doi: 10.1111/j.1472–4669.2011.00279.x

Arp, G., 1995, Lacustrine bioherms, spring mounds, and marginal carbonates of the Ries-Impact-Crater (Miocene, Southern Germany): Facies, v. 33, p. 35–89.

Arp, G., Bielert, F., Hoffmann, V.E., and Löffler, T., 2005, Palaeoenvironmental significance of lacustrine stromatolites of the Arnstadt Formation ("Steinmergelkeuper", Upper Triassic, N. Germany): Facies, v. 51, no. 1, p. 419–441.

Arp, G., Reimer, A., and Reitner, J., 2001, Photosynthesis-induced biofilm calcification and calcium concentrations in Phanerozoic oceans: Science, v. 292, no. 5522, p. 1701–1704.

Arp, G., Reimer, A., and Reitner, J., 2003, Microbialite formation in seawater of increased alkalinity, Satonda Crater Lake, Indonesia: Journal of Sedimentary Research, v. 73, no. 1, p. 22.

Arp, G., Thiel, V., Reimer, A., Michaelis, W., and Reitner, J., 1999, Biofilm exopolymers control microbialite formation at thermal springs discharging into the alkaline Pyramid Lake, Nevada, USA: Sedimentary Geology, v. 126, p. 159–176.

Awramik, S.M., 1992, The oldest records of photosynthesis: Photosynthesis Research, v. 33, p. 75–89.

Awramik, S.M., 2006, Palaeontology: respect for stromatolites: Nature, v. 441, no. 7094, p. 700–701.

Awramik, S.M., and Grey, K., 2005, Stromatolites – Biogenicity, Biosignatures, and

Bioconfusion: Proceedings of SPIE, v. 5906, p. 1–9.

Awramik, S.M., and Riding, R., 1988, Role of algal eukaryotes in subtidal columnar stromatolite formation: Proceedings of the National Academy of Science, v. 85, no. 5, p. 1327–1329.

Balch, D., Andrew Cohen, A., Beck, J.W. and Edwards, R.L., 2003, Quaternary ostracode paleoecology and its link to climate change in the Bonneville Basin – a detailed study of the GLAD800 core GSL00-4, Great Salt Lake, Utah: Tucson, University of Arizona, M.S. Thesis Prepublication, 45 p.

Balch, D.P., Cohen, A.S., Schnurrenberger, D.W., Haskell, B.J., Valero Garces, B.L., Beck, J.W., Cheng, H., and Edwards, R.L., 2005, Ecosystem and paleohydrological response to Quaternary climate change in the Bonneville Basin, Utah: Paleogeography, Paleoclimatology, Paleoecology, v. 221, p. 23.

Baskin, R.L., and Allen, D.V., 2005, Bathymetric map for the south part of Great Salt Lake, UT 2005: U.S. Geological Survey Scientific Investigations Map 2005-2894, 1 Plate [Map]. Available online at http://pubs.usgs.gov/sim/2005/2894/

Baskin, R.L., and Turner, J., 2006, Bathymetric map for the north part of Great Salt Lake, UT 2006: U.S. Geological Survey Scientific Investigations Map 2006-2954, 1 Plate [Map]. Available online at http://pubs.usgs.gov/sim/2006/2954/

Baskin, Robert L., 2005, Calculation of area and volume for the south part of Great Salt Lake, Utah: U.S. Geological Survey Open-File Report 2005-1327, 6 p. Available online at http://pubs.er.usgs.gov/publication/ofr20051327

Baskin, Robert L., 2006, Calculation of area and volume for the north part of Great Salt Lake, Utah: U.S. Geological Survey Open-File Report 2006-1359, 6 p. Available online at http://pubs.er.usgs.gov/publication/ofr20061359

Baskin, Robert L., Driscoll N.W., and Wright, V.P., 2011, Lacustrine microbialites in Great Salt Lake; life in a dead lake: AAPG Abstract and Poster, AAPG 2011 Annual Convention and Exhibition, 10-13 April 2011, Houston, Texas.

Baskin, Robert L., Waddell, K.M., Thiros, S.A., Giddings, E.M., Hadley, H.K., Stephens, D.W., and Gerner, S.J., 2002, Water-quality assessment of the Great Salt Lake Basins, Utah, Idaho, and Wyoming – environmental setting and study design: U.S. Geological Survey Water Resources Investigations Report 02-4115, 47 p. Available online at http://pubs.er.usgs.gov/publication/wri024115

Baumgartner, L.K., Spear, J.R., Buckley, D.H., Pace, N.R., Reid, R.P., Dupraz, C. and

Visscher, P.T., 2009, Microbial diversity in modern marine stromatolites, Highborne Cay, Bahamas: Environmental Microbiology, v. 11, p. 2710–2719.

Baumgartner, Laura K., Spear, John R., Buckley, Daniel H., Pace, Norman, R., Reid, R. Pamela, Dupraz, Christophe, and Visscher, Pieter T., 2009, Microbial diversity in modern marine stromatolites, Highborne Cay, Bahamas: Environmental Microbiology v. 11, no. 10, p. 2710–2719.

Becker, J.J., and Sandwell, D.T., 2008, Global estimates of seafloor slope from single-beam ship soundings: Journal of Geophysical Research; Oceans, v. 113, issue C5.

Belovsky, G.E., Stephens, D., Perschon, C., Birdsey, P., Paul, Naftz, D., Baskin, R., Mellison, C., Luft, J., Mosley, R., Mahon, H., Van Leeuwen, J., and Allen, D.V., 2011, The Great Salt Lake Ecosystem (Utah, USA) – long term data and a structural equation approach: Ecosphere, v. 2, no. 3, article 33.

Benson, L., 2001, Western lakes: Developments in Quaternary science, v. 1, p. 185–204.

Benson, L., Currey, D., Lao, Y., and Hostetler, S., 1992, Lake-size variations in the Lahontan and Bonneville basins between 13,000 and 9,000 ^{14}C yr B.P.: Palaeogeography, Palaeoclimatology, Palaeoecology, v. 95, p. 19–32.

Benson, L.V., Currey, D.R., Dorn, R.I. Lajoie, K.R., Oviatt, C.G., Robinson, S.W., Smith, G.I., and Stine, S., 1990, Chronology of expansion and contraction of four Great Basin lake systems during the past 35,000 years: Palaeogeography, Palaeoclimatology, Palaeoecology, v. 78, p. 241–286.

Bortz, L.C., 1987, Heavy-oil deposit, Great Salt Lake, Utah: AAPG Studies in Geology Series No. 25.

Bortz, L.C., Cook, S.A., and Morrison, O.J., 1985, Great Salt Lake Area, Utah: Rocky Mountain Association of Geologists and Denver Geophysical Society, Seismic Exploration of the Rocky Mountain Region, p. 275–281.

Bottjer, D.J., Schubert, J.K., and Droser, M.L., 1996, Comparative evolutionary palaeoecology – assessing the changing ecology of the past: Geological Society of London Special Publications, v. 102, no. 1, p. 1–13.

Bowlin, E.M., Klaus, J.S., Foster, J.S., Andres, M.S., Custals, L., and Reid, R.P., 2011, Environmental controls on microbial community cycling in modern marine stromatolites: Sedimentary Geology, v. 263, p. 45–55, doi:10.1016/j.sedgeo.2011.08.002

Brady, A.L., Slater, G.F., Omelon, C.R., Southam, G., Druschel, G., Andersen, D.T., Hawes, I., Laval, B., and Lim, D.S.S., 2010, Photosynthetic isotope biosignatures in laminated micro-stromatolitic and non-laminated nodules associated with modern, freshwater microbialites in Pavilion Lake, B.C.: Chemical Geology, v. 274, p. 56–67.

Breitbart, M., Hoare, A., Nitti, A., Siefert, J., Haynes, M., Dinsdale, E., Edwards, R., Souza, V., Rohwer, F., and Hollander, D., 2009, Metagenomic and stable isotopic analyses of modern freshwater microbialites in Cuatro Ciénegas, Mexico: Environmental Microbiology, v. 11, no. 1, p. 16–34.

Broecker, W.S., and Kaufman, A., 1965, Radiocarbon chronology of Lake Lahontan and Lake Bonneville II, Great Basin: Geological Society of America Bulletin, v. 76, p. 537–566.

Brothers, D.S., Driscoll, N.W., Kent, G.M., Harding, A.J., Babcock, J.M. and Baskin, R.L., 2009, Tectonic evolution of the Salton Sea inferred from seismic reflection data: Nature Geoscience, v. 2, 581–584. Available online at http://pubs.er.usgs.gov/publication/70037012

Brown, C. J., Hewer, A.J., Meadows, W.J., Limpenny, D.S., Cooper, K.M., and Rees, H.L., 2004, Mapping seabed biotopes at Hastings Shingle Bank, eastern English Channel – part 1 – assessment using sidescan sonar: Journal of the Marine Biological Association of the UK, v. 84, p. 481–488.

Burne, R.V., and Moore, L.S., 1987, Microbialites – organosedimentary deposits of benthic microbial communities: Palaios, v. 2, p. 241–254.

Burne, Robert V., and Johnson, Ken, 2012, Sea-level variation and the zonation of microbialites in Hamelin Pool, Shark Bay, Western Australia: Marine and Freshwater Research, v. 63, p. 994–1004.

Canet, C., Prol-Ledesmaa, R.M., Torres-Alvarado, I., Gilgc, H.A., Villanuevaa, R.E., and Lozano-Santa Cruz, R., 2005, Silica-carbonate stromatolites related to coastal hydrothermal venting in Bahía Concepción, Baja California Sur, Mexico: Sedimentary Geology, v. 174, p. 97–113.

Carozzi, Albert V., 1957, Contribution de 1'étude des propriétés géométriques des oolithes—l'exemple du Grande Lac Sale, Utah, USA. Inst., National Genevé Bulletin, v. 58, p. 1–52.

Carozzi, Albert V., 1962, Observations on algal biostromes in the Great Salt Lake, Utah: Journal of Geology, v. 70, no. 2, p. 246–252.

Casanova, J., 1994, Stromatolites from the east African rift – a synopsis: *in* Bertrand-Sarfati, J., and Monty, C. (eds.), Phanerozoic stromatolites II, p. 193–226.

Chafetz, H.S., and Folk, R.L., 1984, Travertines depositional morphology and the bacterially constructed constituents: Journal of Sedimentary Petrology, v. 54, no 1, p. 27.

Cohen, A.S., Lezzar, K.E., Tiercelin, J.J., and Soreghan, M.R., 1997, New palaeogeographic and lake level reconstructions of Lake Tanganyika; implications for tectonic, climatic and biologic evolution in a rift lake: Basin Research, v. 9, p. 107–132.

Cohen, A.S., Soreghan, M., and Scholz, C., 1993, Estimating the age of ancient lake basins – an example from Lake Tanganyika: Geology, v. 21, p. 511–514.

Cohen, A.S., Talbot, M.R., Awramik, S.M., Dettman, D.L., and Abell, P.I., 1997, Lake level and paleoenvironmental history of Lake Tanganyika, Africa, as inferred from late Holocene and modern stromatolites: GSA Bulletin, v. 109, no. 4, p. 444–460, 8 figs., 4 tables.

Cohen, Andrew S., 1995, Paleoecological approaches to the conservation biology of benthos in ancient lakes; a case study from Lake Tanganyika: Journal of the North American Benthological Society, v. 14, no. 4, p. 654–668.

Cohen, Y., Krumbein, W., and Shilo, M., 1977, Solar Lake (Sinai)–Part 2–Distribution of photosynthetic microorganisms and primary production: Limnology and Oceanography, v. 22, no. 4, p. 609–620.

Coimbra, M.M., Silva, C.G., and others, 2000, Radiocarbon measurements of stromatolite heads and crusts at the Salgada Lagoon, Rio de Janeiro State, Brazil: Nuclear Instruments and Methods in Physics Research Section B – Beam interactions with materials and atoms, v. 172, nos. 1–4, p. 592–596.

Colman, S.M., Kelts, K.R., and Dinter, D.A., 2002, Depositional history and neotectonics in Great Salt Lake, Utah, from high-resolution seismic stratigraphy: Sedimentary Geology, v. 148, nos. 1–2, p. 61–78.

Cooper, J.A.G., Smith, A.M., and Arnscheidt, J., 2013, Contemporary stromatolite formation in high intertidal rock pools, Giant's Causeway, Northern Ireland: preliminary observations: Journal of Coastal Research, Special Issue No. 65, p. 1675–1680.

Corsetti, F.A., Anderson, R.P., Bird, J., Meneske, M., Stefurak, E., Petryshyn, V.A., Tripati, A., Stamps, B.W., Stevenson, B.S., and Spear, J.R., 2013, Ooid formation in the Great Salt Lake, Utah – insights from clumped isotope paleothermometry and molecular biology: Abstract – Geological Society of America – Denver , CO, November 2013.

Couradeau, E., Benzerara, K., Moreira, D., Gerard, E., Kazmierczak, J., Tavera, R., and López-García, P., 2011, Prokaryotic and Eukaryotic community structure in field and cultured microbialites from the alkaline Lake Alchichica (Mexico): PLoS ONE, v. 6, no. 12, e28767, doi:10.1371/journal.pone.0028767

Crittenden, M.D., 1963, New data on the isostatic deformation of Lake Bonneville: U.S. Geological Survey Professional Paper 454-E, Government Printing Office, Washington D.C.

Danforth, W.W., 1997, Xsonar/ShowImage - A complete system for rapid side scan sonar processing and display: U.S. Geological Survey Open-File Report 97-686, 99 p.

Della Porta, Giovanna, and Barilaro, Federica, 2011, Non-marine carbonates – facies, diagenesis and porosity development: AAPG Search and Discovery article #30173.

Dinter, D.A., and Pechmann, J.C., 1999, Multiple Holocene earthquakes on the East Great Salt Lake fault, Utah – evidence from high-resolution seismic reflection data: EOS, Transactions of the American Geophysical Union, v. 80, no. 46, supplement, F734.

Dinter, D.A., and Pechmann, J.C., 1999, Sublacustrine paleoseismology – evidence for recent earthquakes on the East Great Salt Lake fault, Utah: Association of Engineering Geologists, 42nd Annual Meeting Abstracts with Program, p. 62–63.

Dinter, D.A., and Pechmann, J.C., 2000, Late Quaternary slip rates and recurrence intervals of large earthquakes on the East Great Salt Lake fault, Utah – estimates from high-resolution seismic reflection data: Geological Society of America, Abstracts with Programs, 2000 Annual Meeting, v. 32.

Dinter, D.A., Pechmann, J.C., Kelts, K., Schnurrenberger, D., Haskell, B., Valero-Garces, B., Nielson, D. M., Kruger, N., Cohen, A., and Dean, W., 2000, Holocene paleoseismology of the East Great Salt Lake fault: Preliminary results of an integrated coring/high-resolution reflection seismic study of a submerged active normal fault: EOS, Transactions of the American Geophysical Union, v. 81.

Dinter, David A., 2001, Seismic risk in the Wasatch Front region, Utah from the east Great Salt Lake normal fault – estimates from high-resolution seismic reflection data; Geological Society of America Annual Meeting, November 5–8, 2001, Session No. 144, Paper No. 144-0.

Dix, George R., Patterson, R. Timothy, and Park, Lisa E., 1999, Marine saline ponds as sedimentary archives of late Holocene climate and sea-level variation along a carbonate platform margin; Lee Stocking Island, Bahamas: Paleogeography, Paleoclimatology, Paleoecology, v. 150, p. 223–246.

Du Preez, C., and Tunnicliffe, V., 2012, A new video survey method of microtopographic laser scanning (MiLS) to measure small-scale seafloor bottom roughness: Limnology and Oceanography Methods, v. 10, p. 899–909.

Duane, M.J., and Al-Zamel, A.Z., 1999, Syngenetic textural evolution of modern sabkha stromatolites (Kuwait): Sedimentary Geology v. 127, p. 237–245.

Dupraz, C., and Visscher, P.T., 2005, Microbial lithification in marine stromatolites and hypersaline mats: Trends in Microbiology, v. 13, no. 9, p. 10.

Dupraz, C., Pattisina, R., and Verrecchia, E.P., 2006, Translation of energy into morphology – simulation of stromatolite morphospace using a stochastic model: Sedimentary Geology, v. 185, p. 185–203.

Dupraz, C.R., Reid, P., Braissant, O., Decho, A.W., Norman, R.S., and Visscher, P.T., 2009, Processes of carbonate precipitation in modern microbial mats: Earth-Science Reviews, v. 96, p. 141–162.

Eardley, A.J., 1938, The sediments of Great Salt Lake, Utah: Bulletin of the American Association of Petroleum Geologists, v. 22, p. 1305–1411.

Eardley, A.J., Shuey, R.T., Gvosdetsky, V., Nash, W.P., Picard, M.D., Grey, D.C., and Kukla, G.J., 1973, Lake cycles in the Bonneville Basin, Utah: Geological Society of America Bulletin, v. 84, p. 211–216.

Eardley, A.J., 1962, Glauber's salt bed west of Promontory Point, Great Salt Lake, Utah: Utah Geological and Mineralogical Survey Special Studies 1, 12 p.

Eardley, A.J., 1962, Gypsum dunes and evaporite history of the Great Salt Lake Desert: Utah Geological and Mineralogical Survey Special Study 2, 27 p.

Eardley, A.J., and Gvosdetsky, V., 1960, Analysis of Pleistocene core from Great Salt Lake, Utah: Geological Society of America Bulletin, v. 71, no. 9, p. 1323–1344.

Eardley, A.J., and Stringham, B., 1952, Selenite crystals in the clays of Great Salt Lake: Geological Society of America Bulletin, v. 63, no. 12, p. 1362–1362.

EDCUtah, 2013, Utah Demographics: Economic Development Corporation of Utah.

Eggleston, J.R., and Dean, W.E., 1976, Freshwater stromatolitic bioherms in Green Lake, New York, *in* Walter, M.R. (ed.), Stromatolites: Developments in sedimentology 20: Elsevier Scientific Publishing Company, Amsterdam, p. 479–488.

Elser, J., Schampel, J., Garcia-Pichel, F., Wade, B., Souza, V., Eguiarte, L., and others, 2005, Effects of phosphorus enrichment and grazing snails on modern stromatolitic microbial communities: Freshwater Biology, v. 50, p. 1808–1825.

Elser, J.L., Watts, J., Schampel, J.H., and Farmer, J., 2006, Early Cambrian food webs on a trophic knife-edge? – a hypothesis and preliminary data from a modern stromatolite-based ecosystem: Ecological Letters, v. 9: p. 295–303.

ESRI, 2010, ArcGIS Desktop – Release 10.1: Environmental Systems Research Institute, Redlands, CA.

Farias, M.E., and others, 2011, Modern stromatolite ecosystems at alkaline and hypersaline high-altitude lakes in the Argentinean Puna, *in* V.C. Tewari and J. Seckbach (eds.), Stromatolites: interaction of microbes with sediments, cellular origin, life in extreme habitats and astrobiology, v. 18, p. 427–441, doi 10.1007/978-94-007-0397-1_19

Fenneman, N.M., 1931, Physiography of the western United States: New York, McGraw-Hill, 534 p.

Ferris, F., Thompson, J., and Beveridge, T., 1997, Modern freshwater microbialites from Kelly Lake, British Columbia: Canadian Palaios, v. 12, p. 213–219.

Foster, J.S. and Green, S.J., 2011, Microbial diversity in modern stromatolites: *in* Tewari V.C., and Seckbach, J. (eds.), Stromatolites: Interaction of microbes with sediments, cellular origin, life in extreme habitats, and astrobiology, v. 18, pp. 383–405, DOI 10.1007/978-94-007-0397-1_17

Frémont, J.C., 1845, Report of the exploring expedition to the Rocky Mountains in the year 1842 and to Oregon and North California in the years 1843–44: Printed by order of the Senate of the United States, v. 174.

Friedlander, Alan M., and Parrish, James D., 1998, Habitat characteristics affecting fish assemblages on a Hawaiian coral reef: Journal of Experimental Marine Biology and Ecology, v. 224, p. 1–30.

Friedman, A., Pizarro, O., Williams, S.B., and Johnson-Roberson, M., 2012, Multi-scale measures of rugosity, slope and aspect from benthic stereo image reconstructions: PLoS ONE, v. 7, no 12, p. e50440.

Frost, N.J., Burrows, M.T., Johnson, M.P., Hanley, M.E., and Hawkins, S.J., 2005, Measuring surface complexity in ecological studies: Limnology and Oceanography Methods, vol. 3, p. 203–210.

Garrett, P., 1970, Phanerozoic stromatolites - noncompetitive ecologic restriction by grazing and burrowing animals: Science, v. 169, no. 3941, 171–173.

Gebelein, C.D., 1976, The effect of the physical, chemical and biological evolution of the Earth: *in* Walter, M.R. (ed.), Stromatolites: Developments in sedimentology 20: Elsevier Scientific Publishing Company, Amsterdam, p. 499–515.

Getis, A., and Ord, J. K., 1992, The analysis of spatial association by use of distance statistics: Geographical Analysis, v. 24, no. 3, 189–206.

Gibson, M.A., Gischler, E., and Oschmann, W., 2006, Preliminary interpretation of a stromatolite field in Laguna Bacalar, Quintannaroo Mexico: *in* Carbonates – then and now; how much has changed? Geological Society of America, Southeastern Section - 55th Annual Meeting, 23–24 March 2006, paper no. 17-4.

Gilbert, G. K., 1890, Lake Bonneville: U.S. Geological Survey Monograph 1, 438 p., U.S. Government Printing Office, Washington D.C.

Gilbert, G.K., 1875, Report on the geology of portions of Nevada, Utah, California and Arizona examined in the years 1871 and 1872: Report on U.S. Geographical and Geological Surveys West of the 100th Meridian, v. 3, Geology, part 1, p. 17–187.

Gilbert, G.K., 1882, Contributions to the history of Lake Bonneville: U.S. Government Printing Office, Washington D.C.

Gilbert, G.K., 1886, The inculcation of scientific method by example, with an illustration drawn from the Quaternary geology of Utah: American Journal of Science, v. 184, p. 284–299.

Gischler, E., Gibson, M.A., and Oschmann, W., 2008, Giant Holocene freshwater microbialites, Laguna Bacalar, Quintana Roo, Mexico: Sedimentology, v. 55, no. 5, p. 1293–1309.

Gischler, E., Golubic, S., Gibson, M.A., Oschmann, W., and Hudson, J.H., 2011, Microbial mats and microbialites in the freshwater Laguna Bacalar, Yucatan Peninsula, Mexico: *in* Reitner, J., and others (eds.), Advances in stromatolite geobiology, lecture notes in earth sciences, v. 131, doi 10.1007/978-3-642-10415-2_13

Gray, J.S., 1974, Animal-sediment relationships: Oceanography and Marine Biology Annual Review, v. 12, p. 223–261.

Great Salt Lake Advisory Council, 2012, Economic Significance of the Great Salt Lake to the State of Utah: prepared by Bioeconomics, Inc., Missoula, Montana.

Grim, R.E., Kulbricki, G., and Carozzi, A.V., 1960, Clay mineralogy of the sediments of the Great Salt Lake, Utah: Geological Society of America Bulletin, v. 71, no. 4, p. 515–519.

Grotzinger, J.P., and Knoll, A.H., 1999, Stromatolites in Precambrian carbonates – evolutionary mileposts or environmental dipsticks?: Annual Reviews in Earth Planet Science, v. 27, p. 313–358.

Hahl, D.C., and Langford, R.H., 1964, Dissolved-mineral inflow to Great Salt Lake and characteristics of the salt lake brine – Part II, technical report: Utah Geological and Mineralogical Survey, Water Resources Bulletin 3, 40p.

Halley R. B., 1976, Textural variation within Great Salt Lake algal mounds: *in* Walter, M.R. (ed.), Stromatolites: Developments in sedimentology 20: Elsevier Scientific Publishing Company, Amsterdam.

Halley, R.B., 1977, Ooid fabric and fracture in the Great Salt Lake and the geologic record: Journal of Sedimentary Petrology, v. 47, no. 3, p. 1099–1120.

Harris, P.M., Ellis, J., and Purkis, S.J., 2012, Analogs for carbonate deposition in early rift settings: SEPM Short Course Notes 55. DVD.

Harris, Peter T., 2012, Biogeography, benthic ecology, and habitat classification schemes: *in* Seafloor Geomorphology as Benthic Habitat, Chapter 4, p. 61–87.

Hedberg, L.L. and Parry, W.T., 1971, Clay mineralogy at the brine-sediment interface in the south arm of Great Salt Lake, Utah: Utah Geological and Mineralogical Survey Special Studies 35.

Henkart, P., 2003, SIOSEIS: Scripps Institution of Oceanography, La Jolla, CA. Available online at http://sioseis.ucsd.edu

Hofmann, H.J., 1994, Proterozoic carbonaceous compressions ("metaphytes" and "worms"): *in* Bengtson, S. (ed.), Early life on Earth, Columbia University Press, New York, p. 342–357.

Horel, John, 2014, Temperature data for Great Salt Lake, Utah: Written communication, March 2014.

Horodyski, Robert J., and Vonderhaar, Stephen P., 1975, Recent calcareous stromatolites from Laguna Mormona (Baja California) Mexico: Journal of Sedimentary Petrology, v. 45, no. 4.

Horodyski, Robert J., Bloeser, Ann Bonnie, and Vonderhaar, Stephen, 1977, Laminated algal mats from a coastal lagoon, Laguna Mormona, Baja California, Mexico: Journal of Sedimentary Petrology, v. 47, no.2, p. 680–696.

HyPack, 2013, HyPack Hydrographic Survey Software: HyPack, Inc., Middletown, CT, USA.

Irish, Jennifer L., and Lillycrop, W. Jeff, 1999, Scanning laser mapping of the coastal zone – the SHOALS system: Journal of Photogrammetry and Remote Sensing, v. 54, nos. 2–3, p. 123–129.

ISO, 1997, Geometrical Product Specifications (GPS) – Surface texture – Profile method – Terms, definitions and surface texture parameters: International Organization for Standardization, ISO 4287, 1997.

Jahnert, Ricardo J., and Collins, Lindsay B., 2011, Significance of subtidal microbial deposits in Shark Bay, Australia: Marine Geology, v. 286, p. 106–111.

Jahnert, Ricardo J., and Collins, Lindsay B., 2012, Characteristics, distribution and morphogenesis of subtidal microbial systems in Shark Bay, Australia: Marine Geology, v. 303–306, p. 115–136.

Jahnke, L., Embaye, T., Hope, J., Turk, K., Van Zullen, M., Des Marais, D., and others, 2004, Lipid biomarker and carbon isotopic signatures for stromatolite-forming, microbial mat communities and Phormidium cultures from Yellowstone National Park: Geobiology, v. 2, p. 31–47.

Johnson, J., and Grotzinger, J.P., 2006, Affect of sedimentation on stromatolite reef growth and morphology, Ediacaran Omkyk Member (Nama Group), Namibia: South African Journal of Geology, v. 109, pp. 87–96.

Kawaguchi, T., and Decho, A.W., 2002, Isolation and biochemical characterization of extracellular polymeric secretions (EPS) from modern soft marine stromatolites (Bahamas) and its inhibitory effect on $CaCO_3$ precipitation: Prep Biochem

Biotechnology, v. 32, no. 1, p. 51–63.

Kazmierczak, J., and Kempe, S., 2006, Genuine modern analogues of Precambrian stromatolites from caldera lakes of Niuafo'ou Island, Tonga: Naturwissenschaften, v. 93, p. 119–126, doi 10.1007/s00114-005-0066-x

Kazmierczak, J., Kempe, S., Kremer. B., Lopez-Garc?a, P., Moreira, D., and Tavera, R., 2011, Hydrochemistry and microbialites of the alkaline crater lake, Alchichica, Mexico: Facies, v. 57, p. 543–570, doi 10.1007/s10347-010-0255-8

Knauth, L.P., 1998, Salinity history of the Earth's early ocean: Nature, v. 395, no. 6702, p. 554–555.

Kowalewska, A. and Cohen, A.S., 1998, Reconstruction of paleoenvironments of the Great Salt Lake Basin during the late Cenozoic: Journal of Paleolimnology, v. 20, p. 381–407.

Krumbein, W., Cohen, Y., and Shilo, M., 1977, Solar Lake (Sinai) – Part 4 – Stromatolite cyanobacterial mats: Limnology and Oceanography, v. 22, p. 635–656.

LaCono, V., and others, 2011, Unveiling microbial life in new deep-sea hypersaline Lake Thetis – Part I – Prokaryotes and environmental settings: Environmental Microbiology, v. 13, no. 8, p. 2250–2268, doi:10.1111/j.1462-2920.2011.02478.x

Last, Fawn M., Last,William M., and Halden, Norman M., 2010, Carbonate microbialites and hardgrounds from Manito Lake, an alkaline, hypersaline lake in the northern Great Plains of Canada: Sedimentary Geology, v. 225, p. 34–49.

Leatherman, S.P., 1987, Field measurement of microtopography: Journal of Coastal Research, v. 3, no. 2, p. 233–235.

Lim, D.S.S., Laval, B.E., Slater, G., and others, 2009, Limnology of Pavilion Lake, B.C., Canada – Characterization of a microbialite forming environment: Fundamental and Applied Limnology, Archiv für Hydrobiologie, v. 173/4, p. 329–351.

Logan, B.W., 1961, Cryptozoon and associate stromatolites from the Recent, Shark Bay, Western Australia: Journal of Geology, v. 69, p. 517–533.

Logan, B.W., Rezak, R., and Ginsburg, R.N., 1964, Classification and environmental significance of algal stromatolites: Journal of Geology, v. 72, no. 1, p. 68–83.

Lopez-Garcia, P., Kazmierczak, J., Benzerara, K., Kempe, S., Guyot, F., and Moreira, D., 2005, Bacterial diversity and carbonate precipitation in the giant microbialites from the highly alkaline Lake Van, Turkey: Extremophiles, v. 9, p. 263–274, doi 10.1007/s00792-005-0457-0

Madison, R.J., 1970, Effects of a causeway on the chemistry of the brine in Great Salt Lake, Utah: Utah Geological Survey Water Resources Bulletin 14, 52 p.

McCall, Joseph, 2010, Lake Bogoria, Kenya – hot and warm springs, geysers and Holocene stromatolites: Earth-Science Reviews, v. 103, p. 71–79.

McCormick, M.I., 1994, Comparison of field methods for measuring surface topography and their associations with a tropical reef fish assemblage: Marine Ecology Progress Series, v. 112, nos. 1–2, p. 87– 96.

McNair, G., 2010, Coastal Zone mapping with airborne LiDAR bathymetry: Norwegian University of Life Sciences Department of Mathematical Sciences and Technology, M. Sc. Thesis, 100 p.

Mikulich, M.J., and Smith, R.B., 1974, Seismic-reflection and aeromagnetic surveys of the Great Salt Lake, Utah: Geological Society of America Bulletin, p. 991–1002, 1 pl.

Mohapatra, G.K., and Johnson, R.A., 1998, Localization of listric faults and thrust fault ramps beneath the Great Salt Lake basin, Utah – evidence from seismic imaging and finite element modeling: Journal of Geophysical Research, v. 103, p. 10047–10063.

Moore, L.S., and Burne, R.V., 1994, The modern thrombolites of Lake Clifton, Western Australia: *in* Bertrand-Sarfati, J. and Monty, C. (eds.), Phanerozoic stromatolites II, Kluwer Academic Publishers, Boston, Massachusetts: p. 3–29.

Moran, P.A.P., 1950, Notes on continuous stochastic phenomena: Biometrika, v. 37, p. 17–33.

Morris, R.C., and Dickey, P.A., 1957, Modern evaporite deposition in Peru: AAPG Bulletin, v. 41, no. 11, p. 2467–2474.

Morrison, R.B., 1966, Predecessors of Great Salt Lake: *in* Stokes, W.L. (ed.), The Great Salt Lake – guidebook to the geology of Utah: v. 20, p. 77–104, Utah Geological Society, Salt Lake City, Utah.

Moutoux, Thomas E.,1995, Palynological and tephra correlations among deep wells in the modern Great Salt Lake, Utah, USA – implications for a Neogene through Pleistocene climatic reconstruction: Unpublished M. Sc. Thesis, University of

Arizona Department of Geosciences, Tucson, AZ.

Moyer, Ryan P., Riegl, Bernard, Banks, Kenneth, and Dodge, Richard E., 2003, Spatial patterns and ecology of benthic communities on a high-latitude South Florida (Broward County, USA) reef system: Coral Reefs, v. 22, p. 447–464.

NASA, 2003, Image ISS07-E-13002, Great Salt Lake: National Aeronautics and Space Administration - Earth Observatory - International Space Station image ISS07-E-13002; acquired 19 August 2014, accessed 03 February 2014, online at http://eoimages.gsfc.nasa.gov/images/imagerecords/4000/4148/ISS007-E-13002_lrg.jpg

O'Leary, M.J., Hearty, P.J., and McCulloch, M.T., 2008, U-series evidence for widespread reef development in Shark Bay during the last interglacial: Palaeogeography, Palaeoclimatology, Palaeoecology, v. 259, pp. 424–435.

Osborne, Robert H., Licari, Gerald R., and Link, Martin H., 1982, modern lacustrine stromatolites, Walker Lake, Nevada: Sedimentary Geology, v. 32, p. 39–61.

Oviatt, C.G., 1997, Lake Bonneville and global climate change: Geology, v. 11, p. 19–30.

Oviatt, C.G., and Thompson, R.S., 2002, Recent developments in the study of Lake Bonneville: *in* Gwynn, W. (ed.), Great Salt Lake - An overview of change: Special publication of the Utah Department of Natural Resources, Utah Geological Survey, p. 1–6.

Oviatt, C.G., Currey, D.R., and Miller, D.M., 1990, Age and paleoclimatic significance of the Stansbury shoreline of Lake Bonneville, northeastern Great Basin: Quaternary Research, v. 33, p. 291–305.

Oviatt, C.G., Currey, D.R., and Sack, D., 1992, Radiocarbon chronology of Lake Bonneville, eastern Great Basin, U.S.A.: Palaeogeography, Palaeoclimatology, and Palaeoecology, v. 99, p. 225–241.

Oviatt, C.G., Habiger, G.D., and Hay, J.E., 1994, Variation in the composition of Lake Bonneville marl – a potential key to lake-level fluctuations and paleoclimate: Journal of Paleolimnology, v. 11, p. 19–30.

Oviatt, C.G., Madsen, D.M., and Schmitt, D.N., 2003, Late Pleistocene and Early Holocene rivers and wetlands in the Bonneville basin of western North America: Quaternary Research, v. 60, p. 200-210.

Oviatt, C.G., McCoy, W.D., and Nash, W.P., 1994, Sequence stratigraphy of lacustrine deposits – a Quaternary example from the Bonneville basin, Utah: Geological Society of America Bulletin, v. 106, p. 133–144.

Oviatt, C.G., Miller, D.M., McGeehin, J.P., Zachary, C., and Mahan, S., 2005, The Younger Dryas phase of Great Salt Lake, Utah, USA: Paleogeography, Paleoclimatology, Paleoecology, v. 219, p. 22.

Oviatt, C.G., Sack, D., and Currey, D.R., 1994. The Bonneville basin (Quaternary), western United States: *in* E. Gierlowski-Kordesch and K. Kelts (eds.), Global Geological Record of Lake Basins – Volume 1, New York, Cambridge University Press, p. 371–375.

Oviatt, C.G., Thompson, R.S., Kaufman, D.S., Bright, J., and Forester, R.M., 1999, Reinterpretation of the Burmester core, Bonneville basin, Utah: Quaternary Research, v. 52, p. 180-184.

Papineau, D., Walker, J.J., Mojzsis, S.J., and Pace, N.R., 2005, Composition and structure of microbial communities from stromatolites of Hamelin Pool in Shark Bay, Western Australia: Applied and Environmental Microbiology, v. 71, p. 4822–4832.

Parker, B.C., and Wharton, R.A., 1985, Physiological ecology of bluegreen algal mats (modern stromatolites) in Antarctic oasis lakes: Archiv fuer Hydrobiologie supplement AHBSA-8, v. 71, no. ½, p. 331–348.

Parker, B.C., Simmons, G.M. Jr., Love, F.G., Wharton, R.A., and Seaburg, K.G., 1981, Modern stromatolites in Antarctic Dry Valley: BioScience, v. 31, no. 9, p. 656–661.

Pedone, B.A., and Folk, R.L., 1996, Formation of aragonite cement by nannobacteria in the Great Salt Lake, Utah: Geology, v. 24, p. 763–765.

Pedone, V.A., and Dickson, J.A.D., 2000, Replacement of aragonite by quasi-rhombohedral dolomite in a Late Pleistocene tufa mound, Great Salt Lake, Utah, USA: Journal of Sedimentary Research, v. 70, no. 5, p. 1152–1159.

Penrose, J.D., Siwabessy, P.J.W., Gavrilov, A.N., Parnum, I.M., Hamilton, L.J., Bickers, A., Brooke, B., Ryan, D.A., and Kennedy, P., 2005, Acoustic techniques for seabed classification: CRC Coastal Zone Estuary and Waterway Management, 130 p.

Pinckney, J.L., and Reid, R.P., 1997, Productivity and community composition of stromatolitic microbial mats in the Exuma Cays, Bahamas: Facies, v. 36, p. 204–

207.

Post, F.J., 1977, The microbial ecology of the Great Salt Lake: Microbial Ecology, v. 3, p. 143–165.

Powell, J.W., Gilbert, G.K., Dutton, C.E., Drummond, W., and Thompson, A.H., 1879, Report on the lands of the arid region of the United States- with a more detailed account of the lands of Utah - with maps (Vol. 3): U.S. Government Printing Office, Washington D.C.

Pratt, B.R., 1982, Stromatolite decline – a reconsideration: Geology, v. 10, p. 512–515.

Priscu, J.C., Fritsen, C.H., Adams, E.E., Paerl, H.W., Lisle, J.T., Dore, J.E., Wolf, C.F., and Mikucki, J.A., 2005, Perennial Antarctic lake ice – a refuge for cyanobacteria in an extreme environment: *in* Castello, J.D., and Rogers, S.O. (eds.), Life in Ancient Ice: p. 22–49.

Rasmussen, K.A., Macintyre, I.G., and Prufert, L., 1993, Modern stromatolite reefs fringing a brackish coastline, Chetumal Bay, Belize: Geology, v. 21, p. 199–202.

Rawley, E.V., 1974, The Great Salt Lake biotic system: State of Utah, Department of Natural Resources, Division of Wildlife Resources publication 74-13, 431 p.

Regan, John, 2009, Effect of climate change and eutrophication on the thrombolites and microbial mats within Lake Clifton: Honours dissertation, Bachelor of Engineering (Environment), University of Western Australia, November 2009.

Reid, R.P., Macintyre, I.G., Browne, K.M., Steneck, R.S. and Miller, T., 1995, Modern marine stromatolites in the Exuma Cays, Bahamas – uncommonly common: Facies v. 33, p. 1–17.

Reid, R.P., Visscher, P.T., Decho, A.W., Stolz, J.F., Bebout, B.M., Dupraz, C., Macintyre, I.G., Paerl, H.W., Pinckney, J.L., Prufert-Bebout, L., Steppe, T.F., and DesMarais, D.J., 2000, The role of microbes in accretion, lamination and early lithification of modern marine stromatolites: Nature, v. 406, no. 6799, p. 989–992.

Rezak, Richard, 1957, Stromatolites of the Belt Series in Glacier National Park and vicinity, Montana: Geological Survey Professional Paper 294-D, p. 127–154.

Riding, R., 2006, Microbial carbonate abundance compared with fluctuations in metazoan diversity over geological time: Sedimentary Geology, v. 185, no. 3, p. 229–238.

Riding, R., 2011, Microbialites, stromatolites, and thrombolites: *in* J. Reitner and V. Thiel (eds.), Encyclopedia of Geobiology, Encyclopedia of Earth Science Series, Springer, Heidelberg, p. 635–654.

Risk, M.J., 1972, Fish diversity on a coral reef in the Virgin Islands: Atoll Research Bulletin, v. 193, p. 1–6.

Romani, Anna M., and Sabater, Sergi, 1998, A stromatolitic cyanobacterial crust in a Mediterranean stream optimizes organic matter use: Aquatic Microbial Ecology, v. 16, p. 131–141.

Rowan, D.J., Kalff, J., and Rasmussen, J.B., 1992, Profundal sediment organic content and physical character do not reflect lake trophic status, but rather reflect inorganic sedimentation and exposure: Canadian Journal of Fisheries and Aquatic Sciences, v. 49, no. 7, p. 1431–1438.

Sack, D., 1989, Reconstructing the chronology of Lake Bonneville – an historical overview: *in* Tinkler, K.J. (ed.), History of geomorphology, Unwin Hyman, London, p. 223–256.

Sandberg, Philip A., 1975, New interpretations of Great Salt Lake ooids and of ancient non-skeletal carbonate mineralogy: Sedimentology, v. 22, p. 497–537.

Sanson, G.D., Stolk, R., and Downes, B.J., 1995, A new method for characterizing surface roughness and available space in biological systems: Functional Ecology, v. 9, p. 127–135.

Santos, F., Peña, A., Nogales, B., Soria, E., Garcia del Cura, M.Á., González-Martin, J.A. and Antón, J., 2010, Bacterial diversity in modern freshwater stromatolites from Ruidera Pools Natural Park, Spain: Systematic Applied Microbiology, v. 33, p. 209–221.

Schopf, J. William, 2006, The first billion years – When did life emerge?: Elements, v. 2, p. 229–233.

Schouten, S., Rijpstra, I.C., Kok, M., Hopmans, E.C., Summons, R.E., Volkman, J.K., and Sinninghe, D.J.S., 2001, Molecular organic tracers of biogeochemical processes in a saline meromictic lake (Ace Lake): Geochimica et Cosmochimica Acta, v. 65, no. 10, p. 1629–1640.

Schubert, J.K., and Bottjer, D.J., 1992, Early Triassic stromatolites as post-mass extinction disaster forms: Geology, v. 20, no. 10, p. 883–886.

Spadafora, A., Perri, E., Mckenzie, J.A., and Vasconcelos, C.G., 2010, Microbial biomineralization processes forming modern Ca:Mg carbonate stromatolites: Sedimentology, v. 57, p. 27–40.

Spencer, R.J., Baedecker, M.J., Eugster, H.P., Forester, R.M., Goldhaber, M.B., Jones, B.F., Kelts, K., McKenzie, J., Madsen, D.B., Rettig, S.L., Rubin, M., and Bowser, C.J., 1984, Great Salt Lake, and precursors, Utah – the last 30,000 years: Contributions to Mineralogy and Petrology, v. 86, no. 4, p. 321–334.

Spencer, R.J., Eugster, H.P., Jones, B.F., and Rettig, S.L., 1985, Geochemistry of Great Salt Lake, Utah I – hydrochemistry since 1850: Geochimica et Cosmochimica Acta, v. 49, p. 727–737.

Srivastava, N.K., 1999, Lagoa Salgada (Rio de Janeiro) – Recent stromatolites: *in* Schobbenhaus,C.. Campos, D.A., Queiroz, E.T., Winge, M., and Berbert-Born, M. (eds.), Sítios Geológicos e Paleontológicos do Brasil, Online at http://sigep.cprm.gov.br/sitio041/sitio041english.htm

Steneck, R.S., Miller, T.E., Reid, R.P. and Macintyre, I.G., 1998, Ecological controls on stromatolite development in a modern reef environment: a test of the ecological refuge paradigm: Carbonates and Evaporites, v. 13, p. 48–65.

Stephens, D.W., 1974, A summary of biological investigations concerning the Great Salt Lake, Utah (1861–1973): Great Basin Naturalist, v. 34, no. 3, p. 221–229.

Stephens, D.W., 1990, Changes in lake levels, salinity and the biological community of Great Salt Lake (Utah, USA), 1847–1987: Hydrobiologia, v. 197, p. 139–146.

Stephens, D.W., and Gillespie, D.M., 1976, Phytoplankton production in the Great Salt Lake, Utah, and a laboratory study of algal response to enrichment: Limnology and Oceanography, v. 21, no. 1, p. 74–87.

Stolz, J.F., 1983, Fine Structure of the stratified microbial community at Laguna Figueroa, Baja California, Mexico, I – Methods of in-situ study of the laminated sediments source: Precambrian Research, v. 20, nos. 2–4, p. 479–492.

Thompson, J.B., Ferris, F.G., and Smith, D.A., 1990, Geomicrobiology and sedimentology of the mixolimnion and chemocline in Fayetteville Green Lake, New York: PALAIOS, v. 5, no. 1, p. 52–75.

Tucker, M.E., and Wright, V.P., 1990, Carbonate mineralogy and chemistry: Carbonate Sedimentology, p. 284–313, Wiley-Blackwell.

Tukey, J.W., 1977, Box-and-whisker plots: Exploratory Data Analysis, p. 39–43.

U.S. Department of Commerce, 1992, Monthly normals of temperature, precipitation, and heating and cooling degree days, 1961–90, Utah, Wyoming, and Idaho: Publication No. 81, U.S. Department of Commerce National Weather Service.

USGS – U.S. Geological Survey, 2014, National Water Information System digital data for station 10010100 Great Salt Lake near Saline, UT, accessed 15 February 2014.

Utah Department of Natural Resources, 1992, Utah State Water Plan—Bear River Basin: Division of Water Resources, Salt Lake City, Utah.

Utah Department of Natural Resources, 1997a, Utah State Water Plan—Jordan River basin: Division of Water Resources, Salt Lake City, Utah.

Utah Department of Natural Resources, 1997b, Utah State Water Plan—Utah Lake basin: Division of Water Resources, Salt Lake City, Utah.

Vasconcelos, C., Warthmann, R., McKenzie, J.A., Visscher, P.T., Bittermann, A.G., and van Lith, Y., 2006, Lithifying microbial mats in Lagoa Vermelha, Brazil – Modern Precambrian relics?: Sedimentary Geology, v. 185, p. 175–183, doi:10.1016/j.sedgeo.2005.12.022

Vasconcelos, G., and McKenzie, J., 1997, Microbial mediation of modern dolomite precipitation and diagenesis under anoxic conditions – Lagoa Vermelha, Rio de Janeiro, Brazil: Journal of Sedimentary Research, v. 67, p. 378–390.

Waddell, K.M. and Barton, J.D., 1978, Estimated inflow and evaporation for Great Salt Lake, Utah, 1931–76, with revised model for evaluating the effects of dikes on the water and salt balance of the lake: U.S. Geological Survey Open-File Report 79-258, 61 p.

Waddell, K.M., and Bolke, E.L., 1973, The effects of restricted circulation on the salt balance of Great Salt Lake, Utah: Utah Geological Survey Water Resources Bulletin 18, 54 p.

Waddell, K.M., and Fields, F.K., 1977, Model for evaluating the effects of dikes on the water and salt balance of Great Salt Lake, Utah: Utah Geological Survey Water Resources Bulletin 21, 54 p.

Walter , M. R., Golubic, S., and Preiss, W.V., 1973, Aragonite depositing lakes near the Coorong Lagoon, South Australia: Journal of Sedimentary Petrology, v. 43, no. 4,

p. 1021–1030.

Walter, M.R. (ed.), 1976, Stromatolites – Developments in sedimentology 20: Elsevier Scientific Publishing Company, Amsterdam.

Walter, M.R., Golubic, S., and Preiss, W.V., 1973, Recent stromatolites from hydromagnesite and aragonite depositing lakes near the Coorong Lagoon, South Australia: Journal of Sedimentary Petrology, v. 43, no. 4, p. 1021–1030.

Wold, S.R., and Waddell, K.M., 1994, Salt budget for West Pond, Utah, April 1987 to June 1989: U.S. Geological Survey Water Resources Investigations Report 93-4028, 20 p.

Wold, S.R., Thomas, B.E., and Waddell, K.M., 1997, Water and salt balance of Great Salt Lake, Utah, and simulation of water and salt movement through the causeway: U.S. Geological Survey Water Supply Paper 2450, 64 p.

Wolf-Gladrow, Dieter A., Riebesell, Ulf, Burkhardt, Steffen, and Bijma, Jelle, 1999, Direct effects of CO2 concentration on growth and isotopic composition of marine plankton: Tellus, v. 51B, p. 461–476.

Wright, David T., 1999, The role of sulphate-reducing bacteria and cyanobacteria in dolomite formation in distal ephemeral lakes of the Coorong region, South Australia: Sedimentary Geology, v. 126, p. 147–157.

Wright, V.P., 2012, Lacustrine carbonates in rift settings – the interaction of volcanic and microbial processes on carbonate deposition: Geological Society of London, Special Publications, v. 370, doi: 10.1144/SP370.2

Wurtsbaugh, W.A., Gardberg, J., and Izdepski, C., 2011, Biostrome communities and mercury and selenium bioaccumulation in the Great Salt Lake (Utah, USA): Science of the Total Environment, v. 409, no. 20, p. 4425–4434.

Wurtsbaugh, W.A., 1995, Brine shrimp ecology in the Great Salt Lake, Utah: Performance Report to Utah Division of Wildlife Resources, 35 p.

Wurtsbaugh, W.A., 2009, Biostromes, brine flies, birds and the bioaccumulation of selenium in Great Salt Lake, Utah: Natural Resources and Environmental Issues, v. 15, no. 1, 2 p.

Wurtsbaugh, W.A., and Berry, T.S., 1990, Cascading effects of decreased salinity on the plankton, chemistry, and physics of the Great Salt Lake (Utah): Canadian Journal of Fisheries and Aquatic Sciences, v. 47, no. 1, p. 100–109.

Wurtsbaugh, W.A., and Gliwicz, Z. Maciej, 2001, Limnological control of brine shrimp population dynamics and cyst production in the Great Salt Lake, Utah: Hydrobiologia, v. 466, nos. 1–3, p. 119–132.

Wurtsbaugh, W.A., and Gliwicz, Z.M., 1996, Nutritional controls on brine shrimp reproduction in the Great Salt Lake: Bulletin of the Ecological Society of America, v. 77, no. 3, Supplemental Part 2, p. 493.